Doctoral Dissertation

Identifying environmental sex-determining genes in the branchiopod crustacean *Daphnia magna* (*Vrille* up-regulates *Dsx1* expression)

Nur Syafiqah Mohamad Ishak

January 2018

Department of Biotechnology

Graduate School of Engineering

Osaka University

Table of Contents

Chapter 1 General introduction 5

1.1 Introduction 5

1.2 Diversity of sex-determining pathways among animals 6

1.3 Environmental sex determination (ESD) 10

1.4 Monosex culture 10

1.5 The model organism *Daphnia magna* 12

1.6 Molecular mechanism of male production pathway in *D. magna* 14

1.7 Objective of this study 15

Chapter 2 Late response of *Dsx1* to JH signaling in early embryos 17

2.1 Introduction 17

2.2 Materials and methods 18

2.2.1 *Daphnia* strain and culture condition 18

2.2.2 Artificial male production by JH analog exposure 19

2.2.3 Developmental staging of embryogenesis 19

2.2.4 Total RNA isolation 20

2.2.5 First-strand cDNA synthesis 20

2.2.6 Quantitative real-time PCR 21

2.3 Results 22

2.3.1 cDNA synthesis of early embryos 23

2.3.2 Temporal expression by qRT-PCR analysis 24

2.4 Discussion 27

Chapter 3 Transcription factor *Vrille* activates *Dsx1* expression 29

3.1 Introduction 29

3.2 Materials and methods 31

3.2.1 *Daphnia* strain and culture condition 31

3.2.2 Finding potential binding sites by bio-computational 32
3.2.3 Cloning and sequencing 32
3.2.4 Phylogenic analysis 33
3.2.5 Quantitative real-time PCR 34
3.2.6 Gene knockdown by RNAi 35
3.2.7 Gene overexpression by mRNAs delivery 36
3.2.8 Selection of gRNA target sequences by ZiFiT software 37
3.2.9 Cloning-free method for gRNA *in vitro* synthesis 37
3.2.10 Cas9 protein synthesis in *E. coli* cells 39
3.2.11 Cas9 extraction and purification 40
3.2.12 Cas9 protein *in vitro* cleavage assay 42
3.2.13 Targeted mutagenesis by CRISPR/Cas9 system and genotyping 42
3.3 Results 44
3.2.1 E4BP4 binding site candidate on the *Dsx1* promoter 44
3.2.2 Characterization of *Vri* gene in *D. magna* 45
3.2.3 *Vri* expression levels during embryogenesis 48
3.3.4 *Vri* knockdown in male reduced *Dsx1* expression 49
3.3.5 *Vri* overexpression in female increased *Dsx1* expression 55
3.3.6 Disruption of the enhancer reduced *Dsx1* expression 58
3.4 Discussion 62

Chapter 4 Sequence conservation of the *Ftz-F1* ortholog in *D. magna* and its sexually dimorphic expression 65

4.1 Introduction 65
4.2 Materials and methods 66
4.2.1 *Daphnia* strain and culture condition 66
4.2.2 Total RNA isolation 67
4.2.3 First-strand cDNA synthesis 67

4.2.4 Cloning and sequencing 67
4.2.5 Phylogenic analysis 68
4.2.6 Quantitative RT-PCR 69
4.2.7 Gene knockdown by RNAi 70
4.2.8 Finding potential binding sites by bioinformatics computational 71
4.3 Results 71
4.3.1 Characterization of *Ftz-F1* gene in *D. magna* 71
4.3.2 Features of *D. magna* Ftz-F1 proteins 75
4.3.3 *Ftz-F1* mRNAs expression during embryogenesis 78
4.3.4 Phenotypes of *Ftz-F1* RNAi embryos 81
4.3.5 Ftz-F1 binding site candidates on the *Dsx* promoter 83
4.4 Discussion 85

Chapter 5 General discussion and conclusion 88

5.1 General discussion 88
5.2 Conclusion 93

References 94

List of publications 106

Acknowledgments 107

Chapter 1 General introduction

1.1 Introduction

Sex determination is a fundamental biological process that governs the development of sex characteristic such as development of gonads and most organs, and also affects the sex-specific differences in behavior, physiology and morphology. How sex is determined have intrigued scientists for hundreds of years since the time of Aristotle. Until the sex chromosome was discovered around 1900, the claim that the heat of the male partner determines sex was popular. Thereafter, numerous cytological and genetic studies have shown that sex-determining mechanisms are diverse among organisms that can be broadly divided into two categories according to their primary causal factor: genetic sex determination (GSD) and environmental sex determination (ESD) [1]. Recent advances in biotechnology such as genetic engineering unraveled molecular mechanisms of GSD on various model organisms including mouse, nematode, and fruit fly. In contrast, little is known about the ESD because organisms obligating the ESD system are poor genetic models. To understand how diverse sex determination mechanisms have evolved, investigation on ESD mechanisms is necessary.

Studies of sex determination mechanisms have been applied to various scientific fields. In mammals, knowledge on genes and their proteins involved in sex development contribute to understanding disorder of sex development for medical solutions [2,3]. Besides that, elucidation of the mechanism in insects is necessary to develop new synthetic genetics-based tools, such as the sterile insect technique (SIT), for the control of pest insects [4]. Furthermore, biotechnology solution has been successful for producing a single sex population of crustaceans [5,6], which produces higher yield with greater commercial value.

The water flea crustacean *Daphnia magna* is a newly emerging model for sex determination studies. First, this species utilizes environmental signals to determine sex. It normally reproduces females asexually, but male offspring are produced under stressful conditions as they resort to sexual reproduction. *Daphnia* is also the only environmental sex-determining organism to have both its genome sequenced and genetic engineering tools developed. Therefore, it is a suitable model for understanding the ESD mechanism. On the other hand, *Daphnia* belongs to crustaceans including commercially important species such as shrimp and prawns. Among crustaceans, the most advanced set of the functional genomics tools is available in *D. magna.* Since sex-determining mechanisms are relatively similar between species in the same clade (explained in following section), this makes *D. magna* an important model for investigating crustacean sex-determining mechanisms, which in turn would contribute to the development of monosex culture in crustaceans. However, the knowledge about the molecular pathway of *D. magna* sex determination is still limited.

1.2 Diversity of sex-determining pathways among animals

Sex determination is a basic biological mechanism for an embryo to decide which sex-determining pathway it will adopt. This process will govern the sexual differentiation that regulates subsequent sexual development of those parts of the embryo that differ between sexes. From sexual developments, individual can differ remarkably not only on their gametes and gonads but also in many aspects of its morphology, physiology and behavior [1]. Gamete, which made in organ called gonads, is required from each female and male for sexual reproduction to occur.

Sexual reproduction is a very common phenomenon in the animal kingdom for species propagation and genetic diversity [7].

Cells can determine its sexual fate dependently or independently of their surroundings. The former phenomenon occurs through cell non-autonomous mecahnsims, typically in mammals, where sex-specific hormones produced by gonads orchestrate the development of nearly all sexually dimorphic phenotype [8]. Hormone intervention can also stimulate a wide range of secondary sexual traits regardless of its genotype or development stage [9]. In contrast, under cell autonomous mechanism, sexual determination is dictated by genetic cascades that differ between sexes. Studies in *Drosophila* show that embryos with sexually mosaic genotype will develop with a sexually mosaic phenotype [10]. In this phenomenon, a sex-specific regulatory cascade controls the sexual fate of cells and among the animals, the sex-determining cascades are diverse [11].

The primary cues which trigger sexual development vary through genetic evolution [12,13]; whether it is a strict genetic cue (GSD) or simply from environmental signal (ESD) [1]. The former is attributed to the genetic segregation of genes commonly positioned on sex chromosome, while the latter is initiated by environmental cues such as temperature, nutrition, photoperiod, and population density to induce molecular cascades for activation of alternate sex-determining genes. Numerous studies about GSD mechanisms from various model organisms such as mammals, worms and insects have shown that the pathways are largely different mainly at the upstream of the cascades [11]. As presented in Figure 1, a distinct initial cue initiates a specific transduction mechanism, which then finally leads to sex-specific expression of the major effector of sexual differentiation, the DM-domain gene [11].

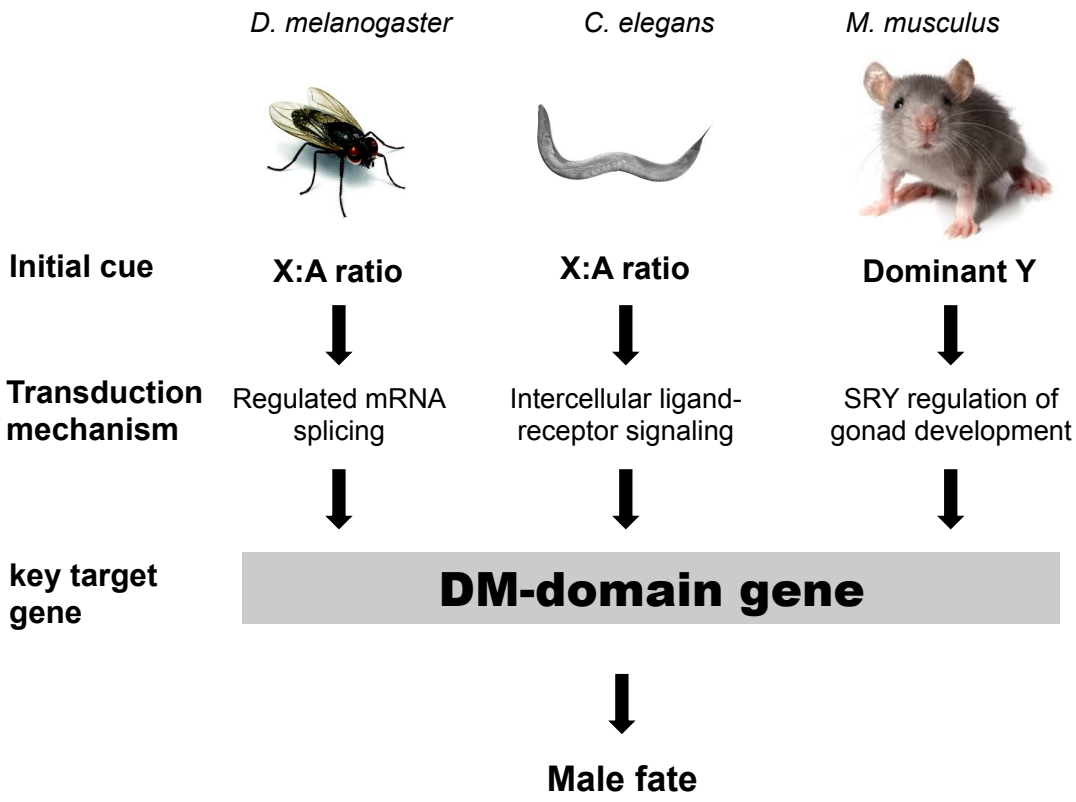

Figure 1: Sex determination pathways in diverse animals. Although the pathway largely differ in the mechanism and gene content, especially at the top of genetic cascades, several systems have homologues key target gene or protein for male sexual differentiation. The key target gene is the DM-domain genes which was named as *Doublesex* (*Dsx1*), *male abnormal 3* (*mab-3*) and *doublesex and male abnormal 3 related transcription factor 1* (*Dmrt1*) in *D. melanogaster, C. elegans* and *M. musculus*, respectively.

Figure 2 shows arthropod sex-determining pathways. Lucas (2008) and Gempe and Beye (2010) have reviewed several sex-determining mechanisms in a number of insect species. In fruit fly, the double dose of X chromosome is responsible for feminizing activity through activation of Sxl^F gene located on the X chromosome. Sxl^F protein is a splicing factor that splices *tra* mRNAs in female to produce Tra^F protein. On the other hand, a single X chromosome leads to the absence of Sxl protein resulting to male *tra* mRNA with premature stop codon [14]. Contrarily, medfly possesses a dominant male determiner M on the Y chromosome, which establishes

masculinizing activity. In the presence of M factor, male *Cc-tra* mRNAs are produced whereas in the absence of M factor, maternally derived Tra directs splicing to produce female *Cc-tra* mRNAs [15]. However, in honeybee, heterozygosity of the *complementary sex determiner* (*csd*) gene activates feminizing activity. This heterozygous Csd directs splicing to form Fem^F mRNAs that encode for the Feminizer (Fem) protein. Homozygous Csd genes are non-active genes which lead *Fem* mRNAs to be spliced into the male form that contains a premature translation stop codon [16]. The *Fem* is apparently an ortholog of the *tra* genes. All in all, these studies demonstrated 1) the diversity of regulatory mechanisms of GSD and importantly 2) conservation of sex-determining genes in the same clade (a group of related organisms).

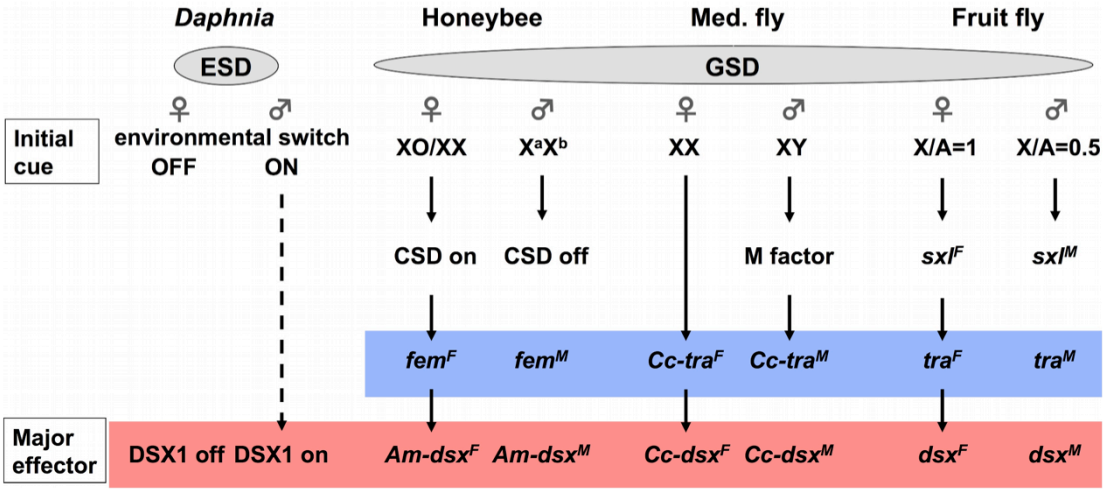

Figure 2: Simplified view of sex-determining pathways in the branchiopod crustacean *Daphnia* and insects. Comparison of GSD pathways in insects model species namely: fruit fly (*Drosphila melanogaster*), Mediterranean fruit fly (Med. Fly, *Ceratitis capitata*) and honeybee (*Apis mellifera*) and ESD pathway of *Daphnia*. The major effector of sexual differentiation *Doublesex* genes are conserved among the species while the upstream regulatory components are diverse [17].

1.3 Environmental sex determination (ESD)

ESD is also widespread, occurring in diverse taxa such as rotifers, nematodes, crustaceans, insects, fishes, and reptiles. Environmental cues involved in ESD include temperature, photoperiod, nutrition, and population density [18]. The ESD has arisen repeatedly during evolution [19], which may imply the adaptive significance of this system in environments. It has long been suggested that selection forces drive the transition between GSD and ESD [1,20]. Previous experiments using a temperature-sensitive mutation created artificially in *Dr. melanogaster* and *C. elegans* also revealed that as a consequence of mutation in a single control gene, GSD could rapidly evolve into ESD [21,22]. Furthermore, orthologs of some genes involved in GSD have been examined in ESD animals. In temperature-dependent sex-determining reptiles, some of those sex-determining genes were expressed in the gonads during the temperature-sensitive period [23]. Also in water flea crustaceans, studies have shown that both ESD and GSD have the same origin and share similar genetic components in their downstream sex-determining cascade (Figure 2), which is the conserved DM-domain transcription factor Dsx1 as the sexual major effector [17,24]. However, a detailed hierarchical cascade of any ESD mechanism has not been reported yet. Therefore, it is important to identify the genes involved in ESD and unravel the upstream molecular regulation involved in sexually dimorphic pathway in order to understand the origin of divergence and evolution of sex determination mechanism.

1.4 Monosex culture

Monosex culture or a single sex culture (either all female or all male) strategy became common practice in fish-based aquaculture [5,25], and subsequently the strategy was applied to crustacean culture. In crustacean aquaculture field, freshwater prawn *Macrobrachium rosenbergii* males grow faster and reach a larger size than

females of the species. These attributes of gender selection in animal breeding are economically advantageous because it lead to higher yields, greater average weights and shorter time to harvest [5]. Because manual segregation of juveniles is extremely laborious, sexual manipulation at genetic level is being implemented in crustacean aquaculture in order to obtain an all-male population. However, the mechanism of sex determination has not been studied extensively in Malacostraca crustacean because of its complex life cycle and difficulties in establishing heterochromosomic sex in this group. Understanding the regulation pathway of sex determination will facilitate the development of biotechnologies for the culture of monosex population of crustacean species [5].

Sex differentiation in malacostracans is regulated by hormone secreted from androgenic gland, in which the absence of AG permits feminization [26]. AG ablation by microsurgical intervention of juvenile at early developmental stage leads to the sexually-reverse male, called as neo-female, which is phenotypically a functional female but has a male genotype [25]. Alternatively, the discoveries of androgenic gland (AG)-specific insulin-like peptides (IAGs) allow feminization to occur by gene silencing in crustacean [6]. Mating neo-females with normal males as broodstock could result in all-male progenies. This process does not involve the use of chemical/hormones and does not involve genetic modification to target organism, hence it is possible to apply it in the aquaculture field. However, current problem is that continuous silencing of the IAG gene is required throughout the lifespan due to the nature of continuous expression of this gene [27]. Therefore, it is necessary to test the silencing of other genes involved in sex-determination and sexual differentiation. Basic research in crustacean sex determination is significant to supplement the biotechnology application on monosex culture of crustacean species.

1.5 The model organism *Daphnia magna*

The *Daphnia magna* is a branchiopod crustacean, which is a waterflea commonly living in freshwater ponds in Europe and Asia. The *D. magna* undergoes switching of its reproductive strategy between parthenogenetic and sexual cycle depending on the environmental living condition [28]. As illustrated in Figure 3, normal healthy *Daphnia* produces female clones through parthenogenesis or asexual reproduction that rapidly increases their population. Alternatively, in response to environmental stimuli such as shortening of photoperiod, lack of food and/or high population density, it produces clonal males, which allows them to undergo sexual reproduction [29]. The environment-dependent production of males is a key process in the life cycle that leads to increased genetic diversity and fitness as a survival strategy to overcome adverse conditions [7].

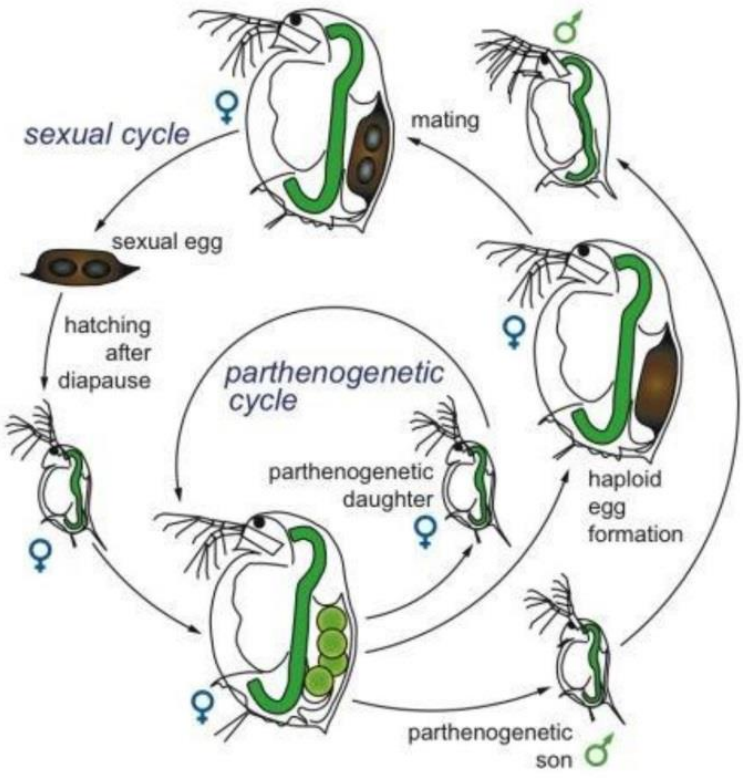

Figure 3: Life cycle of *Daphnia.* The diagram illustrates the parthenogenetic (asexual) and sexual cycle of *Daphnia*. Under normal conditions, female *Daphnia* produces diploid eggs

that develop to be female offspring through parthenogenesis. When *Daphnia* is stimulated by environmental stress, such as shortened photoperiod, food shortage and overcrowded population; the female produces male offspring, and later haploid egg that requires male fertilization. The fertilized egg, which is called resting egg, is enclosed in protective hard shell termed as ephippium. The resting eggs can endure unfavorable condition and diapause over a long time period.

The male offspring produced as environmental response are genetically identical to their sisters and mothers. The first male-specific trait appears at first instar by its shortened rostrum (head shape) and elongated first antennules, as shown in Figure 4, which are clearly distinct from the female's features. Gonads that are located at the both side of gut also exhibit morphological sex in the first instar juveniles [30]. During maturation and development, the male daphniid undergoes more morphological sex differentiation on various somatic tissues [31,32]. For examples, the first thoracic leg armed with the copulatory hook becomes larger in fifth instar, and obtains a modified shape of the breast margin and ventral region [32]. This male continues to mature and masculinize until adulthood, and able to copulate with female with haploid egg requiring fertilization for sexual reproduction to occur. As the result of haploid egg fertilization by male, female *Daphnia* produces sexual egg or resting egg necessary for its survival against the harsh condition [28].

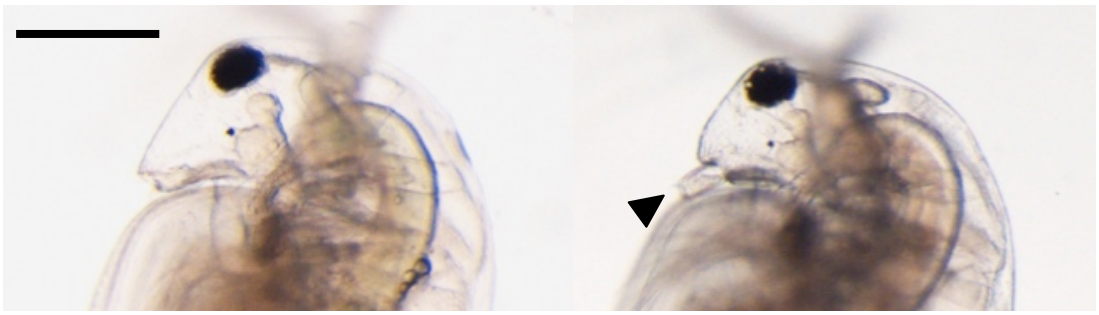

Figure 4: First instar of female (left) and male (right) *Daphnia.* Black arrowhead indicates the first elongated antennae, which is a male-specific phenotype. Scale: 200 μm.

The *D. magna* has emerged as a model organism for studying ESD mechanism because compared to the other ESD animals like turtle and crocodile, its small body size and fast life cycle make *Daphnia* easy to handle and suitable as laboratory experimental animal. In addition, the availability of *Daphnia* genome full sequence [33,34] and gene expression profiles [35] give valuable advantages for ESD research. The advances of genetic manipulation through RNA interference [36], ectopic expression method [37], developing genome editing methods in *D. magna* via TALEN [38–40] and CRISPR/Cas9 systems [41], have allowed us to perform gene function analyses in this model organism. This growing genomics and genes manipulation toolbox for *Daphnia* is providing opportunities to extend laboratory research to analyze gene function for elucidating the molecular mechanism including sex determination.

1.6 Molecular mechanism of male production pathway in *D. magna*

Sex determination is phenotypic in *Daphnia* [28] and it relies on environmental cues to switch the developmental pathway from female to male production [42]. Little is known about the molecular mechanism of male sex determination in *D. magna.* The critical period for male inducing cues has been earlier investigated by Banta and Brown (1929) and Olmstead and LeBlanc (2002) were the first to show production of male juveniles of *D. magna* in response to the sesquiterpenoid hormone methyl farnesoate (MF). Later, other JH analogs (JHAs) in addition to MF have been demonstrated to induce male production ten to four hours before eggs ovulation [44], in which it stimulates germ cells at the late stage of oogenesis leading to development of males from ovulated eggs [45,46]. It is

suggested that environmental cues for sex determination are converted to JH signals neuroendocrinically. These studies also suggest that juvenile hormone could play an important role in understanding male sex-determining pathway of *D. magna.*

A DM-domain transcription factor *Doublesex1* (*Dsx1)* gene, originally identified in *Drosophila melanogaster*, was also discovered in *D. magna.* This gene is expressed in response to the JH signal [17]. Gain- and loss-of-function analyses demonstrated that *Dsx1* gene is a major effector that regulates the male phenotype in *Daphnia.* Unlike *Drosophila Dsx* gene, *Daphnia Dsx1* is sex-specifically expressed; with different transcript abundance for male and female. *Dsx1* is expressed and maintained to regulate development of male traits during embryogenesis [17], suggesting that JH-dependent *Dsx1* activation is necessary for the environmentally dependent production of males. However, the molecular mechanism of *Dsx1* regulation in male sex-determining pathway is still unknown. Other components related to the sex-determining cascade are yet to be discovered.

1.7 Objective of this study

In male sex-determining pathway of *D. magna*, JH and the major effector of sexual differentiation *Dsx1* are currently known to be essential. However, genes that mediates JH signaling and *Dsx1* activation remain unknown (Figure 5). To discover the missing factor(s) that links between JH and Dsx1 in the cascade, identifying and characterizing the genes that are related to sex-determining mechanism is necessary; hence the main objective of this study. To elucidate the ESD mechanism in model organism *D. magna*, I first investigated the timing of JH-dependent activation of *Dsx1* gene during embryogenesis in Chapter 2. Later, I focused on characterizing a candidate gene of transcription factor Vrille (Vri) and its functional analyses in

Chapter 3 to discover the activator of male specific *Dsx1* expression. Lastly, I characterized the transcription factor Ftz-F1 in Chapter 4 to identify other candidate of sex-determining genes.

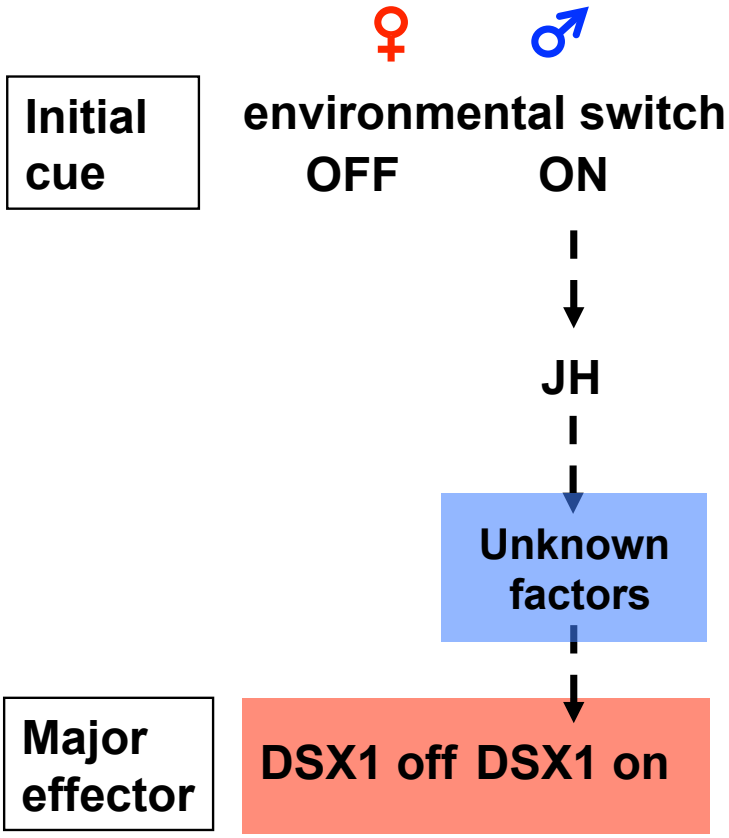

Figure 5: Current progress of molecular mechanism of sex-determining pathway in *D. magna*. Juvenile hormone and Doublesex1 (Dsx1) are known to be involved in male production of *Daphnia*. Identifying other factors is required to understand the molecular cascade of environmental sex determination.

Chapter 2 Late response of *Dsx1* to JH signaling in early embryos

2.1 Introduction

The major effector of sexual differentiation *Dsx* gene was previously discovered in *D. magna* [17]. In the fruit fly *Dr. melanogastor, Dsx* is spliced in the coding region by the *Tra* protein in sex-specific manner at the level of pre-mRNA to produce sex-specific *Dsx* proteins [47]. In contrast, *Dsx1* of *D. magna* shows sexual differences in the transcripts abundances and only encodes for a single coding sequence. It is alternatively transcribed through two promoters, α and β, that utilize two different transcriptional start sites to produce mRNA isoforms which are only different at the 5′ UTR, as shown in Figure 6.

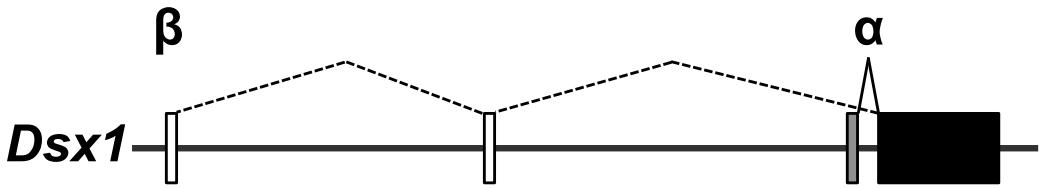

Figure 6: Genomic structure of *Dsx1* gene. The coding exon, *Dsx1-α* 5′ UTR and *Dsx1-β* 5′ UTR are indicated in black, grey and white boxes, respectively.

Alternative promoter usage can influence gene expression in various ways and that includes initiation of transcript, mRNA isoform turnover, and tissue-specific expression [48]. This point suggests that in *D. magna* environmental sex-determining pathway, JH signal could regulate a specific *Dsx1* isoform in different manner, time and space through alternative promoter usage. Although previous study has measured the *Dsx1* expression during embryogenesis, due to the huge gap between each time point [17], the data did not reveal the initiation of each transcript and temporal changes during early embryogenesis. Hence, it was insufficient to understand when JH signal leads to the *Dsx1* activation for male sex determination and differentiation.

In this chapter, I investigated the *Dsx1* expression level during embryogenesis to discover at which time point JH signal initiates the expression of *Dsx1* and which promoter is first controlled by JH. Examining the temporal changes of the two *Dsx1* mRNA transcripts provide information for understanding the nature of JH-dependent *Dsx1* expression in *D. magna.*

2.2 Materials and methods

2.2.1 *Daphnia* strain and culture condition

The *Daphnia magna* (NIES clone) was obtained from the National Institute for Environmental Studies (NIES; Tsukuba, Japan) and cultured in Aachener Daphnien Medium (ADaM) [49] in our laboratory. Eighty juvenile daphniids (less than 24 h age) were cultured in a tank with 5 L of ADaM at 23±1 °C under 16 h light/ 8 h dark photoperiod conditions. They were fed with 4.8×10^8 cells/day of chlorella for a week and then the feeding amount were increased to 9.6×10^8 cells/day from the second week. A previously established transgenic line (HG-1) expresses H2B-GFP protein under the control of *D. magna Elongation Factor 1 α-1* (*EF1 α-1*) promoter/enhancer [50] to provide a high resolution for visualization of active chromatin. This feature enables us to visualize and define embryo developmental stages explained in the section 2.2.3 Developmental staging of embryogenesis. The transgenic line was cultured under the same laboratory condition as the wild-type *Daphnia*.

2.2.2 Artificial male production by JH analog exposure

To obtain male embryos, female adults (2 to 3 weeks-old) at appropriate stage were treated with 1 μg/L of synthetic juvenile hormone analog (JHA), Fenoxycarb (Wako Pure Chemical; Osaka, Japan) [46]. The next ovulated eggs that would develop into male embryos were collected and used for subsequent experiments. The first few and last daphnids that went through ovulation during sampling for every Fenoxycarb exposure were put aside and cultured to validate male offspring production. I confirmed that the Fenoxycarb-exposed daphnia produced 100% male offspring for every conducted experiment.

2.2.3 Developmental staging of embryogenesis

I defined six developmental stages during embryogenesis based on specific developmental landmarks of daphnia embryo (Figure 7). First, a newly ovulated or 0-h post ovulation (hpo) egg is termed as 1-cell stage. At 3-hpo, the embryos were observed to undergo blastulation (blastula) and then the embryos proceed to develop a gastrula. These two stages (blastula and gastrula) are very brief periods, just within few hours. A ring-like gastrulation zone was clearly visible at early gastrula, 6-hpo. Around 9-hpo, the cells were observed to have moved spatially and this stage is termed as late gastrula stage. As the embryo continued to develop, I set the 18-hpo embryos as late embryo I since all five thoracic segments had appeared on the ventral view of embryo. Finally after hatching, I defined 36-hpo embryos as late embryo II stage where the *Daphnia* undergoes further developments including the eyes and antennae before it turned into juvenile.

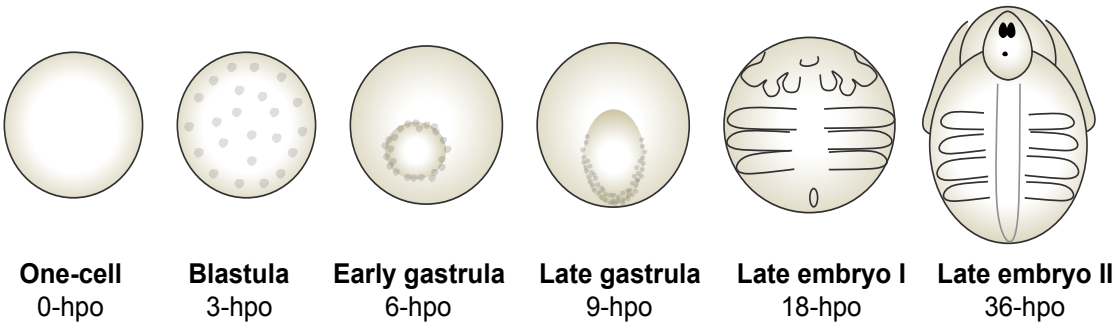

Figure 7: Developmental staging of *D. magna* embryogenesis. Embryonic development was staged at 0-hpo (one-cell), 3-hpo (blastula), 6-hpo (early gastrula), 9-hpo (late gastrula), 18-hpo (late embryo I), and 36 hpo (late embryo II).

2.2.4 Total RNA isolation

Female and male wild-type embryos (25-50 eggs each) at specific stages explained above (2.2.3 Developmental staging of embryogenesis) were collected separately and briefly washed. Homogenization was performed with beads using a Micro Smash machine MS-100 (TOMY; Tokyo, Japan) in the presence of Sepasol-RNA I reagent (Nacalai Tesque Inc.; Kyoto, Japan). Total RNA was isolated according to the manufacturer's protocol and then followed by phenol/chloroform extraction. The amount of purified total RNA was measured with Nanodrop 2000 (Thermo Fisher Scientific).

2.2.5 First-strand cDNA synthesis

The mRNA from purified total RNA was converted to first-strand cDNA using SuperScript III Reverse Transcriptase (Invitrogen; California, USA). One µg of total RNA was added with 250 ng of random primers (Invitrogen), 4 µL of 2.5 mM dNTPs mix (Takara Bio; Shiga, Japan) and ultrapure distilled water (Invitrogen) that would bring the total volume of 13 µL in a PCR tube. The mixture was heated at 65

°C for 5 min and immediately incubated on ice for at least 1 min. Next, 4 μL of 5X First-Strand Buffer (Invitrogen), 1 μL of 0.1 M DTT (Invitrogen), 1 μL of RNase inhibitor RNaseOUT (Invitrogen) and 1 μL of 200 units/μL SuperScript III enzyme were added into the denatured sample. After mixing by pipetting, the reaction sample was incubated in the following conditions: 25°C for 5 min; 50°C for 60 min; 70°C for 15 min. To confirm the cDNA synthesis and check for genomic DNA contamination, *β-Actin* gene was amplified by PCR using a forward primer (5′-GGCAAGGAATAGTTCGATAC-3′) and a reverse primer (5′-CACCGACGTACGAATCCTTCTGACC-3′) and the PCR products were ran on gel electrophoresis.

2.2.6 Quantitative real-time PCR

To measure the *Dsx1* gene expression during embryogenesis, cDNA samples of both females and males at each embryonic stage were prepared in three replicates for quantitative real-time PCR analysis. The reaction mixture was prepared according to the recommended manufacturer's protocol by adding SYBR GreenER qPCR SuperMix Universal reagent (Invitrogen) and each primer set solution to the cDNA samples. The mRNA transcripts were measured with Mx3005P Real-Time QPCR System (Agilent Technologies) by absolute quantification method. This quantification method relates the PCR signal to input copy number using a calibration curve which was obtained by dilution series of plasmid that has sequences corresponding to each primer set. The PCR amplifications were performed in triplicate at the following conditions: 2 in at 50°C and 10 in at 95°C, followed by 40 cycles of 15 sec at 95°C and 1 min at 60°C. Gel electrophoresis and dissociation curve analysis were performed to confirm the correct amplicon size and the absence of non-specific bands.

The primers that specifically amplified α-promoter- and β-promoter-driven transcripts were designed on the 5′ UTR of *Dsx1* gene. The primer sets used for qRT-PCR are listed in Table 1. Normalized expressions were analyzed by quantitating the reference gene of ribosomal protein *L32* expression level using the primer pair of a forward primer: (5′-GACCAAAGGGTATTGACAACAGA-3′) and a reverse primer (5′-CCAACTTTTGGCATAAGGTACTG-3′), and values obtained were used for the calculation of normalization.

Table 1: The primer pairs used to quantitate specific amplification of *Dsx1* gene in qRT-PCR analysis.

Amplify region of *Dsx1*	**Primer sequence (5′−3′)**
Common region	Forward: CCATTCATCATTACCAAATCCCTTC Reverse: AAGTTTGGTGTAGGGGAGGATGAG
α-isoform	Forward: GGGAAAGCTTCGTACCGAAAA Reverse: CAGTAAGGCACCAAAAGGGAAC
β-isoform	Forward: CATTGATGCTGGTTTCACCAA Reverse: GGGGTGCTGTAGATGCTCAAG

2.3 Results

To determine the embryonic stage at which *Dsx1* α- and β- promoters are activated by JH in early embryo, I examined the temporal expression of each isoform. The total RNA from female and male 0, 3, 6, 9, 18 and 36-hpo embryos were purified, reversed transcribed into cDNA and then qPCR was conducted.

2.3.1 cDNA synthesis of early embryos

The *β-Actin* primers were designed to produce 674 bp and 264 bp of genomic DNA and cDNA fragments respectively. Therefore, if an RNA sample was contaminated with genomic DNAs during the isolation step, larger size of PCR products can be observed on the agarose gel after performing RT-PCR reaction with the *β-Actin* primers. In this study, I confirmed that RT-PCR did not show the larger products in all of the cDNA samples used for qRT-PCR, suggesting that there are no genomic DNA contamination that may interfere the expression analysis result. Figure 8 show all results of agarose gel electrophoresis from female and male samples of each stage in triplicates.

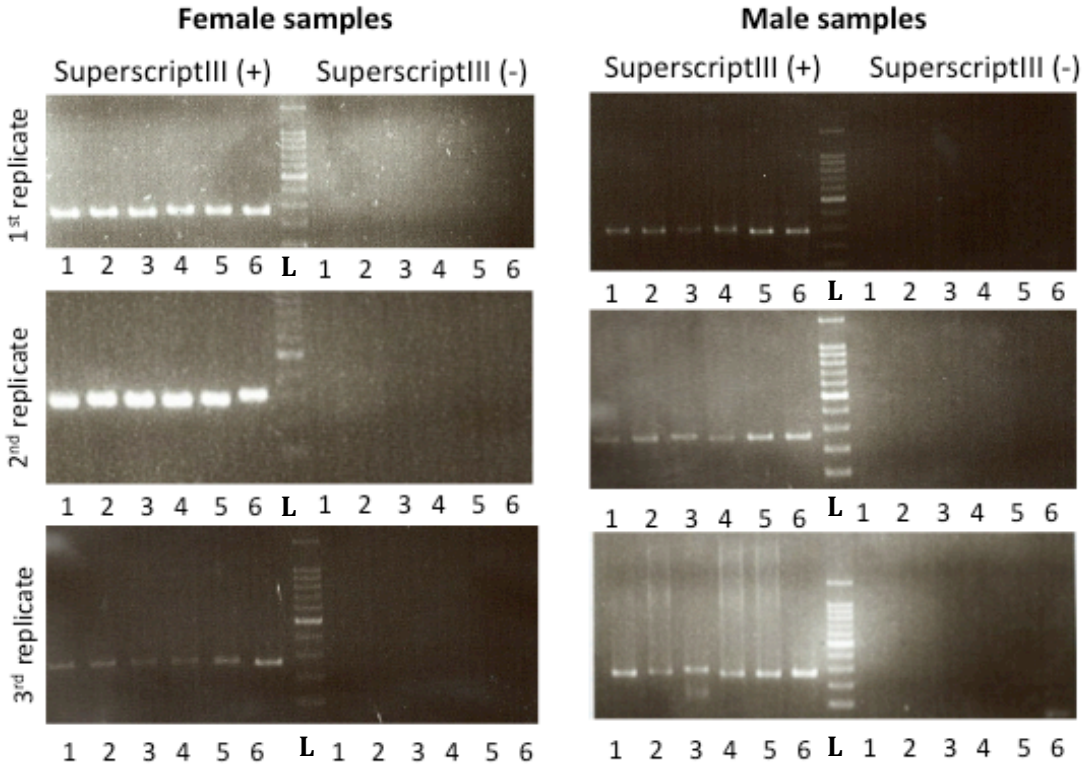

Figure 8: β-Actin RT-PCR products on agarose gel of electrophoresis. Left side shows the samples of first-strand cDNA synthesis reaction with SuperScriptIII enzyme and the right side shows those without the enzyme. The numbers indicate the age of *Daphnia* sample (1: 0-hpo, 2: 3-hpo, 3: 6-hpo, 4: 9-hpo, 5: 18-hpo, 6: 36-hpo, L: ladder for DNA marker).

2.3.2 Temporal expression by qRT-PCR analysis

Before measuring *Dsx1* transcripts levels, I first quantitated a reference gene, ribosomal protein *L32* expression. As shown in Figure 9A, at each developmental stage there was no significant difference in *L32* expression between the sexes. Then, I measured *Dsx1* expression using the primer set that amplifies the *Dsx1* coding region, the common region of two isoforms to reveal the total transcripts amount. Consistent to previous study [17], the *Dsx1* common region showed sexually dimorphic expression as significantly expressed in males. The significant difference was first detected at 9-hpo late gastrula stage (Figure 9B).

To quantify the isoform specific transcripts, the qPCR analyses were performed using primers that amplify the 5'-UTR of each isoform. The result showed that *Dsx1*-α isoform started to be expressed during gastrulation stage at 6-hpo in both sexes; no expression prior this stage (Figure 10A). Male-specific activation of this transcript was observed at 9-hpo and afterward the expression was maintained exclusively in male. However, in female embryos the mRNA transcript gradually depleted starting from 9-hpo. For the *Dsx1-β* (Figure 10B), maternal mRNAs of β-isoform were detected in female and male after ovulation (0-hpo), and were degraded across the blastula to early gastrula (3 to 6-hpo). At 9-hpo, zygotic mRNAs started to be expressed in both sexes and thereafter the male sex-specific expression appeared and was maintained.

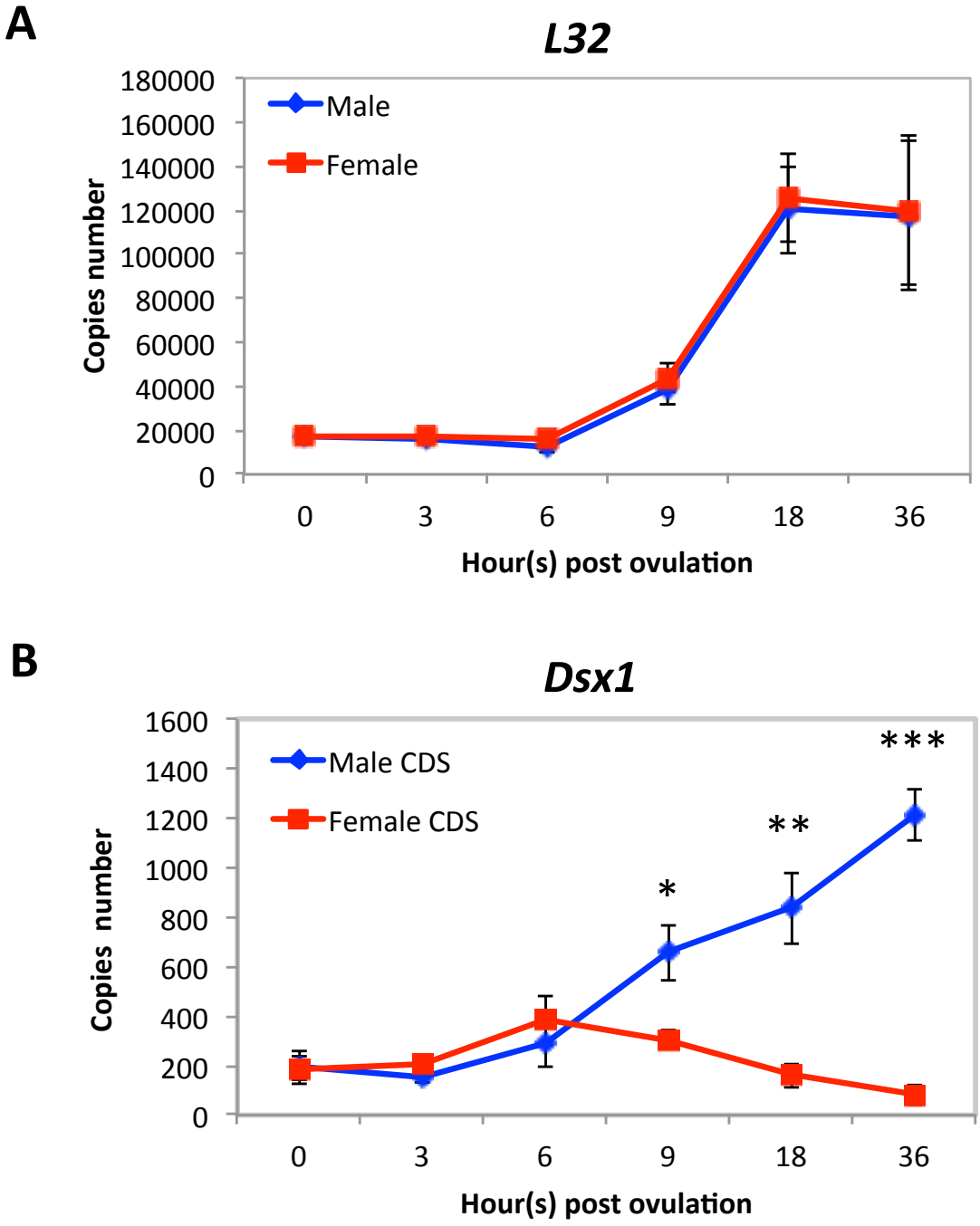

Figure 9: qRT-PCR analyses of (A) L32 reference gene and (B) *Dsx1* CDS transcript expression level. The *L32* gene was chosen as a reference gene for q-PCR assay. The *Dsx1* coding region transcript indicates the total copy number of all mRNA isoform and used as positive control. The expression level was measured as copy number of transcripts per egg. Blue line indicates the result from male samples while red indicates the female samples. (Student's t-test; *, $p \leq 0.05$; **, $p \leq 0.01$; ***, $p \leq 0.001$).

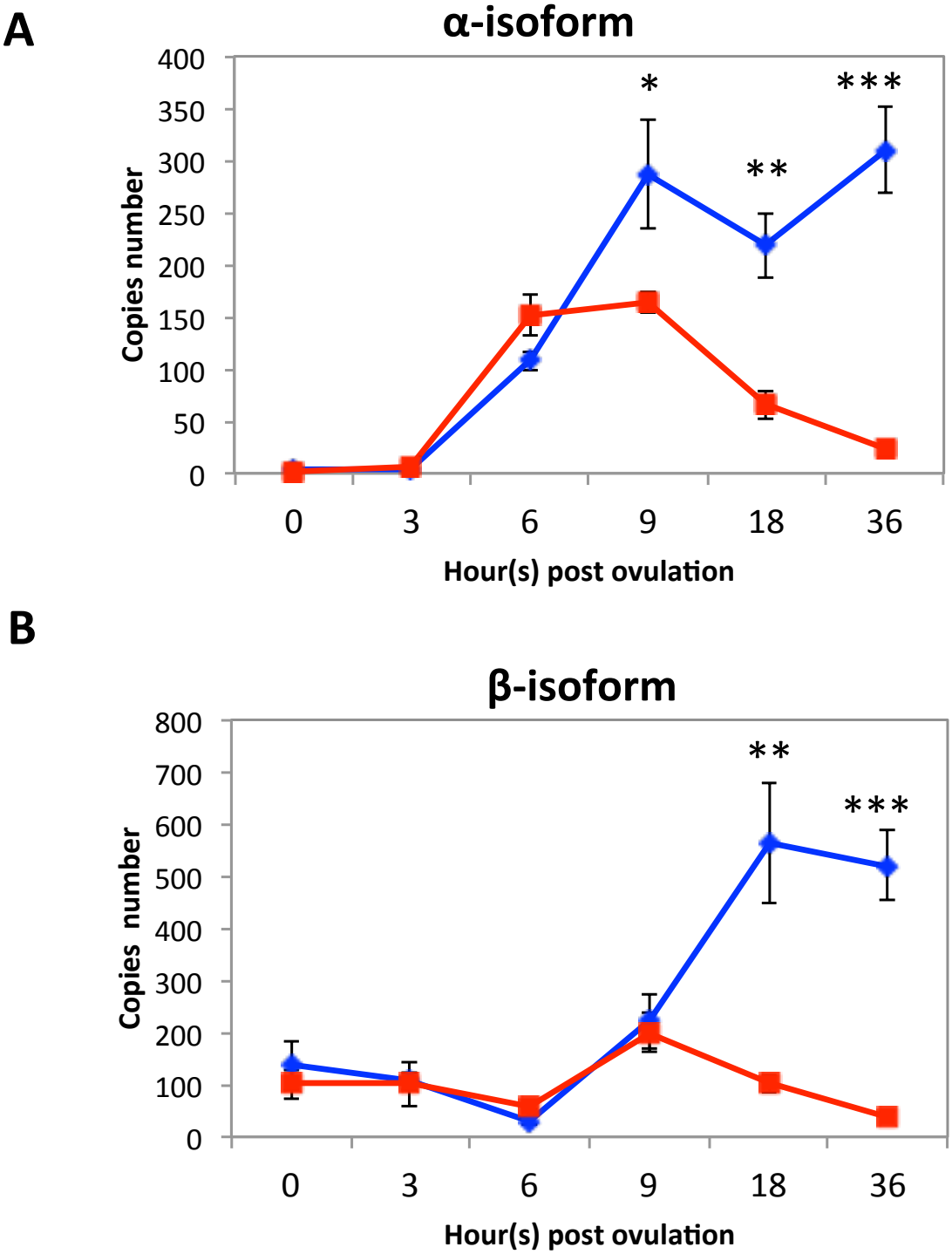

Figure 10: qRT-PCR analyses of (A) α-isoform and (B) β-isoform expression levels. The expression level was measured as copy number of transcripts per egg. Blue line indicates the result from male samples while red indicates the female samples. (Student's t-test; *, $p \leq 0.05$; **, $p \leq 0.01$; ***, $p \leq 0.001$).

2.4 Discussion

To discover the first activation of *Dsx1* during embryogenesis, I examined the temporal changes of two *Dsx1* mRNA transcripts, α- and β-isoform. I simplified both isoforms expression as illustrated in Figure 11. Zygotic transcription of *Dsx1-α* mRNA is largely divided into three phases, 1) initiation: non-specific transcription prior to early gastrula at 6-hpo, 2) up-regulation: male-specific activation during gastrulation from 6 to 9-hpo, and 3) maintenance: constant transcription during late embryogenesis. The *Dsx1-β* male-specific transcription starts three hours later than α-isoform (around 9-hpo) and thereafter become more abundant in male embryos. This finding indicates that *Dsx1-α* promoter might be the first target of JH-signaling genes. Importantly, the time lag between JH action (4 to 10 prior ovulation) and the onset of *Dsx1-α* up-regulation (6 to 9-hpo) suggests that the late response of *Dsx1*. And that it is not the primary JH-responsive gene regulated by JH receptor protein, Methorprene-tolerant (MET) [51], rather there are unknown factor(s) responsible to control the *Dsx1* male-specific expression in gastrula.

Since *Dsx1-α* promoter was discovered as the first target of JH signaling between the two promoters, I speculated that there are transcription factor binding sites in the region upstream of the transcription start site of *Dsx1-α* transcript, where the regulator proteins bind to activate male specific *Dsx1* expression. Further investigation on the *Dsx1-α* promoter sequence analysis might be one of the ways to search for candidate transcription factors that could be involved in *Dsx1* regulation.

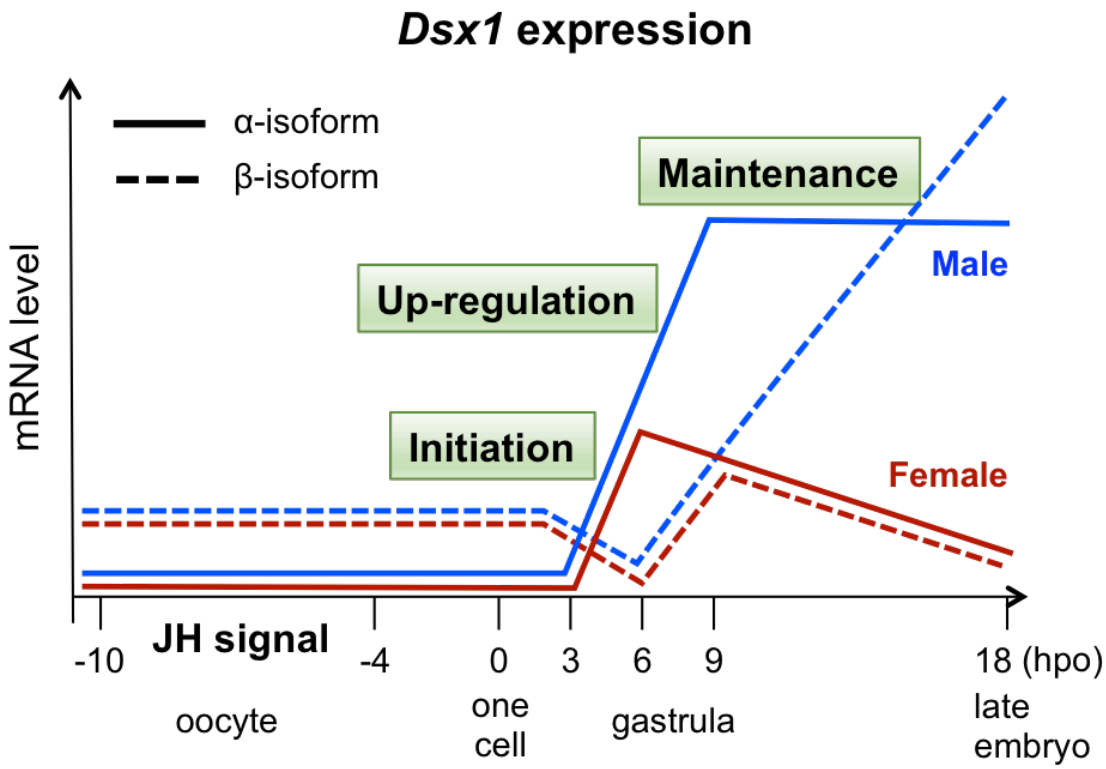

Figure 11: Simplified graph of *Dsx1-α* and *-β* expression during embryogenesis. Schematic representation of the expression patterns of *Dsx1-α* (solid line) and *β* (dash line) mRNAs at various developmental stages of female (red) and male (blue). Four to ten hours before ovulation is the critical period when the developing oocyte is sensitive to JH or JHA for commitment to male trait development. At 0 hpo (hour post oviposition), the embryo is at a one cell stage and only the maternal mRNA of β-isoform is detected both in female and in male. Before embryos become gastrula (initiation phase), non-sex specific *Dsx1-α* transcription starts and maternal *Dsx1-β* transcript is degraded. During gastrulation (up-regulation phase), *Dsx1-α* mRNA increases only in males, and later *Dsx1-β* expression also becomes male-specific. After gastrulation stage (maintenance phase), both isoforms show male-specific expression.

Chapter 3 Transcription factor *Vrille* activates *Dsx1* expression

3.1 Introduction

Great improvement of genome editing techniques such as TALENs and CRISPR/Cas9 system in *D. magna* made targeted sequence knock out and gene fragment knock in possible in this species. Recently, a reporter gene, mCherry red fluorescence protein, was successfully inserted to the downstream of endogenous *Dsx1* promoter in the *Daphnia* genome by Transcription Activator-Like Effector Nuclease (TALEN)-mediate genome editing tool [52]. The red fluorescent expression in this transgenic *Daphnia* is consistent with the putative *Dsx1* expression (Chapter 2) [17]. It was generated from HG-1 transgenic line [50] that made the *Daphnia* also have GFP expression localized in the nucleus of the cell for cell dynamic visualization. This established transgenic strain allow us to easily observe *Dsx1* temporal change expression and spatial localization *in vivo* in a real-time manner by using fluorescence microscopy (Figure 12). With this establishment of *Dsx1* reporter *Daphnia*, it is advantageous to broaden the understanding in *Dsx1* regulation in environmental sex determination.

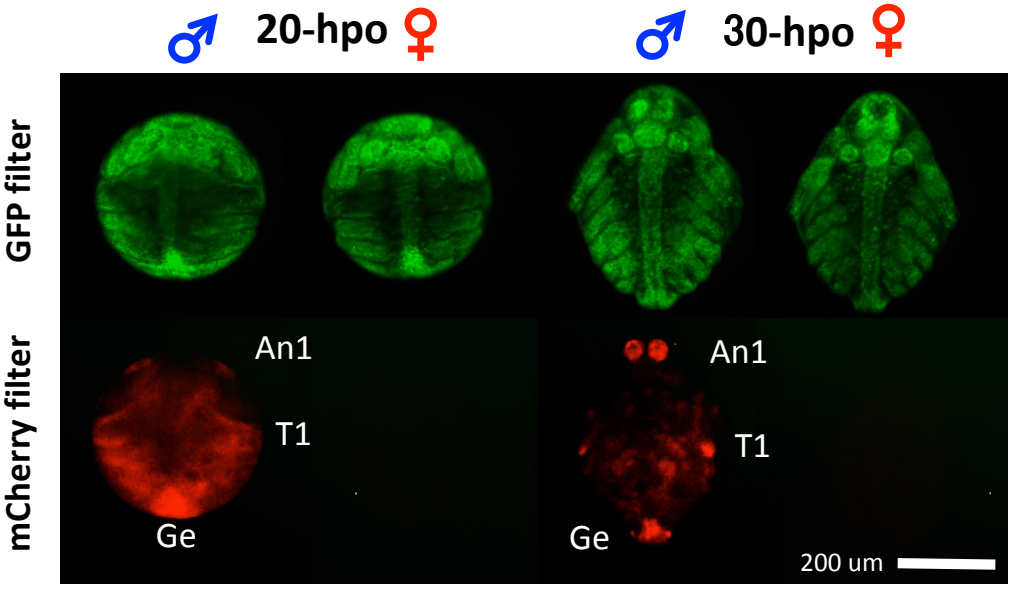

Figure 12: *Dsx1* reporter transgenic *Daphnia*. Male (left) and female (right) embryos of *Dsx1* reporter line at 20 and 40-hpo under GFP and mCherry filters of the fluorescence microscope. Only male daphniids exhibit red mCherry fluorescent A1: first antennae, T1: first thoracic appendage, Ge: genital.

Many studies reported that new sex-determining genes have been identified in sex-determining pathways in several animals as consequence of gene co-option. The co-option occurs when natural selection finds new uses for genes by changes in amino acid coding sequences, changes in spatiotemporal pattern of gene regulation, or both [53]. In the *D. magna* sex determination mechanism, the juvenile hormone (JH) and *Dsx1* were found to be essential. The JH was discovered to drive commitment to male development in oocyte during oogenesis [46] and led to *Dsx1* expression activation, required for controlling male traits development [17]. Considering the possibility of new genes involved in this sex-determining pathway, unknown proteins could be induced by JH signal, which in turn, lead to *Dsx1* up-regulation in *D. magna*. Thus, I searched for potential transcription factor binding sites in the region upstream of the transcription start site of *Dsx1-α* transcript with the aim to identify the transcription factor responsible for male specific up-regulation of *Dsx1-α* mRNA transcription.

Based on the bio-computational analysis, I found a potential enhancer that contains a consensus of the Dsx binding site and an overlapping element for binding of an ortholog of the bZIP transcription factors, *Drosophila* Vrille (Vri) and vertebrate E4BP4/NFIL3. This gene was identified as one of circadian clock genes in many animals including *Daphnia* species [54]. Many studies have reported the involvement of *Vri* and *E4BP4/NFIL3* orthologs in myriad of general development processes such as growth [55], metamorphosis [56], apoptosis [57] and human T cell function [58], both as an activator and a repressor. Furthermore, the *Vri* gene was previously

identified as one of the genes regulated by Dsx protein in male *Drosophila* [59], nevertheless there was no study that reports sex-related function of Vri in any organism. Evolutionary studies have demonstrated that many new sex-determining genes were identified in several animals by gene co-option [60]. These findings signify that there is also a possibility that a new gene can be co-opted in sex-determining pathway and thus *Vri* sex-dimorphic expression is worthy to be studied in order to broaden our understanding in evolution of sex determination mechanism.

In this chapter, after identifying a potential enhancer sequence that contains E4BP4/NFIL3 binding site which overlaps with Dsx binding site, I focused on characterizing the *Vri* gene in *D. magna* by cloning the cDNA and determining its amino acid sequence. I examined *Vri* expression patterns in *D. magna* embryogenesis by qRT-PCR analysis. Then, to study the Vri functions related to sex-determining cascade, I performed functional analyses: 1) the RNAi-mediated knock down and 2) overexpression by mRNA delivery. In addition, I conducted experiment for disruption of Vri binding site on *Daphnia* genome by Cas9 system to examine the function of the sequence concerning the *Dsx1* activation.

3.2 Materials and methods

3.2.1 *Daphnia* strain and culture condition

The *D. magna* (NIES clone) was obtained from the National Institute for Environmental Studies (NIES; Tsukuba, Japan) and cultured under the same laboratory condition mentioned in Chapter 2 (see 2.2.1 *Daphnia* strain and culture condition). The male dapniids were obtained with the same method described in Chapter 2 (see 2.2.2 Artificial male production by JH analog exposure).

3.2.2 Finding potential binding sites by bio-computational

Elements similar to known TF binding sites were searched with TFBIND program [61] using the transcription factor database TRANSFAC R.3.4 to obtain the binding site consensus. Next, because *Dsx1* up-regulation maintenance phase suggests positive feedback regulation of this, I also investigated the binding site consensus of *Dr. melanogaster* Dsx. Then, the locations of hypothetical TF binding sites were searched on genome sequence using RSAT matrix-scan quick and simple method (http://rsat01.biologie.ens.fr/rsa-tools/matrix-scan-quick_form.cgi) [62]. Sequence of *Dsx1-α* promoter from *D. magna* was inserted in the blank space in 'Sequences' table, then consensus sequence of TF binding sites in matrix form in 'Matrix' table. To check whether the binding site sequences are conserved or not in *Daphnia* species, the same computation identification was performed on *Dsx1* gene of *D. pulex.*

3.2.3 Cloning and sequencing

The *Vri* cDNA sequence was amplified from *Daphnia* by 5′ and 3′ rapid amplification of cDNA ends (RACE) methods with a GeneRacer Kit (Invitrogen) and a SMARTer RACE cDNA Amplification Kit (Clontech Laboratories Inc.; Wisconsin, USA), respectively. The primer sequences used for cDNA fragment amplification were as follows: Vri 5′ RACE gene specific primer (5′-TGTTGCTGCCGATTGCGCTGACACTG-3′); Vri 5′ RACE nested primer (5′-CTCGGTCGAACGCCGTCCGCTACTG-3′); Vri 3′ RACE gene specific primer (5′-CCGGCCGTGTACTGCCGCTCAAACTA-3′); and Vri 3′ RACE gene nested primer (GGCTGCCGCTGTTCTGCTGACACTCA-3′). The PCR products excised from an agarose gel after electrophoresis were purified and were cloned into a TOPO vector (Invitrogen) for sequencing analysis. The sequencing reaction was performed using a

BigDye Terminator Cycle Sequencing Kit (PE Applied Biosystems, California, USA) and the DNA sequence were analyzed using the BLAST program

3.2.4 Phylogenic analysis

Amino acid sequences of *Vri* family genes were retrieved from the NCBI database (http://www.ncbi.nlm.nih.gov/) as shown in Table 2; and the conserved sequences, the bZIP domain of each protein, were used to construct the phylogenetic tree. Multiple sequence alignments of the amino acid sequences were constructed using the ClustalW [63] in MEGA program [64]. The following settings were used for the analysis: pairwise alignment parameter: gap opening penalty = 6.00, gap extension penalty = 0.21, and identity protein weight; matrix multiple alignment parameter: gap opening penalty = 10.00, gap extension penalty = 10.00, gap extension penalty = 0.24, delay divergent cut-off = 30%, and gap separation distance = 4. The phylogenetic reconstruction was performed using the p-distance algorithm and the neighbor-joining method was implemented in MEGA.

Table 2: Accession numbers of *Vrille* ortholog genes used in this study.

Common name	Scientific name	Gene name (Definition in NCBI)	Accession no.
Water flea	*Daphnia magna*	Vrille	This work (LC23014)
Fruit fly	*Drosophila melanogaster*	Vrille (isoform A)	NP_477191.1
Sand fly	*Lutzomyia longipalpis*	Vrille	AKN63485.1
Florida carpenter ant	*Camponotus floridanus*	NFIL-3	EFN67066.1
Black garden ant	*Lasius niger*	NFIL-3	KMQ97212.1
Dampwood termite	*Zootermopsis nevadensis*	NFIL-3	KDR6467.1
Body louse	*Pediculus humanus corporis*	NFIL3/E4BP4	XP_00245535.1

Red flour beetle	*Tribolium castaneum*	Vrille	EFA11543.1
Monarch butterfly	*Danaus plexippus*	Vrille	AAT8641.1
Australian ghostshark	*Callorhincus milli*	E4BP4	AFK11403.1
Zebrafish	*Danio rerio*	NFIL3	NM_001004120.2
Mouse	*Mus musculus*	NFIL3	NM_017373.3
Human	*Homo sapiens*	E4BP4	X64318

3.2.5 Quantitative real-time PCR

The cDNA samples of female and male embryos at 0, 3, 6, 18 and 36-hpo (prepared in Chapter 2 experiment) were used in this qRT-PCR analysis. qPCR was conducted with the SYBR GreenER qPCR Supermix Universal (Invitrogen) using the Mx3005P real time (RT)-PCR system (Agilent Technologies). The *Vri* expression was measured using the primer pair as follow: Forward (5'-CATCCACATCACCAGCATCAC-3') and Reverse (5'-CGCGACAACGACCAATCTC-3') and arbitrary copy number of dilution series of standard samples. The *Vri* mRNA expression was normalized with the ribosomal protein L32 expression level.

For *Vri* and *Dsx1* expression validation in knock down (3.2.5 Gene knockdown by RNAi) and overexpression experiment (3.2.6 Gene overexpression by mRNAs delivery), injected embryos were collected after appropriate incubation time for each experiment. After extracting the total RNA and synthesizing cDNA for each sample, qPCR was conducted with the SYBR GreenER qPCR Supermix Universal (Invitrogen) using the Mx3005P (RT)-PCR system (Agilent). Changes of *Vri* expression levels were quantitated and were normalized with the ribosomal protein *L32* expression level. For *Dsx1* expression levels in the *Vri* knock down using

Vri_siRNA_1 and overexpression, the mRNA transcripts were quantitated and were normalized with geometric mean of four reference genes, namely ribosomal protein *L32* and *L8* gene, *β-actine* gene and *Cyclophilin* gene [65], as described previously for more accurate analysis [66]. The primer sets used in this experiment are listed in Table 3 below.

Table 3: The primer pairs used to quantitate specific amplification in qRT-PCR assay.

Gene name	Primer sequence (5′−3′)
Vri	Forward: CATCCACATCACCAGCATCAC Reverse: CGCGACAACGACCAATCTC
Dsx1	Forward: CCATTCATCATTACCAAATCCCTTC Reverse: CCATTCATCATTACCAAATCCCTTC
L32	Forward: GACCAAAGGGTATTGACAACAGA Reverse: CCAACTTTTGGCATAAGGTACTG
L8	Forward: GGTACTATTGTTTGCAATGTTGAGG Reverse: GTCTTCTTGGTATCGGTATTGTGAC
β-actin	Forward: TGTCTCTCTCTGTCCACGCTTTTC Reverse: TGTTGGGTGTCCTTGTGTGTC
Cyclophilin	Forward: GACTTTCCACCAGTGCCATT Reverse: AACTTTCCATCGCATCATCC

3.2.6 Gene knockdown by RNAi

The RNAi method [36] was performed by microinjection of 100 μM siRNAs for gene silencing, targeting *Vri* gene sequence of the following: Vri_siRNA_1 (5′-GCAUCCACAUCACCAGCAU-3′) and Vri_siRNA_2 (5′-GGCAGCAACAACGGCAACAU-3′). A random sequence of control siRNA (5′-GGUUAAGCCGCCUCACAUTT-3′) that do not affect *Daphnia* development [67] was used as a negative control. The siRNA oligonucleotides were dissolved in DNase/RNase-free water (Life Technologies Inc).

Microinjection was performed as previously described [36]. Eggs were obtained from adult *Daphnia* (*Dsx1* reporter line) at 2–3 weeks of age, directly after

ovulation and placed in ice-cold M4 medium with 80 mM sucrose. The specific RNAs for each experiment were mixed with either Alexa Fluor 568 dye (Life technologies Inc.) or Lucifer Yellow dye (Life technologies Inc.) with final concentrations of 0.01 μM and 1 μM respectively, as an injection marker. Microinjection was performed on ice and the injected eggs were incubated in a 96-well plate at 23 °C for the appropriate time.

Phenotypes of injected eggs at certain developmental stages were carefully observed under the microscope. The *Vri* and *Dsx1* expressions in siRNAs injected embryos were validated by qRT-PCR analysis (see 3.2.4 Quantitative real-time PCR).

3.2.7 Gene overexpression by mRNAs delivery

Chimeric *Vri* cDNA harboring the 5′ UTR and 3′ of *Xenopus laevis β-globin* gene was designed and subcloned downstream the T3 promoter on the pRN3 vector [68] as a template for mRNA synthesis. The *Vri* CDS of this plasmid was replaced with *GFP* CDS fused with *Minos* transposase for the template of control mRNA, to investigate the effects of *β-globin* UTRs on mRNA stability and/or translation efficiency. These plasmids were linearized by BsaAI restriction enzyme, purified through phenol/chloroform extraction. *In vitro* transcription by T3 RNA polymerase and poly-A tail addition were performed according to the manufacturers' protocols of the commercial kits mMessage mMachine T3 kit (Life Technologies Inc.) and Poly(A) Tailing kit (Life Technologies Inc.), respectively. The synthesized mRNAs, as illustrated in Figure 14, were column purified using RNeasy Mini Kit (Qiagen), followed by phenol/chloroform extraction, ethanol precipitation, and dissolution in DNse/RNase-free water. The synthesized mRNAs were then prepared in several

concentrations and mixed with dye for injection marker mentioned in above section (3.2.5 Gene knockdown by RNAi).

Microinjection was performed into female eggs both in wild-type and *Dsx1* reporter strain. Phenotypes of injected eggs at certain developmental stages were carefully observed under the microscope. The *Vri* and *Dsx1* expressions in mRNAs-injected embryos were validated by qRT-PCR analysis (see 3.2.4 Quantitative real-time PCR).

Figure 13: Capped, polyadenylated mRNAs structure constructed for overexpression expression.

3.2.8 Selection of gRNA target sequences by ZiFiT software

The target sequences of gRNA were determined using ZiFiT software from the website (http://zifit.partners.org/ZiFiT/ChoiceMenu.aspx) [69]. After choosing the CRISPR/Cas Nucleases option, the sequence of *Dsx1-α* was inserted in blank space, the length of target site was set to 20 nt, and the T7 promoter was selected. The result listed several identified target sites for the subsequent Cas9 system experiment.

3.2.9 Cloning-free method for gRNA *in vitro* synthesis

For the syntheses of gRNAs, the templates were prepared by cloning free method [70]. The sense synthetic oligo contains three main parts: a T7 promoter (shown in bold), a variable targeting sequence (N_{18}) and the first 20 nt of the Cas9 binding scaffold sequence. The full sequence is as follows: (5′-

GAAA**TTAATACGACTCACTATAGG**NNNNNNNNNNNNNNNNNNGTTTTA GAGCTAGAAATAGC-3′). While the anti-sense synthetic oligo contains 80 nt full sequence of the Cas9 protein binding scaffold where the underlined nucleotides denote the complementary sequence between two oligo sequences: (5′-AAAA GCACCGACTCGGTGCCACTTTTTCAAGTTGATAACGGACTAGCCTTATTTT AACTTGCTATTTCTAGCTCTAAAAC-3′). The PCR reaction (Table 4) was performed with PrimeSTAR polymerase (Takara Bio; Shiga, Japan) with the cycle condition shown in Table 5.

Table 4: Reaction mixture for PCR using PrimeSTAR polymerase.

Reagent	Volume
5X PrimeSTAR Buffer	10 µL
2.5 mM dNTP mix	4 µL
Sense, antisense oligos mix (100 µM each)	1 µL
PrimSTAR polymerase	1 µL
MilliQ water	34 µL
Total	50 µL

Table 5: The PCR cycle condition.

Temperature	Duration	Cycle no.
98°C	5 min	1
98°C	10 sec	30
55°C	30 sec	
68°C	15 sec	
78°C	7 min	1

After purification by phenol/chloroform extraction, the DNA fragments were used as templates for *in vitro* transcription using MEGAscript T7 kit (Life Technologies Inc.), followed by column purification with mini Quick Spin RNA gel columns (Roche diagnostics GmbH; Mannheim, Germany), phenol/chloroform

extraction, ethanol precipitation, and dissolution in DNase/RNase-free water. The amount of purified RNA was measured with Nanodrop 2000.

3.2.10 Cas9 protein synthesis in *E. coli* cells

A modified pCold-based vector with Ampicillin resistance and containing sequence encoding for Cas9 protein with N-terminal 10x His-tag and C-terminal Nuclear Localization Signal (NLS) was a gift from Dr. Asako Sugimoto, previously generated in Cas9 research of *C. elegans* [71]. The plasmid construct, which also contained a cold-inducible promoter (Takara Bio), was transformed into the *E. coli* strain BL21(DE3) for Cas9 protein expression. Successful transformation colonies were screened by colony PCR using the following primer sequence: Cas9 forward (5′-ACAAATAGCGTCGGATGG-3′) and reverse (5′-CGCTTTAGCATCTACTCCAC-3′).

A single colony was inoculated into 2 mL of LB broth with ampicillin (100 mg/mL final concentration) and were incubated at 37°C as the first pre-culture. After 8 h incubation (OD_{590} = 1.5), 200 µL of the first pre-culture was diluted into 50 mL of LB containing ampicillin medium as the second pre-culture and divided into 8 tubes of 5 mL culture medium in each tube. The second pre-cultures were incubated overnight at 37°C (OD_{590} = 1.6-1.7). Next, each of the second pre-cultures was diluted into 500 mL of 2x YT medium containing ampicillin (100 mg/mL final concentration) in 1 L flask (total culture = 4 L). The cells were cultured until the OD_{590} reached around 0.5 by incubating at 37°C for 2.5 h. Then, the Cas9 protein expression was induced by shifting the temperature to 16°C followed by the addition of 250 µL of 1 M IPTG (0.5 mM final concentration). After 24 h incubation at 16°C and 90 rpm rotation, cells were collected from 1 L culture each by centrifugation at 4000 rpm for

10 min (GRX-200 High Speed Refrigerated Centrifuge, TOMY). The pellets were washed with H buffer (20 mM HEPES pH 7.5, 500 mM NaCl, 1 mM TCEP) two times before freezing with liquid nitrogen. The cell pellets were stored at -80°C.

3.2.11 Cas9 extraction and purification

The thawed cell pellet from 1 L culture was suspended in 20 mL H buffer (20 mM HEPES pH 7.5, 500 mM NaCl, 1 mM TCEP 10% glycerol) and two tablets of protein inhibitor cocktail (Roche diagnostics GmbH) were added into the suspended cells. Glycerol was added to the buffer solution to increase protein solubility and stability during protein extraction and then purification was performed. The cells were divided into 10 mL each in 50 mL tubes and placed on ice before sonication. The cells were disrupted through sonication using the following parameters: 50% duty cycle, output 4, 30 sec. Sonication was repeated for 15 min or until the liquid become translucent, as shown in Figure 14. Lysed cells were centrifuged at 4°C, 150,000 rpm for 30 min and then supernatant was collected and filtered with Millipore (size 0.45 μm) before performing column chromatography.

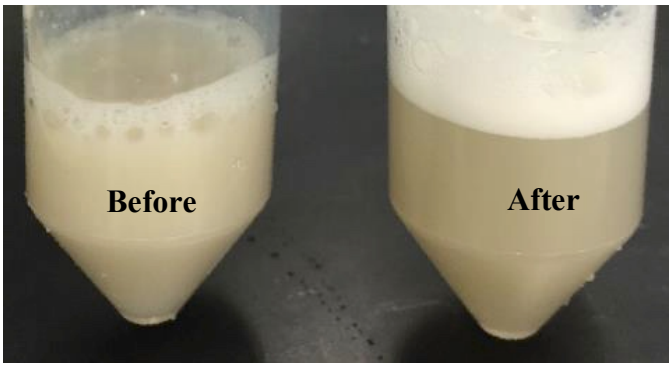

Figure 14: Suspended cell pellet before sonication (Before) and after the sonication completed (After).

The column was set up on a suitable rack and 500 µL of Ni-NTA Superflow resin (Qiagen) was added into the column. After the resin settled down, the resin was equilibrated with Equilibrium buffer (Table 6) and the filtered supernatant sample added with 10 mM imidazole was loaded and flow through was collected. The resin was washed with 5 mL of Wash buffers #1 and #2. Each wash was repeated four times. The bound protein was eluted by stepwise elution (50 to 350 mM imidazole) using Elution buffers #1, #2, #3, and #4. Each elution was repeated four times as fractions were collected and ran for SDS-PAGE.

Table 6: The following reagents were used for nickel column chromatography experiment. H buffer (20 mM HEPES pH 7.5, 500 mM NaCl, 1 mM TCEP, 10% glycerol).

Reagent	Concentration (final)		Volume
	H-Buffer	Imidazole	
Equilibrium		10 mM	5 mL
Wash 1		20 mM	20 mL
Wash 2		25 mM	20 mL
Elution 1	1 X	50 mM	4 mL
Elution 2		150 mM	4 mL
Elution 3		250 mM	4 mL
Elution 4		350 mM	4 mL

The eluted samples were concentrated by centrifugal ultrafiltration according to the manufacturer's protocol (Amicon Ultra-0.5 Centrifugal Filter, Merck Millipore). The buffer was then changed to 1 M NaCl concentration for second column chromatography purification to remove DNA contamination. The second column chromatography was performed under the same conditions described above except for the NaCl concentration (1 M). Elution was performed using 0.5 mL of 50 and 150 mM imidazole solution. Each elution was repeated six times (Table 7). The

eluted protein was analyzed by SDS-PAGE to confirm its purity and was dialyzed against the storage buffer (20 M HEPES pH 7.5, 150 mM KCl, 1 mM TCEP, 10% glycerol). Finally, the sample was concentrated by centrifugal ultrafiltration to have a final volume of 200 µL, was frozen with liquid nitrogen and was stored at -80°C.

Table 7: The following reagents were prepared for second nickel column chromatography experiment. H buffer (20 mM HEPES pH 7.5, 1 M NaCl, 1 mM TCEP, 10% glycerol).

Reagent	Concentration (final)		Volume
	H-Buffer	Imidazole	
Equilibrium		10 mM	5 mL
Wash 1		20 mM	20 mL
Wash 2	1 X	25 mM	20 mL
Elution 1		50 mM	3 mL
Elution 2		150 mM	3 mL

3.2.12 Cas9 protein *in vitro* cleavage assay

To examine the ability of designed gRNAs and Cas9 protein in executing double strand breaks, 300 ng of the plasmid harboring the target sequence was incubated with 1 µM Cas9 protein and 2 µM gRNA at 37°C for 1 hour in reaction buffer that contains 20 mM HEPES (pH 7.5) 150 mM KCl, 0.5 mM DTT, 0.1 mM TCEP and 10 mM $MgCl_2$. To stop the reaction, 0.5 M EDTA was added to the reaction mixture and the cleavage of the plasmid by Cas9 and gRNA was observed by running the gel electrophoresis.

3.2.13 Targeted mutagenesis by CRISPR/Cas9 system and genotyping

The *in vitro* synthesized RNA with Cas9 protein was mixed and were incubated for 5 min at 37°C to make gRNA-Cas9 complexes [71]. To prepare the

injection solutions, the gRNA-Cas9 complexes were mixed with either Alexa Fluor 568 dye (Life technologies Inc.) or Lucifer Yellow dye (Life technologies Inc.) with final concentrations of 0.01 μM and 1 μM respectively, to serve as injection marker. The microinjection was performed on ice using wild-type and transgenic *D. magna* eggs, as described previously [36]. The eggs collected immediately after ovulation were placed in ice-cold M4 medium containing 80 mM sucrose to prevent the egg membrane from hardening before injection and the injected eggs were incubated in a 96-well plate at 23°C for the appropriate time. Phenotypes of injected eggs at certain developmental stages were carefully observed under the fluorescence microscope.

To characterize the somatic mutation on the Vri binding site generated by Cas9 protein, target loci were amplified by PCR from genomic DNA isolated from each injected egg. To extract the genomic DNA, injected embryos were homogenized individually in 90 μL of 50 mM NaOH with zirconia beads. The sample was heated at 95°C for 10 min, followed by a neutralization step through the addition of 10 μL of 1 M Tris-HCl (pH 7.5). The sample was centrifuged at 13,000 g for 5 min and the supernatant was used as PCR template. PCR was performed with HS Ex Taq polymerase (Takara Bio) using a primer pair designed as follows: Vri-bs forward (5′-GATGTCACGAAATCTGAGGTC-3′) and Vri-bs reverse (5′-GATCTAAACACCTTGGCGTAAC-3′), which amplified 214 bp including the enhancer region. The PCR products were analyzed using native PAGE gel electrophoresis. To characterize the heritable mutagenesis, injected *Daphnia* were cultured separately until they produced offspring. The offspring were pooled (around 8-10 daphniids) and genomic DNA extraction and genomic PCR were performed as mentioned above.

3.3 Results

3.2.1 E4BP4 binding site candidate on the *Dsx1* promoter

To find candidate transcription factors (TFs) that activate *Dsx1* male-specific expression from 6-hpo, I analyzed a sequence with 7,899 bp upstream the transcription start site of *Dsx1-α* mRNA. Of the thousands of potential TF binding sites found in this study, I found an element similar to the fat body enhancer of the *Drosophila* yolk protein gene 1 that contains a Dsx binding site and overlapping bZIP protein binding site, which regulated tissue- and sex-specific expression [72]. Thereafter, I searched for the consensus sequence of bZIP protein E4BP4 binding site from the transcription factor database TRANSFAC R.3.4 and consensus sequence for binding sites of *Dr. melanogaster* Dsx with TFBIND program. Interestingly, an element similar to the *Drosophila* fat body enhancer was found on the *D. magna Dsx1* promoter sequence, illustrated in Figure 15A. In *Daphnia* species, the binding site for bZIP protein matched the binding site consensus of mammalian E4BP4/NFIL3. To investigate the conservation of the position and sequence of this element, I performed analysis on the *Dsx1* promoter of *D. pulex.* The same element was also found in *D. pulex* (Figure 15B), and thus, I annotated this element as a candidate enhancer sequence of *Dsx1*.

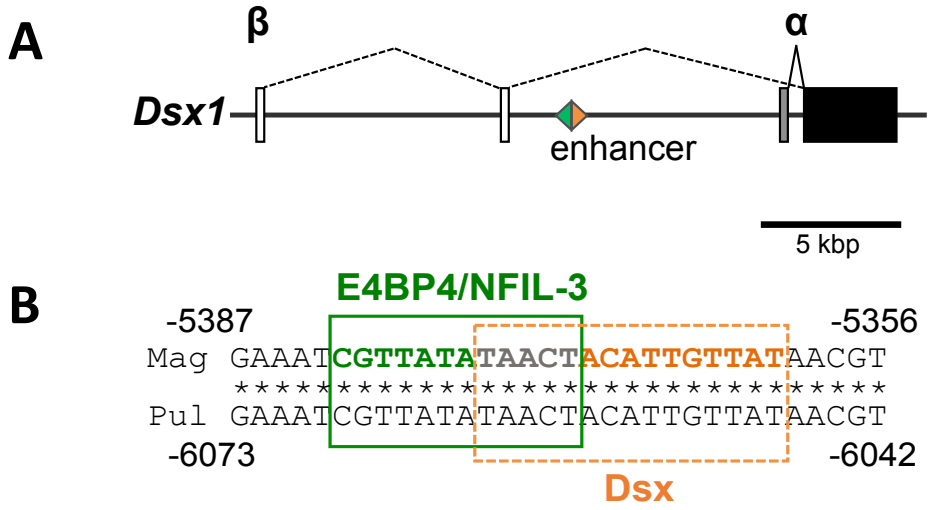

Figure 15: Candidate Vri binding site of the enhancer element on *Dsx1* promoter. (A) Position of the enhancer sequence on *D. magna* Dsx1 locus. (B) Sequence of the enhancer that contains a bZIP protein binding site (green box) overlapped with a Dsx binding site (orange box). This sequence is conserved between *D. magna* (Mag) and *D. pulex* (Pul).

3.2.2 Characterization of *Vri* gene in *D. magna*

To investigate the existence of an E4BP4/NFIL3 ortholog in *D. magna,* I performed a BLAST search using an amino acid sequence of the human E4BP4/NFIL3 against the *D. magna* genome database, and found one ortholog that shows high homology in the bZIP domain to E4BP4/NFIL3 protein. To determine the full-length of *Vri* cDNA in *D. magna,* I performed 5′ and 3′ RACE reactions and obtained a single 2,394 bp nucleotide sequence that encodes for 797 amino acids (Figure 16). No sex-specific transcript was found from the RACE experiments. The deduced amino acid sequence obtained from the cDNA sequence was compared to the protein sequence of Vri ortholog of other animals. The multiple alignments revealed that *D. magna Vri* protein contains the conserved basic leucine zipper (bZIP) domain (Figure 17A). The domain consists a basic region that mediates sequence

specific DNA binding properties and the leucine zipper that is required to dimerize two DNA binding region.

```
  1 ATGGTGACTGAGAATCATTCACATCAGCATTCTCAGCAGATCCAGCACCAGCACGCACAGCGCAACGGGCGCTATTTGCAGCAGACGCCA 90
  1  M  V  T  E  N  H  S  H  Q  H  S  Q  Q  I  Q  H  Q  H  A  Q  R  N  G  R  Y  L  Q  Q  T  P  30

 91 TCACACCATCAAGACGCTCACGAGGAACGCGCTATGGTAATTCAACAGCACCCGGCTTCCATTCCGATGTCTGGCGAGCCGCCACGCAAC 180
 31  S  H  H  Q  D  A  H  E  E  R  A  M  V  I  Q  Q  H  P  A  S  I  P  M  S  G  E  P  P  R  N  60

181 GGTTCGTCTGCAAACTCCCAGCAGCACGCCAATAGCGTTTCGCATCTCAACGCCGCCATGGAGGAAAGAGCGGTGGCTCTTCAAGCCGCG 270
 61  G  S  S  A  N  S  Q  Q  H  A  N  S  V  S  H  L  N  A  A  M  E  E  R  A  V  A  L  Q  A  A  90

271 GCCGCCGTTGCCGCCGCCGTCACCGGATTTAATTCCGCCAATTTGTCGGTCGGTATGGACTTGTCCGGTCTCGTCCCAGTAGGTCTCATG 360
 91  A  A  V  A  A  A  A  V  T  G  F  N  S  A  N  L  S  V  G  M  D  L  S  G  L  V  P  V  G  L  M  120

361 AATCACTTGCAGCACAACAATGAGCAGCAGCAACATAACTCGCCAAACAACAACAACAACAACAGCAACAGCAACCAGCAGAGGAAA 450
121  N  H  L  Q  H  N  N  E  Q  Q  Q  H  N  S  P  N  N  N  N  N  N  N  S  N  S  N  Q  Q  R  K  150

451 CAGCGCGAGTTCATTCCGGATAATAAAAAAGACGACAGCTACTGGGATCGGCGGAGGCGCAACAACGAGGCGGCTAAACGTTCACGCGAG 540
151  Q  R  E  F  I  P  D  N  K  K  D  D  S  Y  W  D  R  R  R  R  N  N  E  A  A  K  R  S  R  E  180

541 AAGCGTCGTCTCAACGACATGGTACTGGAGAGTCGCGTCCTGGAATTGACCAAGGATAATCACATCCTTCGCGCCCAGCTATCGGCCGTT 630
181  K  R  R  L  N  D  M  V  L  E  S  R  V  L  E  L  T  K  D  N  H  I  L  R  A  Q  L  S  A  V  210

631 CGCGACAAATACGGAATCAACCCAGATGCTCTCGTTTCGATTGACCAAGTTCTGGCCACTTTGCCGTCTCCTGATCAGGTCCTTAGTCTA 720
211  R  D  K  Y  G  I  N  P  D  A  L  V  S  I  D  Q  V  L  A  T  L  P  S  P  D  Q  V  L  S  L  240

721 CCACGCCCTCGTTCTCGCCTCCTGTCCGGCATGAGTCCGTCTTTGGGTTCCGGTCGCGGTGGCGGATCGGTCTCGCCGTCGCCCAGCAAT 810
241  P  R  P  R  S  R  L  L  S  G  M  S  P  S  L  G  S  G  R  G  G  G  S  V  S  P  S  P  S  N  270

811 CGCAGCCTCTCACCGCCCATGTCACAGCAGTCACAAATGCATTCGCACCAGCCACATCACCAGCCGAATCAACATCAGCAACAGAGGCAG 900
271  R  S  L  S  P  P  M  S  Q  Q  S  Q  M  H  S  H  Q  P  H  H  Q  P  N  Q  H  Q  Q  Q  R  Q  300

901 TCCGTTCTGATGTCGATGAACCGGGCACACAGGTCTCCTAGTCCGGTAGCGGTAGGACCAGGACAGGGTTCGGGTTCGGCATCTATGCAG 990
301  S  V  L  M  S  M  N  R  A  H  R  S  P  S  P  V  A  V  G  P  G  Q  G  S  G  S  A  S  M  Q  330

991 CAGCAGCATTCGTACGCCAGCGGCCATCACCATCAGCAGCATCACCAGCACGGCTTTCGCTATCAACCTGCCGGAGAGTTGGCTGGAACG 1080
331  Q  Q  H  S  Y  A  S  G  H  H  H  Q  Q  H  H  Q  H  G  F  R  Y  Q  P  A  G  E  L  A  G  T  360

1081 GGCGGCAATCACGCGTATCAGCATCAGCAGCAGCATCAACATGCACAGCATTCTCAGCCAATTAAAACTCAACAAAGAGTACTAGAGAGG 1170
361  G  G  N  H  A  Y  Q  H  Q  Q  Q  H  Q  H  A  Q  H  S  Q  P  I  K  T  Q  Q  R  V  L  E  R  390

1171 TCTCTGCCGCCTCTTCCAGCACTGACTCCTGTGCCCGTCATTTCTCCCAATCACCAGCTGGAGATGGGAGGGTCATCAGTGGAAGGAGCT 1260
391  S  L  P  P  L  P  A  L  T  P  V  P  V  I  S  P  N  H  Q  L  E  M  G  G  S  S  V  E  G  A  420

1261 CACCAGCACCCTCTTCCAGGAGCGGATAGGGTTGGTTCGAATGGCAACGTAGCACCAGTTGCGGCTTTCTTCGACCTGTGTTCATCGTCA 1350
421  H  Q  H  P  L  P  G  A  D  R  V  G  S  N  G  N  V  A  P  V  A  A  F  F  D  L  C  S  S  S  450

1351 AGCAGCAGCAGTTCGAGCAGTTCTAGCAGCCACCCGGGCTCAAGTAGCGGTGACGACGGAAGCCATTCTCCGATTGATCCGGCCGTGGCA 1440
451  S  S  S  S  S  S  S  S  S  S  S  H  P  G  S  S  S  G  D  D  G  S  H  S  P  I  D  P  A  V  A  480

1441 GCCGGCCGTGTACTGCCGCTCAAACTACGCCACAAAACCCACCTGGGTGAAAGGGACGTAGCGGCCGCCACCGCTTCGGCTGCCGCTGTT 1530
481  A  G  R  V  L  P  L  K  L  R  H  K  T  H  L  G  E  R  D  V  A  A  A  T  A  S  A  A  A  V  510

1531 CTGCTGACACTCAACGAGATCAAACACGAGCCGGAAGGGATCGAAGACAGTCCTTCGGCAGTCGACTCGGCAGTTGACAGCGTTTCTGCT 1620
511  L  L  T  L  N  E  I  K  H  E  P  E  G  I  E  D  S  P  S  A  V  D  S  A  V  D  S  V  S  A  540

1621 GAAATGAACAACAACAGTATGAGTGACCATCACAGCCAAGTTCATCACCATGGCCTGCATCACCATGCCAACCACCTCAGCCACCACCAT 1710
541  E  M  N  N  N  S  M  S  D  H  H  S  Q  V  H  H  H  G  L  H  H  H  A  N  H  L  S  H  H  H  570

1711 CATCAACAACAGCCACAACAGCAATCGCACCAGAACGCCCAACAACATCAACAACTGCAGCATCCACATCACCAGCATCACCTAAACAGT 1800
571  H  Q  Q  Q  P  Q  Q  Q  S  H  Q  N  A  Q  Q  H  Q  Q  L  Q  H  P  H  H  Q  H  H  L  N  S  600

1801 AGCGGACGGCGTTCGACCGAGTCGAGCGATGATCGCGATTCGGGAATCTCATCAGGTGGAGATTGGTCGTTGTCGCGCAGTTCGTCACGG 1890
601  S  G  R  R  S  T  E  S  S  D  D  R  D  S  G  I  S  S  G  G  D  W  S  L  S  R  S  S  S  R  630

1891 TTTAGTAGCAGCAGCAGTGGCAGCAATGCCAGTGTCAGCGCAATCGGCAGCAACAACGGCAACATTGTTGGCCATTTGTACCACGCACAT 1980
631  F  S  S  S  S  S  S  G  S  N  A  S  V  S  A  I  G  S  N  N  G  N  I  V  G  H  L  Y  H  A  H  660

1981 CATCAACATCAGCCAGCGTCGAAGAGAATGAGGATGAGCCCCAATTCTCCTGTTGTGGACCACCAACATCAAAATGAGCACCCGCACATG 2070
661  H  Q  H  Q  P  A  S  K  R  M  R  M  S  P  N  S  P  V  V  D  H  Q  H  Q  N  E  H  P  H  M  690

2071 CAACATCAGCAGGCGGTGCAGAGGCGCTTCACCGCTGCCCGAGCTAGCCAACAACAACAGCAACAAGTGATGAACAATCAAGAGGTAGAC 2160
691  Q  H  Q  Q  A  V  Q  R  R  F  T  A  A  R  A  S  Q  Q  Q  Q  Q  Q  V  M  N  N  Q  E  V  D  720

2161 GAGGAGGAGAATGACCCGGCTTCTGGCATCGTTCATGAAAGATTGGTATTGGTCGGTGGCAACGAGTCTTCGGATGAGAATAACGACGAA 2250
721  E  E  E  N  D  P  A  S  G  I  V  H  E  R  L  V  L  V  G  G  N  E  S  S  D  E  N  N  D  E  750

2251 CTTCGTTCCCATATTGCTCGATTGGCCTCCGAATTGGAGTCTCTCAAAACGATGATGCTCGGTGGTGGCGGCACCTCGGCAGCTGGATCG 2340
751  L  R  S  H  I  A  R  L  A  S  E  L  E  S  L  K  T  M  M  L  G  G  G  G  T  S  A  A  G  S  780
```

```
2341 GCGTCGACCATTCGGAACTGTAAAAGCAGCAGTACCAACTTTCGGCTTCATTGA 2394
 781  A  S  T  I  R  N  C  K  S  S  S  T  N  F  R  L  H  *  798
```

Figure 16: Nucleotide and deduced amino acid sequences of *Vri* from *D. magna.* Black shaded amino acids indicate the putative bZIP domain and grey shaded nucleotide is the sequence that was removed for *Vri* overexpression experiment. The underlined sequences are the target sites for Vri_siRNA_1 and Vri_siRNA_2 accordingly.

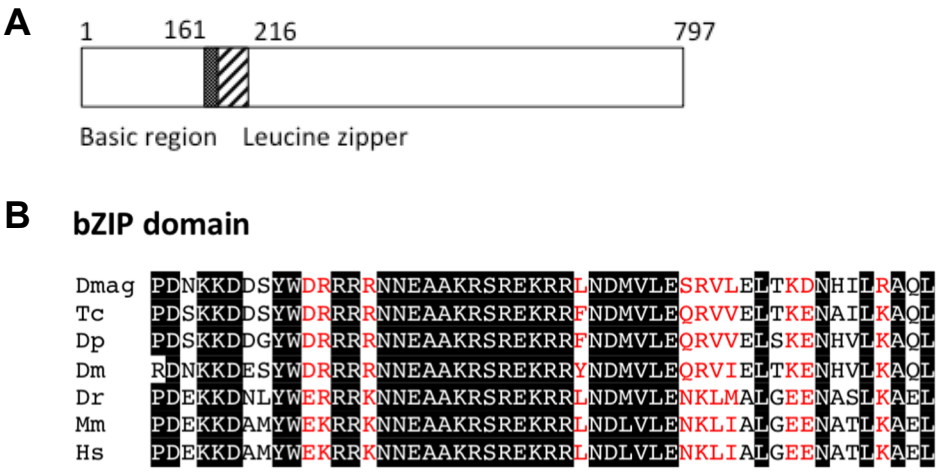

Figure 17: (A) The protein structure of Vri from *D. magna* and (B) the alignment of its bZIP domain with other Vri and E4BP4/NFIL3 proteins. The numbers indicate the location of amino acid. Dmag is *D. magna,* Tc is *T. castaneum* (red beetle), Dp is *D. plexippus* (monarch betterfly), Dm is *Dr. melanogaster* (fruit fly), Dr is *Da. rerio* (zebrafish), Mm is *M. musculus* (mouse) and Hs is *H. sapiens* (human). Black shaded indicates the same amino acids while red indicates the same type of amino acid in one position.

To analyze the evolutionary relationship of *D. magna* Vri, a phylogenetic tree with 13 other related proteins was constructed by neighbor-joining method, using the bZIP domain amino acid sequence (Figure 18B). The phylogenetic tree revealed that *Daphnia* Vri ortholog is most closely related to the insects' E4BP4/NFIL3 ortholog Vrille (Figure 18). This result was in good agreement with the taxonomic relationship between crustacean and insects, consistent with the previous hypothesis that insect originated from branchiopod crustaceans [73].

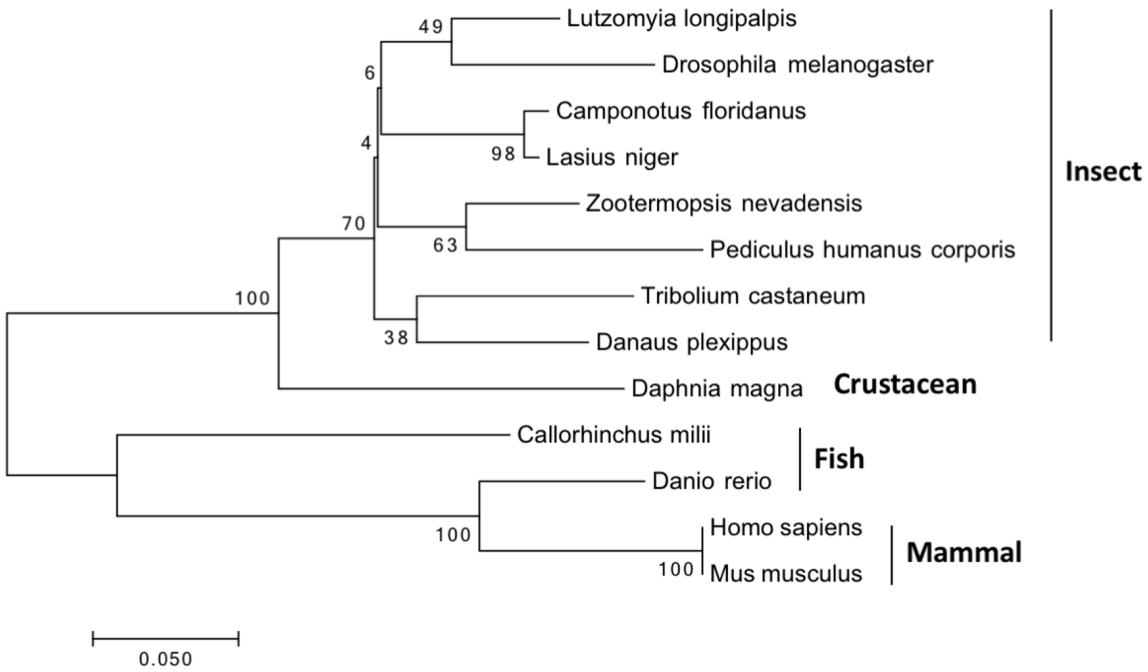

Figure 18: Phylogenetic tree using the amino acid sequences of the bZIP domain of Vri and E4BP/NFIL3 transcription factors. The percentages of replicated tree in which the associated taxa clustered together in the bootstrap test (1,000 replicates) are shown next to the branches. The bar indicates branch length and corresponds to the mean number of the differences ($P<0.05$) per residue along the each branch. Evolutionary distances were computed using the p-distance method.

3.2.3 *Vri* expression levels during embryogenesis

I analyzed the temporal expression pattern of *Vri* by qRT-PCR during *D. magna* embryogenesis, and the result is presented in Figure 19. At early stages of embryogenesis, *Vri* expression in males was significantly higher than that in females at 0, 3, and 6-hpo. At 6-hpo, *Vri* transcript became more abundant but retained the sexually dimorphic expression pattern (Figure 19A). At the later embryonic stages (18 and 36-hpo), *Vri* expression increased both in males and females and lost its sexual dimorphism (Figure 19B).

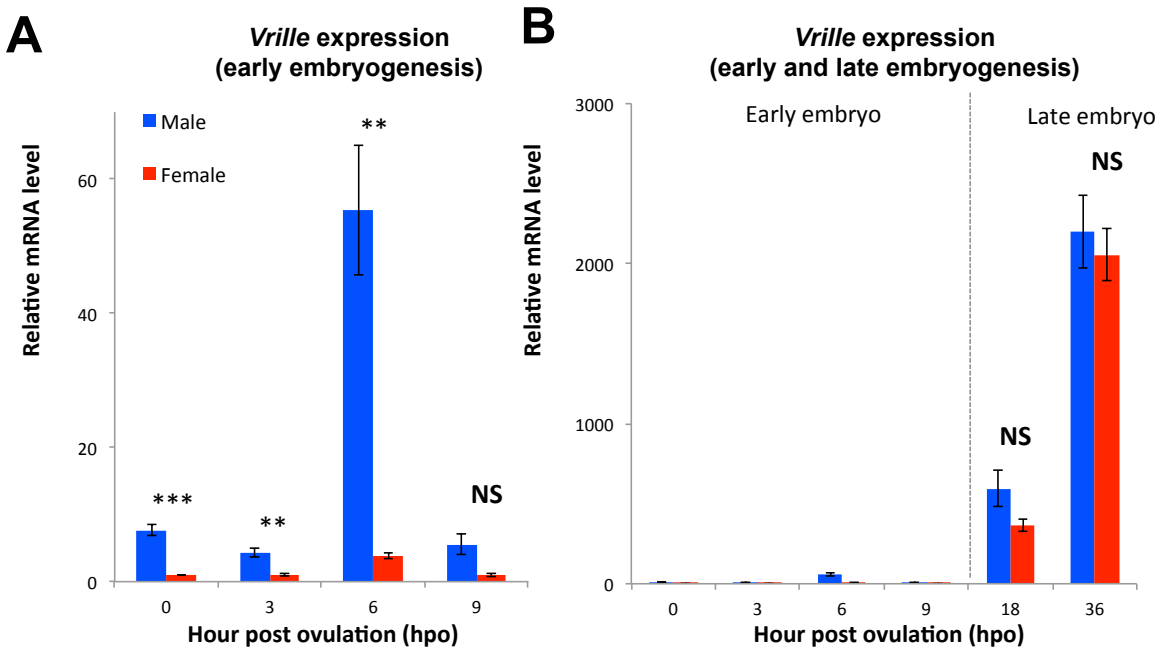

Figure 19: *Vri* expression during embryogenesis of *D. magna*. (A) Sexual dimorphism of *Vri* expression at early embryogenesis stages (0, 3, 6, and 9-hpo). (B) Non-sex specific *Vri* expression in the late embryos (18 and 36-hpo). The *Vri* expression levels were normalized to the reference gene expression levels (ribosomal protein L32). The normalized expression in female embryos at 0-hpo was set to one. (Student's t-test: *, P<0.05; **, P<0.01; ***, P<0.001; NS = No significant different)

3.3.4 *Vri* knockdown in male reduced *Dsx1* expression

To examine the roles of the *D. magna* Vri gene especially for sex determination, *Vri* expression was knocked down using RNAi method [36] in male and female embryos. To confirm specificity of phenotype induced by *Vri* RNAi, two siRNAs were designed. Vri_siRNA_1 and Vri_siRNA_2 both target the *Vri* coding sequence but their target sequences are different (Figure 16). The phenotypes of the cell and tissue influenced by *Vri* RNAi during embryogenesis were observed using

H2B-GFP expressing *Daphnia* that allows visualization of individual cells in an embryo [50].

Based on the GFP expression pattern as presented in Figure 20A, development of male embryos injected with Vri_siRNA_1 and Vri_siRNA_2 seemed to be normal at around 10 to 11-hpo. At 20-hpo, Vri-siRNA_1-injected embryos developed cephalic appendages such as second antennae but did not start thoracic segmentation in contrast to control embryos. Vri_siRNA_2-injected embryos died due to more severe phenotype in which the segmental structures were not formed. At 30-hpo, Vri_siRNA_1-injected embryos showed abnormal segmentation of thoracic appendages, and undeveloped posterior and anterior region of the embryos, which prevented us from investigating sex-reversal in sexually dimorphic structure such as the first antennae. These RNAi-dependent deformities were also observed in female embryos (Figure 20B), but for Vri_siRNA_1-injected female embryos they were able to hatch before the abnormal developments led to embryo lethality. The data of *Vri* RNAi microinjection for phenotypes observation are summarized in Table 8 below.

Table 8: Summary of the *Vri* siRNA microinjection experiment for phenotype observation.

siRNA	Sex of egg	Injected egg	Hatched	Swimming juvenile
Vri_1	Female	17	11	0
	Male	20	0	0
Vri_2	Female	11	0	0
	Male	9	0	0
Cntrl_siRNA	Female	10	10	10
	Male	8	8	8

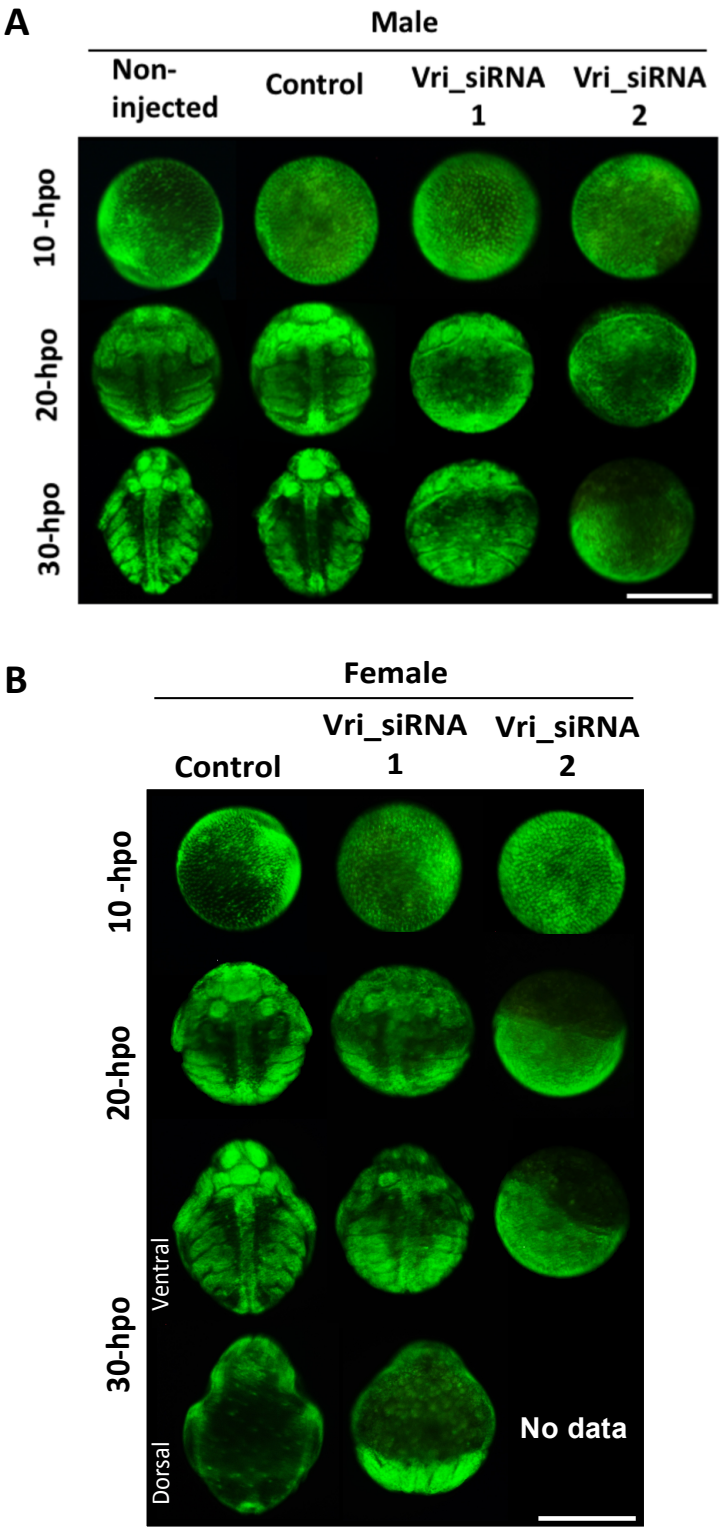

Figure 20: Effects of *Vri* RNAi on embryonic development. The phenotypes of (A) male and (B) female *Vri* RNAi embryos at 10, 20 and 30-hpo. Two *Vri* siRNAs were injected into the transgenic line and control siRNA was used as negative control. The injected embryos were brighter compared to non-injected ones because of the fluorescence from Lucifer yellow dye co-injected with siRNAs. Scale bar: 200μm.

To exclude the possibility that the developmental defect affects *Dsx1* expression, I analyzed *Dsx1* expression levels in RNAi embryos at 11-hpo by qRT-PCR, and I validated that the *Vri* expression level was negligible in both of the RNAi embryos (Figure 21). The qRT-PCR analysis also revealed that *Dsx1* expression was reduced in both Vri_siRNA_1 and Vri_siRNA_2 siRNAs-injected wild-type males as shown in Figure 22.

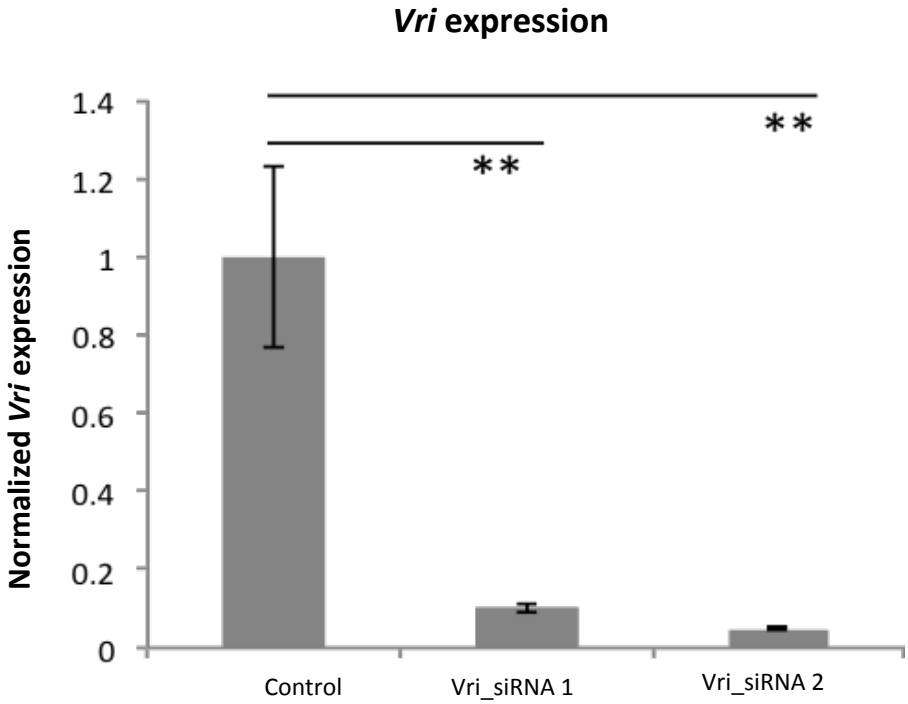

Figure 21: *Vri* expression levels in siRNA-injected embryos at 11-hpo. The *Vri* expression levels were normalized to the reference gene expression levels (ribosomal protein L32). The normalized expression in control-siRNA-injected embryos set to one. (Student's t-test: **, $P<0.01$).

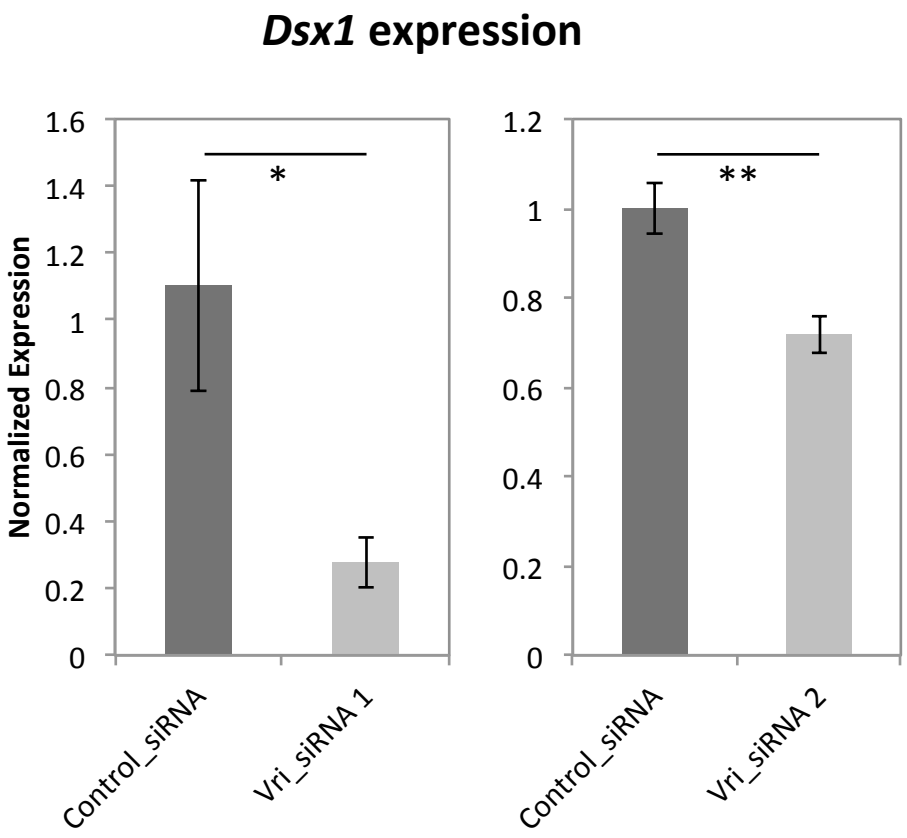

Figure 22: *Dsx1* expression level in siRNA-injected male embryos at 11-hpo measured by qRT-PCR. Control_siRNA, Vri_siRNA_1 and Vri_siRNA_2 indicate control-, Vri_siRNA_1- and Vri_siRNA_2-injected males, respectively. Each experiment was performed in biological triplicate. For each replicate, nine or ten embryos were pooled in one tube, subjected to total RNA extraction and used for quantitation. (Student's t-test; *, $P<0.05$; **, $P<0.01$).

To further analyze where *Vri* RNAi reduced the expression, I utilized a transgenic *Daphnia,* which was a *Dsx1* reporter strain that expresses a red fluorescence protein mCherry under the endogenous *Dsx1* promoter/enhancer [52]. At 20-hpo, in control male and female *Daphnia,* the mCherry fluorescence appeared exclusively in male embryos and is localized in the first antennae, which are the first organs to appear as a male-specific trait in *Daphnia.* In addition, mCherry-expressing cells could be seen in thoracic appendages, and remarkably in posterior growth zone (Figure 23). In Vri_siRNA_1-injected male embryos, mCherry signal could be seen

only in the posterior growth zone but with weaker intensity. Vri_siRNA_2-injected embryos did not show any red fluorescence (Figure 23). However, due to severe effect of *Vri* silencing during embryonic processes, we could not exclude the possibility that some of the structures that normally express the mCherry reporter were not properly formed when *Vri* was silenced. I summarized the injection experiment in Table 9.

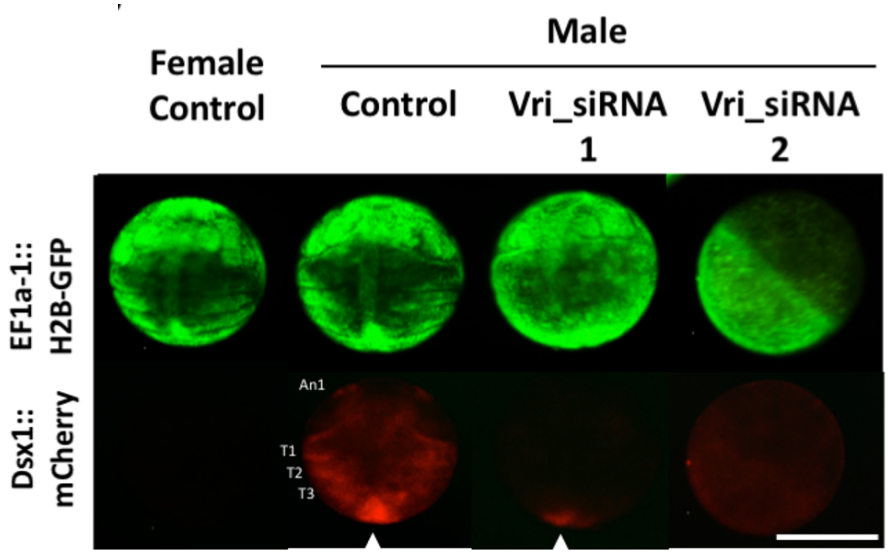

Figure 23: Spatial expression pattern of mCherry as a reporter of *Dsx1* gene expression at 20-hpo. An1 is first antennae, T1 is thoracic appendage 1, T2 is thoracic appendage 2, T3 is thoracic 3, arrowheads indicate posterior growth zone. Scale bar: 200 µm.

Table 9: Summary of *Vri* RNAi experiments using the *Dsx1* reporter strain.

siRNA	Sex	Injected	Hatched	Juvenile	Declined of mCherry fluorescence
Vri_siRNA_1	Male	20	0	0	90% (18/20)
Vri_siRNA_2	Male	9	0	0	88.9% (8/9)
Control_siRNA	Male	8	8	8	0% (0/8)

3.3.5 *Vri* overexpression in female increased *Dsx1* expression

To test whether transient expression of *Vri* in early embryos is sufficient to activate *Dsx1* and trigger male development, I induced transient ectopic expression of *Vri* in female by delivering capped, polyadenylated mRNAs into ovulated eggs via microinjection. I first attempted to establish a system to mimic the transient expression of *Vri* in early male embryos. We constructed *GFP* mRNA harboring the 5′ UTR and 3′ UTR sequences obtained from *X. leavis β-globin* gene and injected this chimeric *GFP* mRNA into female eggs. As exhibited in Figure 24, the UTRs led to expression at early embryogenesis (3 to 10-hpo) but not in later stages. Hence, to study the Vri function in sex-determining pathway, I linked the *X. laevis β-globin* UTRs to the *Vri* CDS and injected the mRNA into wild-type eggs that would develop into females.

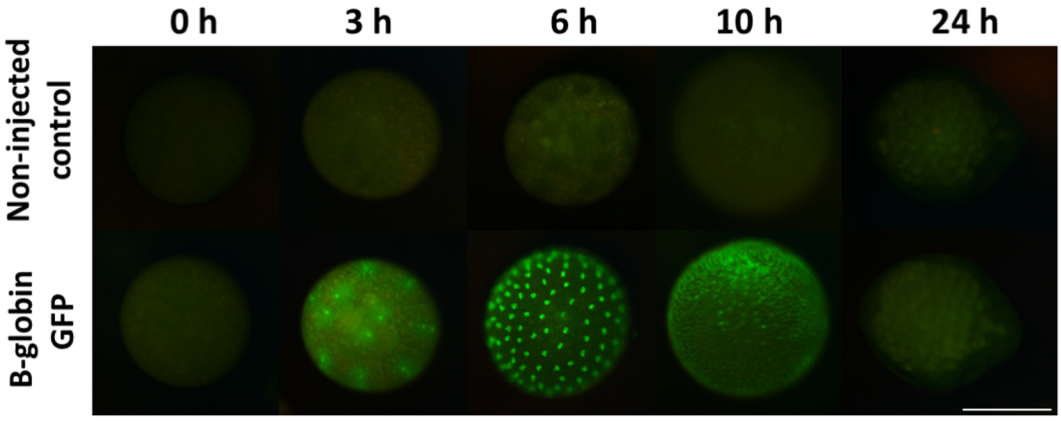

Figure 24: Temporal change of fluorescence in embryos injected with *GFP* mRNA harboring *X. laevis β-globin* UTRs. GFP was fused with Minos transposase, which resulted in nuclear localization of GFP as previously reported [68]. Scale bar: 200 μm.

Although injecting the chimeric *Vri* mRNA induced high embryonic lethality, the juveniles that survived showed a partial elongation of the male-specific trait first antennae (Figure 25), in an mRNA concentration-dependent manner, as summarized

in Table 10. Consistent with this masculinized phenotype, I confirmed the up-regulation of *Dsx1* expression levels in *Vri* mRNA-injected daphniids by qRT-PCR at 48 to 50-hpo. The qRT-PCR result is shown in Figure 26A. However, low viability and lethality prevented the observation of further masculinization phenotypes in the injected female animals.

Figure 25: Phenotype of *Vri* mRNA injected female juveniles at 72-hpo. Black arrowheads indicate the first antennae, the male-specific trait that can be observed at this stage. Scale bar: 200 µm.

Table 10: Masculinization of 1st antennae by *Vri* overexpression in females.

mRNA	Conc. (ng/µL)	Injected eggs	Swimming juveniles	Viability	Elongated 1st antennae
Vrille	1000	64	8	13%	75% (6/8)
	250	34	6	18%	67% (4/6)
	62.5	16	5	31%	0% (0/5)
GFP	800	29	24	83 %	0% (0/24)

In addition, by using the *Dsx1* reproter strain, I tested the effects of the same chimeric *Vri* mRNA on *Dsx1* activation in females. From the mRNA injection, I detected high and widespread *mCherry* epxression mainly in the thoracic appendages at 50-hpo (Figure 26B). To confirm whether Vri's DNA binding activity was neccessary for *Dsx1* activation, I modified the *Vri* mRNA by removing the amino acid

sequence of bZIP domain. This mutated Vri could still increase *Dsx1* epxression level in injected female embryos but showed a lower transactivation activity (Figure 26B). Table 11 summarized the microinjection and red fluorescence observation.

Table 11: Activation of *mCherry* by *Vri* overexpression in female embryos from the *Dsx1* reporter strain at 20-hpo.

mRNA	Concentration	Red fluorescence
Vrille (full length)	1 µg/µl	100% (5/5)
	250 ng/µl	100% (12/12)
	62.5 ng/µl	100% (13/13)
Vrille (w/o bZIP)	1 µg/µl	80% (8/10)
GFP	1 µg/µl	0% (0/9)

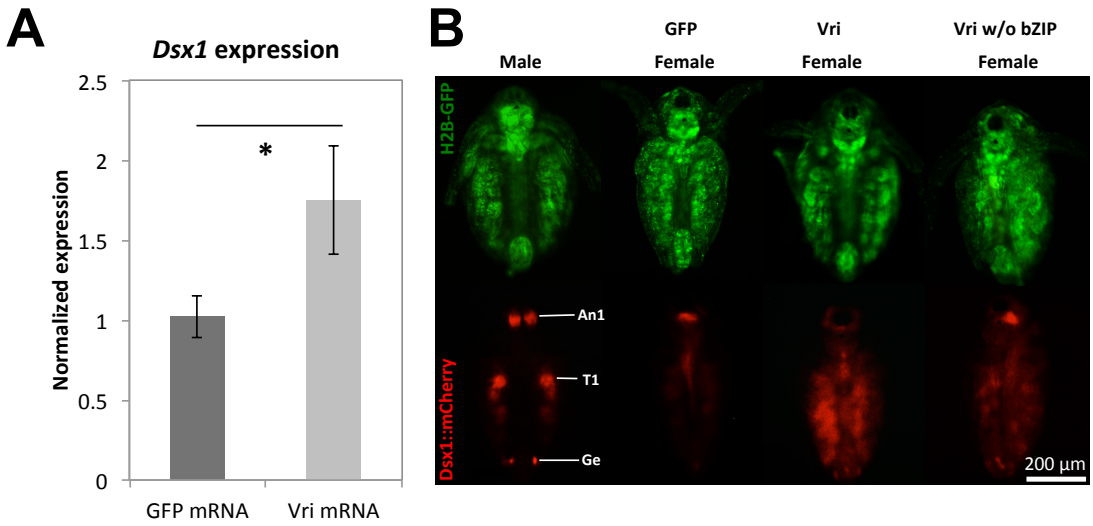

Figure 26: Effects of *Vri* over-expression on *Dsx1* expression. (A) *Dsx1* expression level in *Vri* mRNA-injected embryos at 50-hpo measured by qRT-PCR. *GFP* mRNA was used as a negative control. This experiment was performed with four biological replicates. For each replicate, one daphniid was subjected to total RNA extraction and the cDNA was used for quantification. (Student's t-test; *, P<0.05) (B) Spatial expression pattern of *mCherry* as a reporter of *Dsx1* gene expression at 50-hpo. Non-injected male displays mCherry expression in the 1st antennae (An1), first thoracic leg (T1), and genital (Ge). GFP-, Vri-, and Vri without bZIP indicate negative control female injected with *GFP* mRNA, females injected with *Vri* harboring its full-length CDS, and females injected with mRNA encoding bZIP domain lacking Vri, respectively. Scale bar: 200 µm.

3.3.6 Disruption of the enhancer reduced *Dsx1* expression

To test whether the enhancer element, which contains bZIP binding site overlapped with Dsx binding site, is required for *Dsx1* activation and male trait development, I tried to disrupt the sequence on the genome by CRISPR/Cas9 system. Due to the low GC content (23%) of the enhancer, I could not obtain a suitable sequence that can be directly targeted by TALENs and gRNAs to make a double strand break. More than 50% of GC content is preferred to get a good binding stability in DNA genome. Alternatively, I designed separate gRNAs (gRNA-1 and gRNA-2) near to the enhancer as illustrated in Figure 27A. For the Cas9, Cas9 mRNA was initally co-injected with gRNAs for targeted mutagenesis in *D. magna* [41]. To improve the knock out efficiency, I expressed the Cas9 protein in *E. coli* cells, purified and used the Cas9 protein for microinjection (Figure 27B). The Cas9 protein was tested to mutate the *Eyeless* [41] and *Scarlet* gene (Ismail *et al.,* unpublished), and based on the mutant phenotype, knock out efficiency was increased up to 36.4% and 38.5%, compared to 8.3% 3.4% efficiency made by Cas9 mRNA injection, respectively. I then tested the functionality of newly designed gRNAs (gRNA-1 and gRNA-2) and Cas9 protein by Cas9/gRNA complex *in-vitro* cleavage assay. As shown in Figure 27C, the Cas9-gRNA complexes successfully cut the plasmid (linearized band) that contained target sequences, indicating that the gRNAs and Cas9 protein could introduce targeted double strand break.

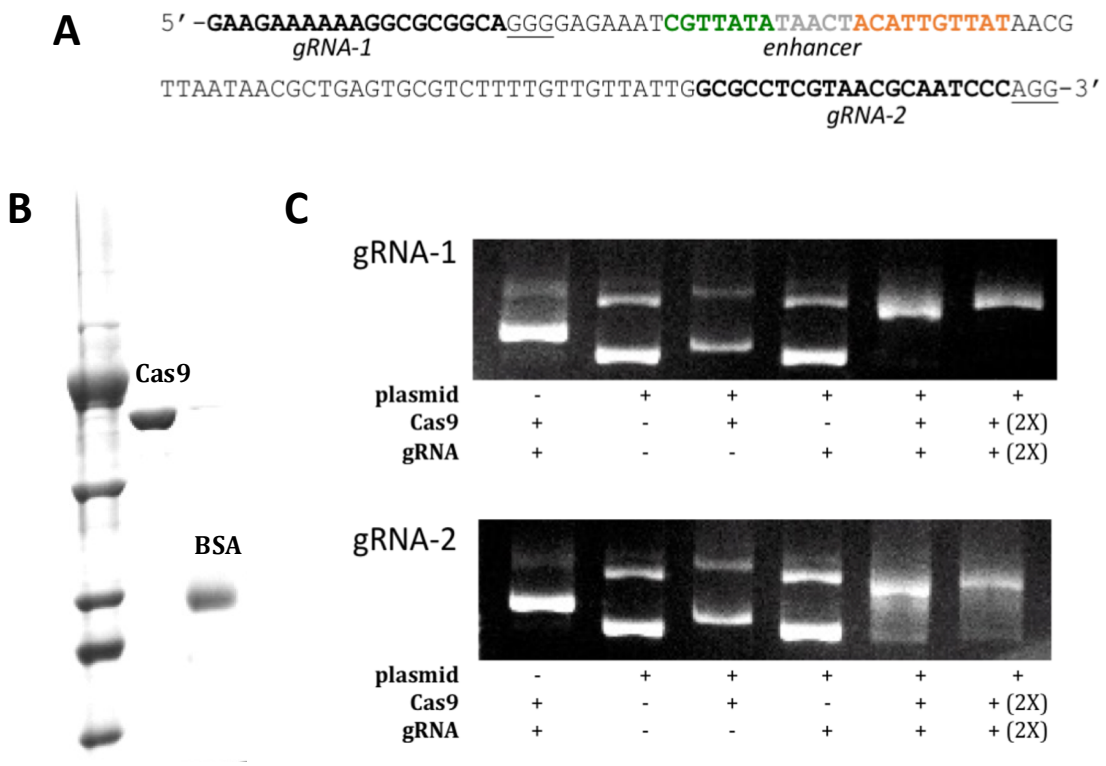

Figure 27: The design of gRNAs and Cas9/gRNA functionality tests. (A) The sequence of gRNA target sites (bold) located near the enhancer region. The underlines show the PAM sequences. (B) SDS-PAGE gel indicates that the Cas9 protein was successfully purified from the *E. coli* cells. (C) Gel electrophoresis after the Cas-9 protein *in-vitro* cleavage assays. The positive result can be interpreted by detecting the linear band of the plasmid on the gels. 2X means double amount of each Cas9 protein and gRNA.

Next, I injected the two gRNAs with Cas9 protein into the *Dsx1* reporter strain eggs to show the development into male and evaluated effects of enhancer disruption on *Dsx1* expression and the morphological phenotypes. At 36-h after injection, I found four different phenotypes from 12 injected embryos, the phenotypes are presented in Figure 28A. Four injected-embryos (#1, #2, #3, and #4) exhibited Phenotype-1 in which embryonic development was delayed and showed weaker mCherry fluorescence than control but at the later stages, they could have normal male traits development. Two embryos (#5 and #6) showed Phenotype-2 wherein

eggs development was disturbed and mCherry signal was weak with abnormal localization. Phenotype-3 was observed in three injected-embryos (#7, #8, and #9), showing the most severe deformities without mCherry expression. The remaining three embryos (#10, #11, and #12) showed no apparent change in phenotype compared to non-injected control (Phenotype-4). The abnormal development of these eggs prevented us from observing sex specific trait or feminized phenotypes.

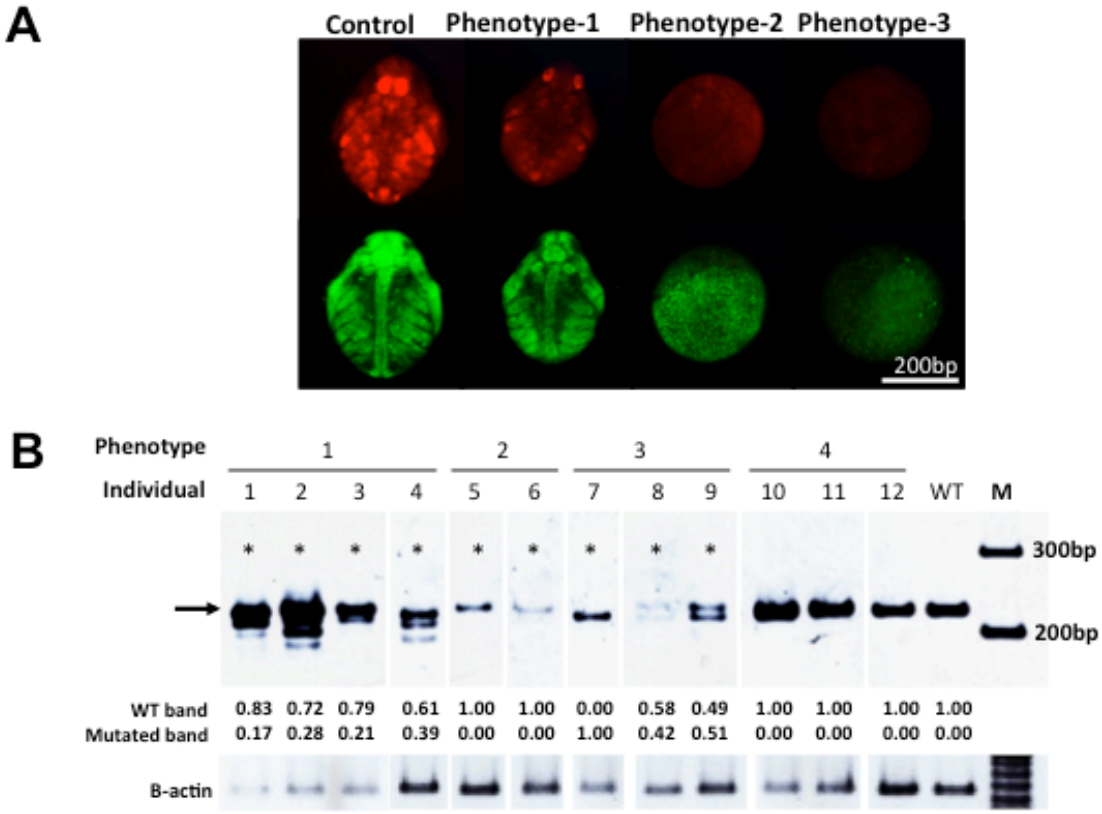

Figure 28: Disruption of enhancer region by the CRISPR/Cas9 system. (A) Spatial expression pattern of *mCherry* at 36-hpo. The Cas9 protein was co-injected with a pair of gRNA-1 and gRNA-2 into 12 male embryos of *Dsx1* reporter strain. Scale bar: 200 μm. (B) PAGE analysis of PCR products by genomic PCR to amplify a region that includes the enhancer. Original size of the PCR product should be 214 bp, indicated by the black arrow. Asterisks show the individuals that contain mutations. The numbers under the images of the PAGE gel indicate intensity of wild-type (WT) and mutated band measured by ImageJ application. M denotes DNA marker.

To examine the correlation between the introduced mutation and the observed phenotypes, I extracted genomic DNA from each embryo described above and performed genomic PCR to amplify 214 bp sequence including the enhancer region. Native PAGE results, shown in Figure 28B, demonstrated that some PCR products were either smaller sizes than what was expected from the wild-type sequence, while some have reduced intensity compared to the wild-type band. These suggest that large and small in-del mutations in the enhancer region has occurred. Then, I measured the intensity of each band and calculated the ratio of intensity of smaller bands to the expected band size. I observed that the more severe the injected-embryos phenotype was (Figure 28A), the higher was the ratio (Figure 28B). These result indicate that the enhancer may be a *cis*-regulator element for male-specific *Dsx1* expression.

In addition, I attempted to generate enhancer knock out mutants by injecting the Cas9 protein-gRNA complexes and collecting the offspring of the injected daphniids. For this purpose, neither somatic (Table 12) nor heritable mutation (Table 13) was detected from female eggs injection. Meanwhile, using male eggs, the injection led to high embryonic lethality (>90%) as shown in Table 13. I was able to collect offspring from feminized male embryos by *Dsx1* RNAi, but no mutant line was generated from the survived daphniids.

Table 12: Somatic mutagenesis in female for disrupting the *Dsx1* enhancer by utilizing the CRISPR/Cas9 system.

Sex	Cas9 protein	gRNAs	Injected	Juvenile	Screened	Somatic mutation
Female	1 μM	2 μM each	19	13	12	0
	2.5 μM	5 μM each	45	11	11	0

	2.5 μM	2.5 μM each	43	33	16	0

Table 13: Heritable mutagenesis in female and male for disrupting the *Dsx1* enhancer.

Sex	Cas9	gRNAs	Injected	Juvenile	Adult	Screened	Mutated enhancer
Female	1 uM	2 uM each	29	17	14	14	0
	0.5 uM	1 uM each	13	7	5	5	0
Male (coinjection with dsx1 siRNA)	0.5 uM	1 uM each	66	11	8	8	0
	1 μM	1 μM each	66	4	3	3	0
	-	-	22	15	15	-	-

3.4 Discussion

Results in previous chapter have shown that in response to JH signal, *Dsx1-α* transcript is up-regulated before early gastrulation at 6-hpo and is maintained in later embryogenesis for regulation of male trait development. In this chapter, a hypothetical enhancer element that contains a consensus sequence for binding of the bZIP transcription factor orthologs, the *Drosophila* Vri and vertebrate E4BP4/NFIL3, was found on *Dsx1* promoter. The binding site overlapped with a consensus sequence of Dsx binding site and this overlapping structure of the enhancer is similar to the fat body enhancer of the *Drosophila* yolk protein gene 1 [72], which was the *cis*-regulator for tissue- and sex-specific expression. Since, *Dsx1* up-regulation also suggests positive feedback regulation of this gene, it is reasonable to hypothesize that the Vri works together with Dsx1 protein, binds to the enhancer to activate the male-specific *Dsx1* transcription.

I discovered that the *Vri* gene has male sex-specific expression during early embryonic development and is highly expressed during the gastrulation stage (6-hpo). The gene encoded for a single cDNA sequence; no other splicing pattern was found. Since *Vri* gene is a bZIP transcription factor that was previously identified as a circadian rhythm gene [54], my findings suggest a potential new role for *Vri* gene in early embryogenesis with the hypothesis that it has been co-opted into sexually dimorphic pathway of *D. magna*.

To further this study, I investigated the function of Vri regarding *Dsx1* expression by loss- and gain-function analyses, and disruption of an enhancer harboring a consensus sequence of the Vri binding site. Vri siRNAs do not only cause morphological defects, but also cause reduction of *Dsx1* expression and loss of *Dsx1* reporter gene activity in regions known to give rise to male-specific structures. Ectopic expression of *Vri* by mRNA injection resulted in masculinization of morphology and *Dsx1* reporter gene activity in females. Lowered and increased levels of *Vri* gene caused early lethality. Using Cas9-mediated somatic mutagenesis approach to target the bZIP/Dsx binding site region in the *Dsx1* locus, the males with genomic defects at the *Dsx1* locus were correlated to have morphological phenotype effects. These results suggested that Vri directly regulates the transcriptional output of *Dsx1*.

Our findings indicate that Vri functions as an activator of the *Dsx1* gene in *Daphnia*. In *Drosophila*, Vri regulates various developmental processes such as cell growth, proliferation and flight [55,74], as well as metamorphosis [56] and tracheal integrity [75]. In addition to these processes, Vri is required for circadian oscillation by repression of *Clock* transcription [76]. In mammals, the Vri ortholog E4BP4/NFIL3 is also reported as a clock-controlled gene. It competes for the binding

site of the PAR-protein. Both *Drosophila* Vri and mammalian E4BP4/NFIL3 are well known transcriptional repressors. However, in the human immune response system, E4BP4/NFIL3 was identified as an activator of the *IL3* promoter [58] and was also shown to up-regulate *IL-10* and *IL-13* [77]. It is essential for lineage commitment of innate lymphoid cells (ILCs) [78]. In natural killer cell development, E4BP4/NFIL3 interacts with the histone ubiquitinase MYSM1 and maintains an active chromatin state at the *Id2* locus [79]. In *Daphnia* sex determination, Vri works at the gastrulation stage when lineage commitment occurs. These similarities in regulation at the genetic and cellular levels may suggest that the molecular mechanism of Vri-dependent *Dsx1* activation is similar to that of E4BP4/NFIL-3 function in human ILCs.

In targeted mutagenesis using Cas9 system, I could not introduce any mutation into Vri binding site at the *Dsx1* promoter/enhancer on the genome in females. In contrast, this mutagenesis introduced deletion at the target site on the genome in males and reduced *Dsx1* expression. These results suggest that this enhancer may be silenced via close chromatin in females but is required for *Dsx1* activation in males. I also discovered that deletion of the enhancer led to embryonic lethality in males, even though I could not shed light on the mechanism underlying this high mortality. However, these clear differences of phenotypes between males and females in targeted mutagenesis experiments indicate a male-specific role of this enhancer. Further study is needed to understand the epigenetic regulation at *Dsx1* locus.

As a conclusion, the results in this chapter demonstrate co-option of the bZIP transcription factor Vri upstream of the *Dsx1* in the environmental sex-determining cascade of the crustacean *D. magna.* The data suggest the remarkably plastic nature of gene regulatory network in sex determination.

Chapter 4 Sequence conservation of the *Ftz-F1* ortholog in *D. magna* and its sexually dimorphic expression

4.1 Introduction

To identify other sex-determining genes involved in *D. magna* cascade, I performed literature review related to sex determination in various organisms. One possible candidate is a member of the orphan nuclear receptor family Fushi tarazu factor-1 (Ftz-F1), which is involved in genetic regulation of various developmental processes [80]. It was first identified in *Dr. melanogaster* and subsequently, *Ftz-F1* orthologs have been isolated from many animals recorded in several different names such as steroidogenic factor-1 (Sf-1) [81], adrenal-4-binding protein (Ad4BP) [82], and nuclear hormone receptor-25 (nhr-25) [83]. Vertebrate *Ftz-F1* orthologs are known to function in genetic sex determination (GSD). In particular, the mammalian Ftz-F1 homolog Sf-1 has been found to be essential for the proper development of the adrenal-gonadal axis, strongly linked to steroidogenesis [84] and it also plays a critical role in mammalian sex determination that involved the testis-determining pathway [85]. Additionally, the zebrafish *Ftz-F1* genes have been linked to the process of sex determination and differentiation, as they are involved in early development of urogenital tissue and as well as regulation of steroidogenic cells and their gene expression [86].

While many studies have demonstrated the function of *Ftz-F1* orthologs in GSD, their roles in the environmental sex-determining pathway have not been known yet. Previous study from Dubrovsky *et al.* (2011) has reported that the *Drosphila* Ftz-F1 nuclear receptor functions as a competence factor that facilitates JH activation of gene expression. Hence, I questioned whether *Ftz-F1* could be one of the mediators

for JH signaling in *D. magna* and also if it conserve the functions for sex determination in *Daphnia*.

In this study, I identified an *Ftz-F1* ortholog in *D. magna* and characterized its cDNAs and amino acid sequences. Additionally, I searched for potential Ftz-F1 binding sites on *Dsx1* promoter to examine the possibility of Ftz-F1 to be involved in the sex-determination cascade. Subsequently, I examined the temporal expression pattern of *Ftz-F1* gene during embryogenesis and compared the sexual differences of the gene expression. To investigate the gene functions, I performed *Ftz-F1* gene silencing by RNAi method via siRNAs delivery into *Daphnia* eggs. This study is important to understand the evolution of Ftz-F1 orthologs and the molecular basis of JH signaling in ESD mechanism.

4.2 Materials and methods

4.2.1 *Daphnia* strain and culture condition

All of the wild-type (WT) and transgenic *D. magna* share the same genetic background (NIES clone). The HG-1 transgenic line mentioned in Chapter 2 was also utilized in the gene knock down experiments in this chapter. The *Daphnia* were cultured under the same laboratory conditions mentioned in Chapter 2 (see 2.2.1 *Daphnia* strain and culture condition). The male daphniids were obtained with the same method described in Chapter 2 (see 2.2.2 Artificial male production by JH analog exposure).

4.2.2 Total RNA isolation

Female and male daphniids were collected separately and briefly washed. Homogenization was performed with beads using a Micro Smash machine MS-100 (TOMY) in the presence of Sepasol-RNA I reagent (Nacalai Tesque Inc.). Total RNA was isolated according to the manufacturer's protocol and then followed by phenol/chloroform extraction. The amount of purified total RNA was measured using Nanodrop 2000 (Thermo Fisher Scientific). One μg of each RNA sample was used to synthesize first-strand cDNA as will be explained in next section.

4.2.3 First-strand cDNA synthesis

The mRNA from purified total RNA was converted to first-strand cDNA using SuperScript III Reverse Transcriptase (Invritrogen; California, USA) with same protocol explained in Chapter 2 (See 2.2.5 First-strand cDNA synthesis).

4.2.4 Cloning and sequencing

Ftz-zF1 cDNA fragments from *D. magna* that encode for the DNA-binding domain (DBD) and the ligand-binding domain (LBD) were obtained from female cDNA by PCR with AmpliTaq DNA polymerase (Applied Biosystems; California, USA) using degenerate primers that were designed based on the conserved amino acid sequences of the DBD (5′-GAAGAACTGTGTCCNGTBTGYGG-3′) and the LBD (5′-ARTTTCATYTGRTCGTCAACCTT-3′). Amplified DNA fragments were cloned into a pGEM-T Easy Vector System (Promega Corp; Wisconsin, USA) and were sequenced.

Full-length cDNAs synthesis was completed by 5′ and 3′ rapid amplification of cDNA ends (RACE) using GeneRacer Kit (Invitrogen) and SMARTer RACE

cDNA Amplification Kit (Clontech), respectively. The primer sequences used for the RACE experiments were as follows: 5′-RACE gene specific primer (5′-TCCTCCGCCGGACGGGTGATTATTTG-3′); 5′-RACE nested primer (5′-TTCGCGGATCAATGGCGGAACTTTAGC-3′); 3′-RACE gene specific primer (5′-ATTCTCCGTCCGGCAGCAGCGTCTAC-3′); and 3′-RACE nested primer (5′-TCCACTTGCCGCATCACTCGGCTATC-3′). The amplification products were then purified from an agarose gel and were cloned into a TOPO cloning kit (Invitrogen) for sequencing. The sequencing reaction was performed using a BigDye Terminator Cycle Sequencing Kit (PE Applied Biosystems) and the DNA sequences were analyzed using the BLAST program.

4.2.5 Phylogenic analysis

Amino acid sequences of Ftz-F1 family genes were retrieved from the NCBI database (http://www.ncbi.nlm.nih.gov/) as shown in Table 14, and the whole amino acid sequences of each protein were used to construct the phylogenetic tree. Multiple sequence alignments of the amino acid sequences were constructed using ClustalW [63] in MEGA version 6.06 [64]. The same settings mentioned in Chapter 3 (see 3.2.4 Phylogenic analysis) were used for the analysis. The phylogenetic reconstruction was performed using the p-distance algorithm and the neighbor-joining method implemented in MEGA.

Table 14: Accession numbers of Ftz-F1 ortholog genes used in this study.

Common name	Scientific name	Gene name (definition in NCBI)	Accession no.
Water flea	*Daphnia magna*	Ftz-F1	This work (LC105700, LC105701)
Water flea	*Daphnia pulex*	Ftz-F1 (Hypothetical protein)	EFX77612.1
German cockroach	*Blattella germanica*	Ftz-F1	CAQ57670.1
Red flour beetle	*Tribolium castaneum*	Ftz-F1	EFA01263.1
Yellow fever mosquito	*Aedes aegypti*	Ftz-F1	AAF82307.1
Silkworm	*Bombyx mori*	Ftz-F1	NP_001037528.2
Shrimp	*Metapenaeus ensis*	Ftz-F1	AAD41899.1
Fruitfly	*Drosophila melanogaster*	Ftz-F1	AAA28542.1
Mouse	*Mus musculus*	Sf-1	AAB28338.1
Zebrafish	*Danio rerio*	Nr5a2	NP_571538.1
Medaka	*Oryzias latipes*	Ftz-F1	BAA32394.1
Roundworm	*Caenorhabditis elegans*	Nhr-25	CAA91028.1

4.2.6 Quantitative RT-PCR

Female and male embryos at several embryonic stages (0, 6, 12, 18, 24, 30, 48, and 72-hpo) were sampled as described in [30,50,88]. To have three biological replicates, the collected embryos at each stage were divided into three groups. Each group was subjected to total RNA isolation and then cDNAs were synthesized from 1 μg of total RNA as described in the section above (4.2.2 Total RNA isolation and 4.2.3 First-strand cDNA synthesis). Of each cDNA pool, 1/120 volume was used as a template for qRT-PCR.

Quantitative real-time PCR was conducted with SYBR GreenER qPCR Supermix Universal (Invitrogen) using the Mx3005P real time (RT)-PCR system (Agilent Technologies). With the appropriate primer pairs, real-time PCR amplifications were performed in triplicate at the following conditions: 2 min at 50°C and 10 min at 95°C, followed by 40 cycles of 15 sec at 95°C and 1 min at 60°C. Gel electrophoresis and dissociation curve analysis were performed to confirm the correct

amplicon size and the absence of non-specific bands. Copy number of *Ftz-F1* mRNAs was measured by quantification method. This relates the PCR signal to the input copy number by using a calibration curve obtained by dilution series of plasmid that contains sequence corresponding to each primer set. Finally, N divided copy number obtained by qRT-PCR from the following calculation, resulting in copy number of transcripts in one embryo.

$$N = \{1\ (\mu g)\ /\ [(amount\ (\mu g)\ of\ purified\ RNAs)/number\ of\ embryos)]/120$$

The primer sets used to amplify a specific region for qRT-PCR are listed in Table 15. Normalized expressions were analyzed by quantitating the reference gene of ribosomal protein *L32* expression level.

Table 15: The primer pairs used to quantitate specific amplification in qRT-PCR assay.

Amplify region of *Ftz-F1*	**Primer sequence (5′−3′)**
Common region	Forward: CGCACACCTTCTCCAAATAA Reverse: TTACCAGTCAACAGTCCCTCAAAA
α-isoform	Forward: ATTCCCTCCAACCTGACGAG Reverse: ATCTTGGAGCTGGATGAGCA
β-isoform	Forward: GGGAGCTCAGCATTTGCATC Reverse: TGAACGGCGACATGGTAGAC

4.2.7 Gene knockdown by RNAi

The RNA-mediated interference method [36] described in Chapter 3 (see 3.2.4 Gene knock down by RNAi) was employed using 100 μM of two siRNA oligos, Ftz-F1_699 siRNA (5′-CCAGUCUCUGACGAUAA-3′) and Ftz-F1_918 siRNA (5′-GCACACACCUUCUCCAAAU-3′). These siRNAs were used to knockdown *Ftz-F1* gene function *in vivo* as delivered into *Daphnia* eggs by microinjection. A random

sequence (5′-GGUUAAGCCGCCUCACAUTT-3′) that did not affect *Daphnia* embryogenesis [67] was utilized as a control siRNA (Control_416 siRNA). The knockdown was performed to a transgenic line HG-1 that expressed H2B-GFP to help visualize embryogenesis under the fluorescence microscope.

The phenotypes of injected embryos were carefully observed by time-lapse imaging from 3 to 30-hpo. At 24-hpo, total RNAs were isolated from two embryos with Control_416 or Ftz-F1_918 siRNA in three replicates and were converted to cDNAs as described above (4.2.2 Total RNA isolation and 4.2.3 First-strand cDNA synthesis). qRT-PCR was performed following the same protocol (4.2.6 Quantitative RT- PCR) using the primers that amplified the common region of *Ftz-F1* gene.

4.2.8 Finding potential binding sites by bioinformatics computational

The possible TF binding sites were searched on genome sequence using RSAT matrix-scan quick and simple method (http://rsat01.biologie.ens.fr/rsa-tools/matrix-scan-quick_form.cgi) [62]. The promoter sequence of *Dsx1* from *D. magna* was inserted in the blank space in ‘Sequences’ table, then the consensus sequence of Ftz-F1 was obtained in matrix form for ‘Matrix’ table [89]. To check whether the binding site sequences are conserved or not in *Daphnia* species, the same computation identification was performed on *Dsx1* gene of *D. pulex.*

4.3 Results

4.3.1 Characterization of *Ftz-F1* gene in *D. magna*

To examine the existence of the *Ftz-F1* ortholog in *D. magna*, the *Ftz-F1* fragment that encodes for the DBD and the LBD region (Figure 29A) were amplified

using degenerated primers. After cloning and sequencing the amplified fragments, BLAST analysis revealed that the putative amino acid sequences showed high homology to *Dr. melanogaster* nuclear hormone receptor *Ftz-F1*. Therefore, this gene was assigned as *D. magna Ftz-F1*.

To obtain full-length *Ftz-F1* cDNA from *D. magna*, I performed 5′ and 3′ RACE using cDNAs of female and male adults. The sequences were assembled into two different isoforms, *αFtz-F1* and *βFtz-F1*, which are composed of 2,763 and 3,078 nucleotides, respectively. Figure 29A shows the common region of both isoform, which contains the DBD and the LBD, based on the alignment of amino acid sequence of signature domain from the BLAST analysis. The sequences differed at the 5′ UTR and 5′ region of ORF, where β-isoform has a longer nucleotide and amino acid sequence as presented in Figure 29B and 29C. From the RACE experiment, I confirmed that the *Ftz-F1* gene showed no sex-specific different in their sequences.

A. Common region

```
GGCGAGTACGAAACGAGCAATGCGGCCAGCAGCAACGCGGCCCTCAGTCCATCACCTCTCATGGATCCTATCGTCATTGTTCCATCCATG 90
 G  E  Y  E  T  S  N  A  A  S  S  N  A  A  L  S  P  S  P  L  M  D  P  I  V  I  V  P  S  M  30

TCTGGCCAATCATCGGCCAGCTCTTTACCACCTGGAACGAGCTCGGCTTCGGGACGACACGACCTGCCCGATACGAAAGAAGGCATCGAA 180
 S  G  Q  S  S  A  S  S  L  P  P  G  T  S  S  A  S  G  R  H  D  L  P  D  T  K  E  G  I  E  60

GAATTGTGTCCGGTTTGCGGCGATAAAGTCTCTGGCTATCATTACGGTCTGCTCACCTGCGAATCGTGCAAGGGATTCTTCAAACGGACC 270
 E  L  C  P  V  C  G  D  K  V  S  G  Y  H  Y  G  L  L  T  C  E  S  C  K  G  F  F  K  R  T  90

GTTCAGAACAAAAAAGCCTATTCTTGCGTCGCTGATCGATCCTGCCACATTGACAAATCACAACGCAAGAGGTGCCCTTATTGCCGATTC 360
 V  Q  N  K  K  A  Y  S  C  V  A  D  R  S  C  H  I  D  K  S  Q  R  K  R  C  P  Y  C  R  F  120

CAAAAGTGCCTTGAAGTCGGCATGAAACTTGAAGCTGTGAGAGCGGACCGAATGCGTGGCGGTCGGAATAAATTTGGACCCATGTACAAA 450
 Q  K  C  L  E  V  G  M  K  L  E  A  V  R  A  D  R  M  R  G  G  R  N  K  F  G  P  M  Y  K  150

CGAGATCGAGCGCGTAAATTGCAGGTGATGCGTGAAAGACAATTGACGACGCCTCGAGGTAGCAACGGTGGAGGTAGCAATCCGTCACCC 540
 R  D  R  A  R  K  L  Q  V  M  R  E  R  Q  L  T  T  P  R  G  S  N  G  G  G  S  N  P  S  P  180

AACAACAGCAACAGCGGAGCAGGGCAGTCTGGAATGTACACGGACATGGGCTATTCTCCGTCCGGCAGCAGCGTCTACGGTGGTGGCAGC 630
 N  N  S  N  S  G  A  G  Q  S  G  M  Y  T  D  M  G  Y  S  P  S  G  S  S  V  Y  G  G  G  S  210

AGTGGCGGTGGTGTCAAGCACGAAATTCAAATTGCCCAAGTTTCTTCGTTGACATCCAGTCCCGATTCCAGCCCGAGTCCACTTGCCGCA 720
 S  G  G  G  V  K  H  E  I  Q  I  A  Q  V  S  S  L  T  S  S  P  D  S  S  P  S  P  L  A  A  240

TCACTCGGCTATCCAGGACCTTCTGGCCAGCCGTTGGGCTCGTTGAACGGTTCTACGGGACCATCCGGATCAGGCGGCCCGCACAATAAC 810
 S  L  G  Y  P  G  P  S  G  Q  P  L  G  S  L  N  G  S  T  G  P  S  G  S  G  G  P  H  N  N  270

AATAATACAAATAACCACAATAATAATAACATGGGCACGACATCGGGAGCGGGACCCTCTCATCCGCACACACCTTCTCCAAATAATCAC 900
 N  N  T  N  N  H  N  N  N  N  N  M  G  T  T  S  G  A  G  P  S  H  P  H  T  P  S  P  N  N  H  300

CCGTCCGGCGGAGGAGGAGGAGGAGGCGCTCCTACACCCCAACAGCATTCCTCCACTTCATCCGTCTCACCGAAAACCTTCCATTTTGAG 990
 P  S  G  G  G  G  G  G  G  A  P  T  P  Q  Q  H  S  S  T  S  S  V  S  P  K  T  F  H  F  E  330

GGACTGTTGACTGGTAACACAATGCTGGGTAATAACAACGTTCCCAATGTCGGAGCCGGATCAGTTAGCGGGGCTAAAGTTCCGCCATTG 1080
 G  L  L  T  G  N  T  M  L  G  N  N  N  V  P  N  V  G  A  G  S  V  S  G  A  K  V  P  P  L  360
```

```
ATCCGCGAATTTGTCCAGTCTCTTGACGATAAAGAATGGCAAAGCGCTTTGTTTGGTCTTCTTCAGAGTCAAACCTACAATCAATGTGAA 1170
 I  R  E  F  V  Q  S  L  D  D  K  E  W  Q  S  A  L  F  G  L  L  Q  S  Q  T  Y  N  Q  C  E  390

GTGGATTTGTTTGAACTGCTGTGTAAGGTGCTGGACCAAAACCTCTTTACCCAAGTGGACTGGGCACGCAATTCCTATTATTTCAAGGAT 1260
 V  D  L  F  E  L  L  C  K  V  L  D  Q  N  L  F  T  Q  V  D  W  A  R  N  S  Y  Y  F  K  D  420

CTAAAGGTTGATGATCAAATGAAGCTGCTCCAGCACGCCTGGTCGGATTTGTTAATTTTGGATCATTTGCATCAACGGTTGCACAATCAC 1350
 L  K  V  D  D  Q  M  K  L  L  Q  H  A  W  S  D  L  L  I  L  D  H  L  H  Q  R  L  H  N  H  450

CTGCCTGACGAATCGTCACTGCCTAACGGACAGAAATTCGACCTTTTATCGCTATCGCTACTCGGTTGTCCATCACTGGCCGAACCCCTT 1440
 L  P  D  E  S  S  L  P  N  G  Q  K  F  D  L  L  S  L  S  L  L  G  C  P  S  L  A  E  P  L  480

CACGACGTTACTGCCCGGCTCACTGAAATACGTTTCGACGTGCCCGACTACGTCTGCCTCAAATTTCTCATGCTCCTCAATTCAGATGTC 1530
 H  D  V  T  A  R  L  T  E  I  R  F  D  V  P  D  Y  V  C  L  K  F  L  M  L  L  N  S  D  V  510

AAGGGATTGATGAATCGACGCCACGTGGTGGAAGCGCAGGAGCAAGTCCAACAAGCTCTTTTTGATTACACACTTAACTGCTACACTCAT 1620
 K  G  L  M  N  R  R  H  V  V  E  A  Q  E  Q  V  Q  Q  A  L  F  D  Y  T  L  N  C  Y  T  H  540

ATCCCTGACAAGTTTGCTAAAATGCTGGCGATCTTACCGGACATTCACGCCATGTCGTCCCGCGGCGAAGAGTATCTCTATTTCAAGCAT 1710
 I  P  D  K  F  A  K  M  L  A  I  L  P  D  I  H  A  M  S  S  R  G  E  E  Y  L  Y  F  K  H  570

CTCAACGGCTGTGCGCCGACACAAACATTACTCATGGAAATGCTTCACGCCAAGCGGAAATGACGAGAGGCATTTTAAACAAAAAACCAT 1800
 L  N  G  C  A  P  T  Q  T  L  L  M  E  M  L  H  A  K  R  K  *                              590

CGCCAGGTAAGATGCATTTTATTTTTGCTCTCAAGTCAACTCATTTCTGTTCTGTATTTATTTATTTGTGAACGTTTTTCTTGGATTTTT 1890
TTTTTTTCTCTTAGATATGAGAATGTGAGTGTGATTGAATGTGTGTGAGTGCGTGTCTCTCTCGAATGAAATTCGGAGATATTGGGAGAA 1980
ACTATTAAAAAAACAAAAC 1999
```

B. α-isoform

```
AGTCGTGCAGCAGTCCCGCACACACACGCCACCGTATTCGCAAGCTGCCAGTGAGATACATCCATCTGGGGAAAAAAAAACGAAATACCCA 90
AACTCTGCAACTGTGTGTGAAAACCGTGTGTGTGTGTGTGTGTGTGTGTATCTATTTTGATAACCAGTGTCAGCCGTCCCGCGTGAAATT 180
TTCAGCAACGAGGTTTTCCGTCAATCATCATAACGTGGTTTAAATTGAAAATAAGGAATCAGTGCTTGGAAGCCAAACTTTGTCGAGTGA 270
TATTCGTGAAAGGGCAAAAAGTGAGCTGTGTTTATTTCGTTTTCGTCTCTTTTCTCTTTCAACAAGGGAGCGTGAATGGGATCCCCCACA 360
AAGCTAAAAAGAAAATAATTCAAATTATCACGGCGAGACGGCTCTACTTGAAAGAGAGAAAACAAAAACACGAGAAAATGGAATGTCAAG 450
                                                                                M  E  C  Q   4

CAGAAGCAGCAGCTTTGTTGCCTTCGTTCAGCGAGCTGACGTCGGCAGGAGTCGTCGGGCGTGACCGCCATGGATCACCGTCAGATGGCA 540
A  E  A  A  A  L  L  P  S  F  S  E  L  T  S  A  G  V  V  G  R  D  R  H  G  S  P  S  D  G   34

GCACTGATGGGTCTCAGCAATCGCAGTTGTCGTCAACTTCGGAATCTTCAGCCGAATTGAGTAAAGAGCTCCGCTTGTCCTCGGCACACG 630
S  T  D  G  S  Q  Q  S  Q  L  S  S  T  S  E  S  S  A  E  L  S  K  E  L  R  L  S  S  A  H   64

CCATGATTTTCCTCTCACAACAGAAACGCG[ATTCCCTCCAACCTGACGAG]CTATCCGCCCACGAAAGTGGGCCCACCTGCCTTCCAGCTG 720
A  M  I  F  L  S  Q  Q  K  R  D  S  L  Q  P  D  E  L  S  A  H  E  S  G  P  T  C  L  P  A   94

ATTCAGATCACCTGA[TGCTCATCCAGCTCCAAGAT]TCACCACAC 764
D  S  D  H  L  M  L  I  Q  L  Q  D  S  P  H  109
```

C. β-isoform

```
CGGTCCGTCTCTCTGACTAGTCGGTGCTGCCCTTTTGTCCGACAATTAAAGTGCATATGATTCTCGTGTTGTTTTGTGCTGTACGACCG  90
CCGTCGTTGTGTGTGTGAAATTCTATTTATTTTTTCCTATCGGTTGTCATCGCATGTGCCGCCCCTGTGTGTTTCGGAATTGCGGTCAACTT 180
TCGCTTTCGGAGCGCCAACAACGCCATCAAGCGGGCAGGTGGTTTCTATAGTGTGTGACTTGTCCTCAATTTTTCCCTCTCTCTCTCTCT 270
TGCTTCCAAACACACACACACATACAGACACGCACAGGAATCTTGTGTGTGAGGATTACAATTCTTTTTGAAAGACTTTTTTTTTTTCGT 360
CTGTGCGTGTGCGTTCTCTTTCCATACCCATAGTGCAACAGGTGTGTGTGTAGCCCTCTGGTGAGCGTTTTTTCGTGCTGCGTATAGCCG 450
CGTTGATTATCATTTTTTTCAAATCTTGTTTAAAAACAATTGTGTGAGATCTCATGTCTATTGGTTGAGATGCTAGTTGACATGGATCTC 540
                                                                M  L  V  D  M  D  L   7

GCAGCTATTGCACCACTCGGAACCAACAGTTCGTCCGGTTTCATAAACTTGTCAGGCCCATCAGTCGATACGGACCAGGTCAGTGTCCAA 630
 A  A  I  A  P  L  G  T  N  S  S  S  G  F  I  N  L  S  G  P  S  V  D  T  D  Q  V  S  V  Q   37

ATCGAACGTTTACACAGCCCCAACGGTGGTGGTGGTGGTGGTGGTGGTTCAAACAGTGGCAATGGACCCAGTGGCCAGCATCATCAC 720
 I  E  R  L  H  S  P  N  G  G  G  G  G  G  G  G  S  N  S  G  N  G  P  S  G  Q  H  H  H   67

ATGGTTGGCCATCCACAGCAACAACAACAACAACTCCATCATCATCACCATCACCACCACCACCTAGC[GGGAGCTCAGCATTTGCATC]AT 810
 M  V  G  H  P  Q  Q  Q  Q  Q  Q  L  H  H  H  H  H  H  H  H  H  L  A  G  A  Q  H  L  H  H   97

AGGACGCTGAGCTCTCCGAATTCTGAATTGTCGATTGCTTCTCTTTCAATGGCTTCATCCAGTCCCGC[GTCTACCATGTCGCCGTTCA]GT 900
 R  T  L  S  S  P  N  S  E  L  S  I  A  S  L  S  M  A  S  S  S  P  A  S  T  M  S  P  F  S  127

GCCAGTAGCAATAACAATAATAATAACAACAACAACAGTAGCTCGTCGGCGGCCATGAGCTATGCAATGAGTCACTTGAGCTCTGGTGGC 990
 A  S  S  N  N  N  N  N  N  N  N  N  S  S  S  S  A  A  M  S  Y  A  M  S  H  L  S  S  G  G  157

GTCGAGGCCGGCGGCAATCTACTGGGTGTGGGCGTGACAGTCGGCCTGACTGGGCTCGATTCCTATTGCATTTACAATCCGAATAACGCA 1080
 V  E  A  G  G  N  L  L  G  V  G  V  T  V  G  L  T  G  L  D  S  Y  C  I  Y  N  P  N  N  A  187
```

Figure 29: Nucleotide and deduced amino acid sequences of *Ftz-F1* in *D. magna.* (A) The *Ftz-F1* common region. Black and grey shaded amino acids indicate the putative DNA-binding domain (DBD) and the ligand-binding domain (LBD) respectively. The Ftz-F1 box

(italicized) and the activation factor-2 (AF-2) core (underlined) motifs are indicated. (B, C) The nucleotide sequence of isoform-specific regions. Deduced amino acid sequences starting from the first methionine for each isoform are indicated. Locations of the primers used in qRT-PCR are emboldened. Numbers on the right indicate the nucleotide and amino acid positions.

Next, I mapped the *Ftz-F1* transcripts to the genomic sequence and examined the exon-intron structure. The genomic structure of *Ftz-F1* gene is composed of 12 exons, spread over ~11 kb of genomic DNA as illustrated in Figure 30A. All exon-intron junctions possess the consensus "GT-AG" nucleotides at their 5′ and 3′ splicing sites. *αFtz-F1* contains all 12 exons except a partial deletion of exon 5, whereas *βFtz-F1* lacks of exon 1-4. The region encoding the DBD is within two exons (Figure 30A; exon 5 and 6, blue boxes) that are separated by a large intron of 2,006 bp, and the LBD is located in four exons, which are exons 9-12, orange boxes in Figure 30A.

I compared the arrangement of the exons of *Ftz-F1* obtained from *D. magna* to the structural organization of *Dr. melanogaster Ftz-F1* gene [90,91] and illustrated it in Figure 30B. I found that the common region between *αFtz-F1* and *βFtz-F1* is similarly composed of eight exons and seven introns in both *D. magna* and *Dr. melanogaster*. Importantly, four of the seven introns positions are conserved between the two species (I, II, III, and IV in Figure 30C). The first intron position (I) is within the DBD and the other three introns (II, III, and IV) are positioned within the LBD. These results show that the DBD and the LBD regions of Ftz-F1 are highly conserved between the two species.

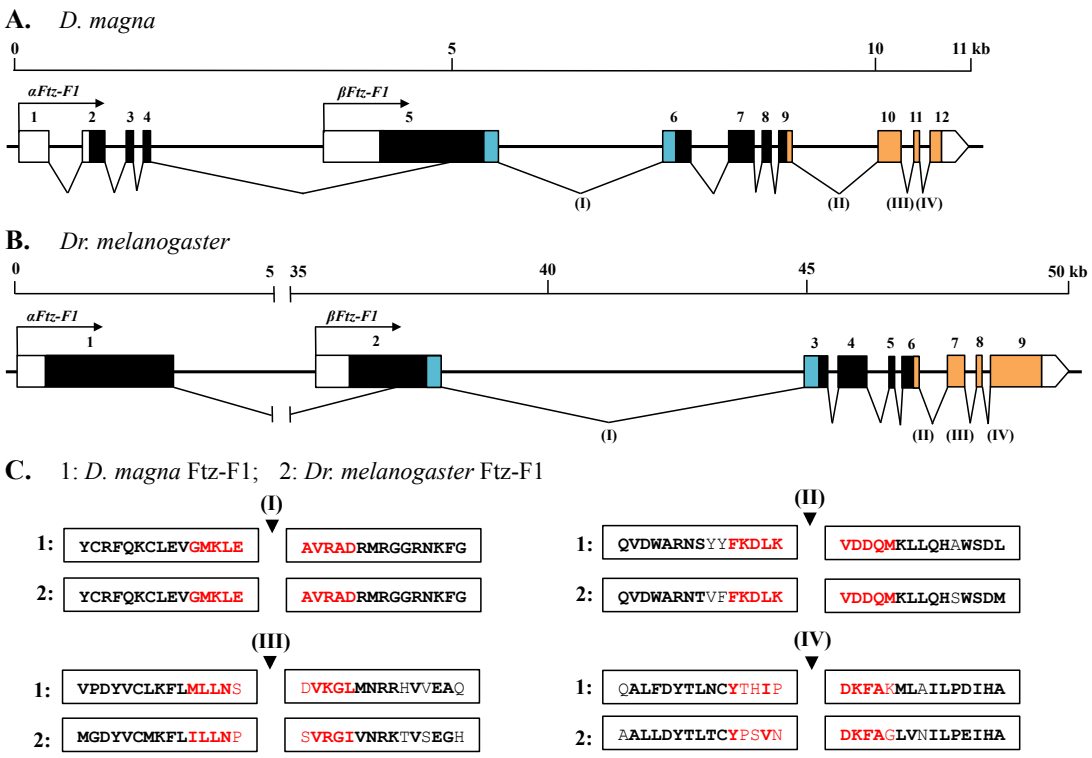

Figure 30:Genomic structural organization of (A) the *D. magna Ftz-F1* gene and (B) the *Dr. melanogaster Ftz-F1* gene. The numbered boxes are exons, and the intervening lines are introns. Colored boxes indicate coding regions; blue represents the DBD, whereas orange represents the LBD. Empty boxes indicate un-translated regions. Each isoform possesses a unique coding sequence at the 5′ end, with black arrows indicating the transcription start site. Scale bars in kilobases are provided at the top of each diagram for the size. Numbers I, II, III, and IV indicate the location of intron splice sites that are conserved between *D. magna* and *Dr. melanogaster*. (C) Putative conserved splice sites mapped to the conserved domain of Ftz-F1 from (1) *D. magna* and (2) *Dr. melanogaster*. The amino acid sequences shown are from DBD (Number I) and LBD (Number II, III, and IV). Red amino acids indicate 10 residues (five residues for pre- and post-introns, respectively) around the intron position assigned as the splice site, whereas further homology upstream and downstream of the intron are represented in black. Bold amino acid residues are residues shared between two species. Black triangles indicate the location of the intron with the splice site.

4.3.2 Features of *D. magna* Ftz-F1 proteins

I compared the obtained amino acid sequences of *D. magna* Ftz-F1 protein with those of those Ftz-F1 orthologs from *Drosophila* and various animals. As a

result, the *D. magna* Ftz-F1 proteins were predicted to have the typical structure of a nuclear structure. This structure consists of an A/B region, a conserved zinc finger DBD at a DNA recognition C region, a hinge D region, and lastly, a LBD followed by an activation function (AF-2) at the E region, as illustrated in Figure 31. Both αFtz-F1 and βFtz-F1 proteins consist of the identical 590 amino acids sequence, which includes the DBD (94 aa) and the LBD (182 aa) regions (Figure 32). They have different amino acid sequence at the A/B region as indicated in Figure 31, where αFtz-F1 and βFtz-F1 has 109 aa and 187 aa, respectively. No conserved motif of Ftz-F1 was found in the A/B region of the α- or β-isoform.

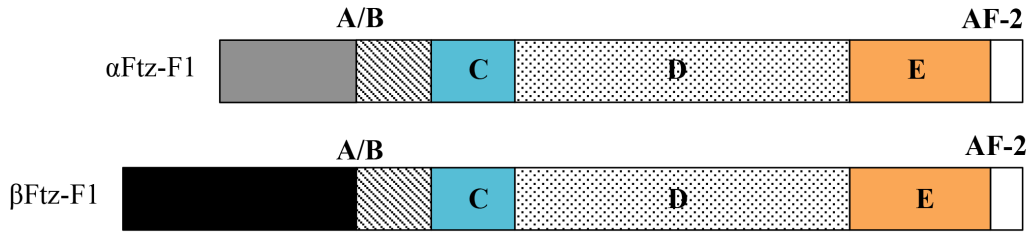

Figure 31: Schematic diagram of the Ftz-F1 protein structures. The protein structures are divided into A/B, C, D, and E regions. Blue box represents the DBD, whereas orange box represents the LBD.

Next, I aligned the DBD and the LBD regions of Ftz-F1 from *D. magna* with other Ftz-F1 othologs, namely, *M. ensis* Ftz-F1, *Dr. melanogaster* Ftz-F1, *B. mori* Ftz-F1, *T. castaneum* Ftz-F1, *M. musculus* Sf-1, and *C. elegans* nhr-25 (Figure 32). In the C region, a DNA sequence recognition region, named the Ftz-F1 box [92], is the most conserved region of the amino acid sequence among species (Figure 32A). In the E region, the LBD signature and AF-2 motif [92,93] were also found in Ftz-F1 of *D. magna* (Figure 32B). Both of these regions were most similar to those of insect orthologs.

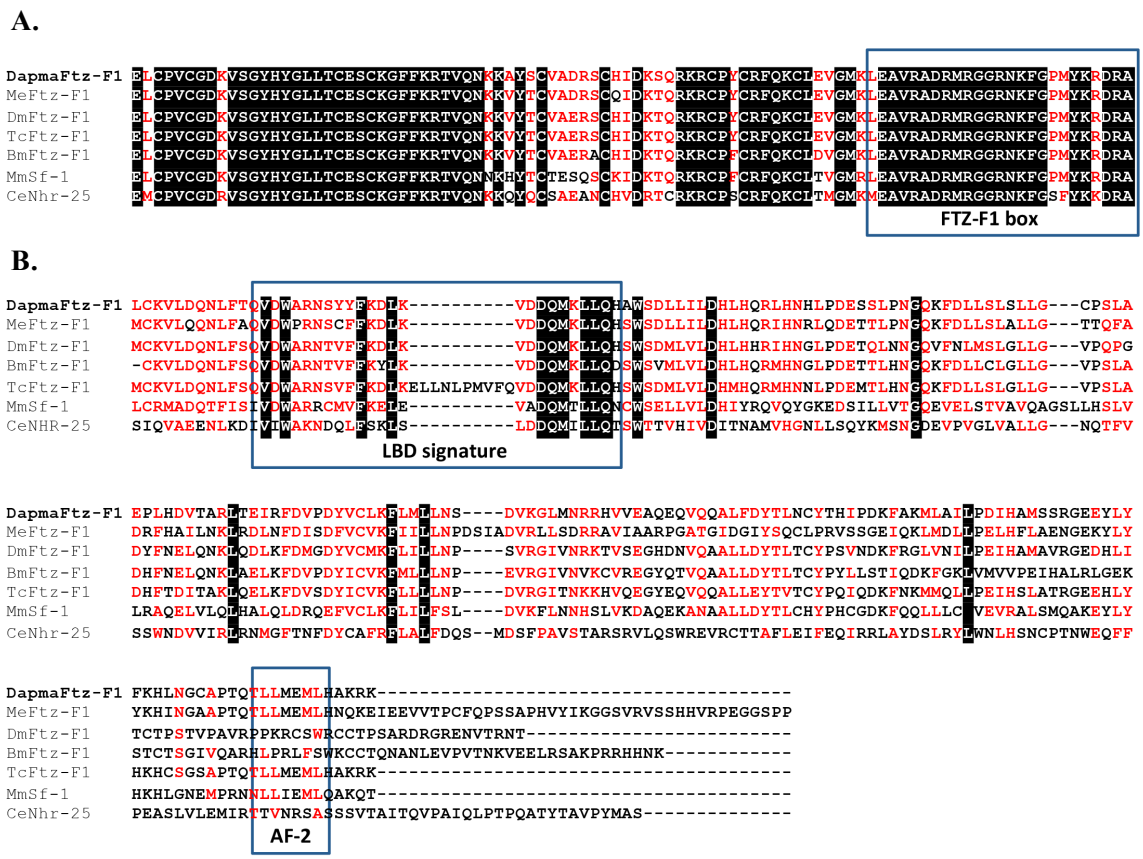

Figure 32: Evolutionary conserved domains of *D. magna* Ftz-F1. (A) Alignment of the DBD amino acid sequences at the C region. (B) Alignment of the LBD at the E region. The Ftz-F1, LBD signature and AF-2 motif are boxed. DmagFtz-F1 is *D. magna* Ftz-F1, MeFtz-F1 is *M. ensis* (shrimp) Ftz-F1, DmFtz-F1 is *Dr. melanogaster* (fruit fly) Ftz-F1, BmFtz-F1 is *B. mori* (silkworm) Ftz-F1, TcFtz-F1 is *T. castaneum* (red beetle) Ftz-F1, MmSf-1 is *M. musculus* (mouse) Sf-1 and CeNhr-25 is *C. elegans* (worm) Nhr-25. Black shaded indicates the same amino acids while red indicates the same type of amino acid in one position.

To analyze the evolutionary relationship of *D. magna* Ftz-F1 protein to other animals, a phylogenetic tree of Ftz-F1 proteins from other 12 Ftz-F1 related proteins listed in Table 14 was constructed (Figure 33). The phylogenetic tree was built through neighbor-joining method, using the whole amino acid sequences. The result in Figure 33 exhibits that the topology of the phylogenetic relationship between Ftz-F1 orthologs was in good agreement with taxonomic relationship between insects and crustaceans. Compared to the Ftz-F1 ortholog of a shrimp belonging to malacostraca

crustacean, the branchiopod crustacean *Daphnia* was more closely related to insect Ftz-F1 orthologs. This result supports the hypothesis that insects originated from branchiopod crustaceans [73].

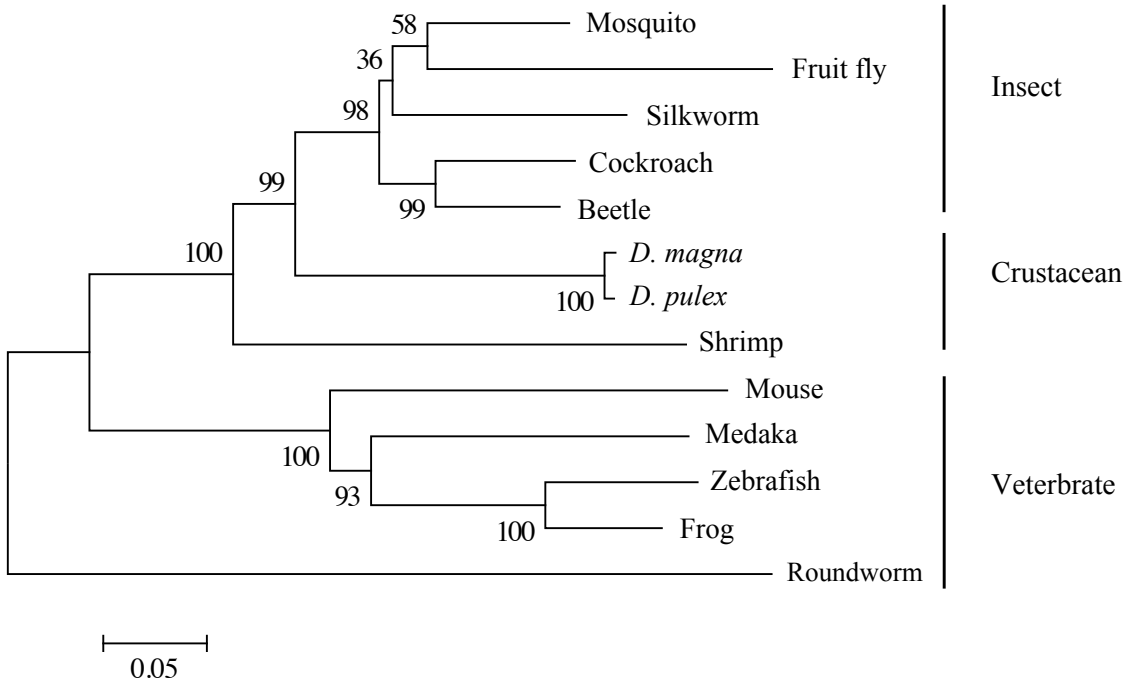

Figure 33: Phylogenetic tree of the amino acid sequences of the Ftz-F1 nuclear hormone receptor subfamily. The percentages of the replicate tree in which the associated taxa clustered together in the bootstrap test (1,000 replicates) are shown next to the branches. The bar indicates branch length and corresponds to the mean number of the differences ($P<0.05$) per residue along each branch. Evolutionary distances were computed using the p-distance method.

4.3.3 *Ftz-F1* mRNAs expression during embryogenesis

Previous study has revealed that the genes related to sex determination and differentiation are known to exhibit sex-specific differences in the abundance of transcripts [17]. Here, I investigated the sexual differences at various embryonic stages using a quantitative real-time PCR assay. Isoform-specific amplification was

achieved by designing primers at the 5′ end of each coding region of *αFtz-F1* and *βFtz-F1* transcript, as indicated in Figures 29B and 29C. The result of qRT-PCR analyses of *Ftz-F1* gene expressions during females and males embryogenesis is presented in in Figure 34.

αFtz-F1 expression just after ovulation (0-hpo) in males was almost two-fold higher than in females as exhibited in Figure 34A. In between the period after ovulation to 12-hpo, *αFtz-F1* expression gradually decreased in both males and females. In later embryonic stages (after 12-hpo), *αFtz-F1* was absent in females except for a detectable peak at 24-hpo; in males it was expressed at each time point but was depleted by 72-hpo, a stage when the embryos become juveniles and swim out from their mother's brood chamber. The temporal change in *βFtz-F1* expression, shown in Figure 34B, was more prominent, especially during early embryogenesis. At 0-hpo, the quantity of *βFtz-F1* mRNA was also two-fold higher in males. This isoform was activated three-fold at 6-hpo during gastrulation stage and then dropped at 12-hpo in both males and females. During middle and late embryogenesis, the *β*-isoform exhibited sexually dimorphic expression; however, its expression was level was lower than that of the *α*-isoform.

I summarized the sexual differences expressions of *Ftz-F1* gene in Table 16. In *D. magna, Ftz-F1* transcripts are dominantly expressed in males during most embryonic stages, except at 24-hpo for *αFtz-F1* mRNAs and 12 and 24-hpo for *βFtz-F1* mRNA. These suggest that *Ftz-F1* may play a role in regulating male trait development during *D. magna* embryogenesis.

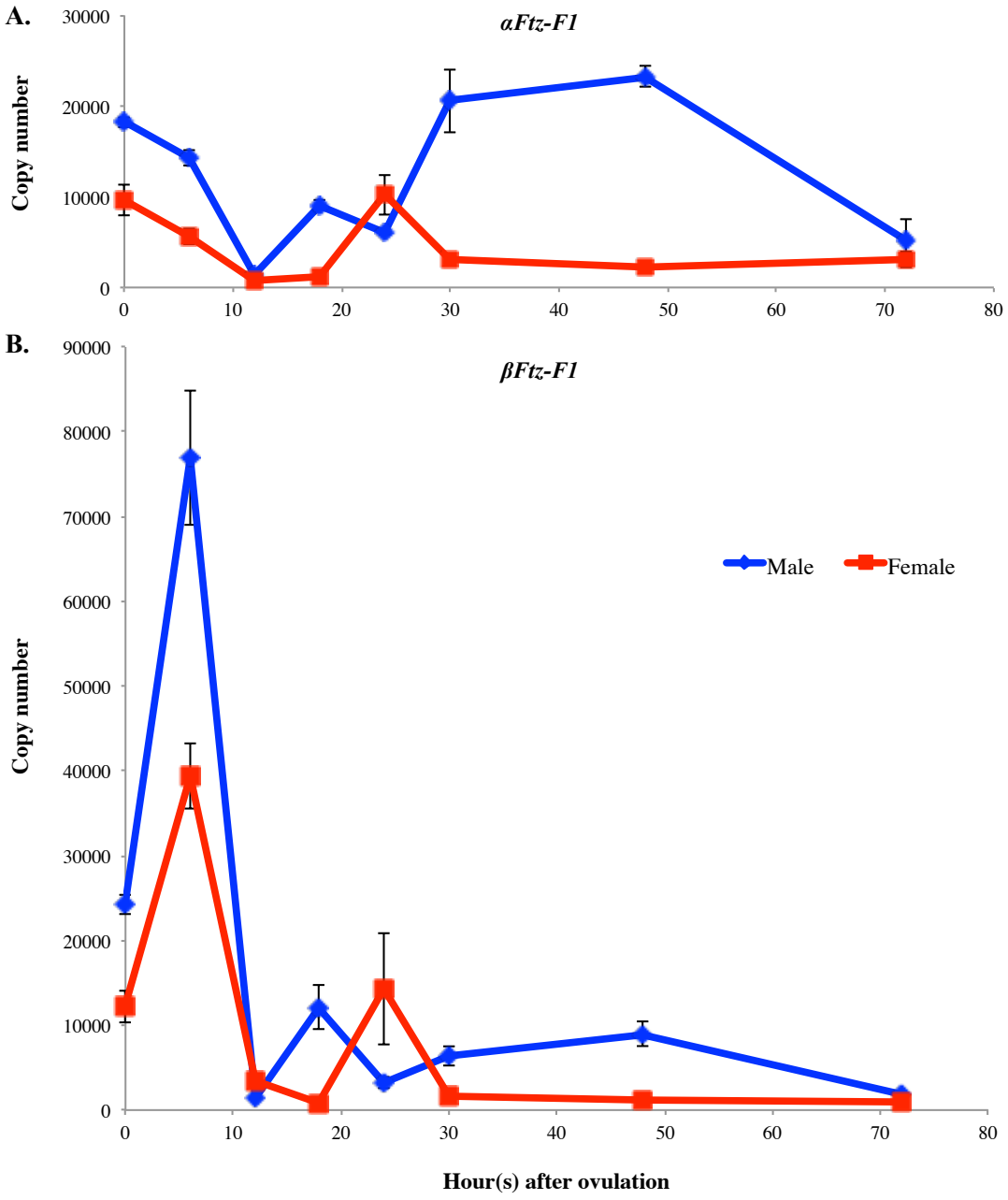

Figure 34: Temporal expression profiles of the *Ftz-F1* in embryonic development stages of *D. magna*. The expression levels of *Ftz-F1* transcripts for (A) *α*-isoform and (B) β-isoform in one embryo of female (red line) and male (blue line). Embryonic development was staged at 0-hpo (single cell egg), 6-hpo (gastrula), 12-hpo (cephalic appendage developing stage), 18-hpo (early thoracic appendage developing stage), 24-hpo (after hatching embryo), 30 hpo (middle carapace developing stage), 48-hpo (further developed thoracic appendages and antennae embryo), and 72-hpo (juvenile *Daphnia*). Results are shown as copy number of transcript per egg that were measured from three independent qPCR and error bars represent standard error values across samples.

Table 16: Sexual differences in *αFtz-F1* and *βFtz-F1* expression in *D. magna* during embryogenesis. *Ftz-F1* expression was normalized using *Ribosomal L32* expression as a reference gene. The fold difference was obtained by normalizing male expression to female expression.

Time (hpo)	*αFtz-F1* expression		*βFtz-F1* expression	
	Fold different	**Std. dev.**	**Fold different**	**Std. dev.**
0	1.88	± 0.09	1.98	± 0.17
6	2.52	± 0.25	1.96	± 0.35
12	1.74	± 0.31	0.41	± 0.05
18	7.32	± 0.72	14.49	± 5.40
24	0.60	± 0.06	0.22	± 0.07
30	6.49	± 1.90	4.12	± 1.30
48	10.33	± 0.87	7.06	± 1.95
72	1.68	± 1.21	1.91	± 0.34

Std. dev. = standard deviation.

4.3.4 Phenotypes of *Ftz-F1* RNAi embryos

To examine the roles of the *D. magna Ftz-F1* gene, I performed *Ftz-F1* gene knock down using RNAi method [36] in male and female embryos. I utilized the transgenic *Daphnia*, which is carrying the GFP gene fused to H2B gene [50], because the nuclear stained with the H2B-GFP protein enhances the visualization of cell dynamics in live embryos. Embryonic development of three *Ftz-F1*-siRNA injected eggs with a control was recorded by time-lapse imaging from 3 to 30-hpo. The snapshots at 6, 9 and 18-hpo of the time-lapse imaging are presented in Figure 35. The development of the knock down embryos was similar to the control egg (non-injected) until the gastrulation stage at 6-hpo. Subsequently, GFP intensity started to weaken (9-hpo) and the development slowed down and did not proceed normally (18-hpo). The siRNAs microinjections are summarized in Table 17. Almost all of the Control_416 siRNA-injected embryos could survive and normally develop. However, all of the *Ftz-F1* siRNA-injected embryos, regardless of its sex, failed to hatch. I

observed that some injected embryos developed eye pigment after 48 h incubation, indicating that the eggs development still slowly continued up to the eye developmental stage. Importantly, there was no difference in the RNAi phenotype between male and female embryos that were observed in this experiment.

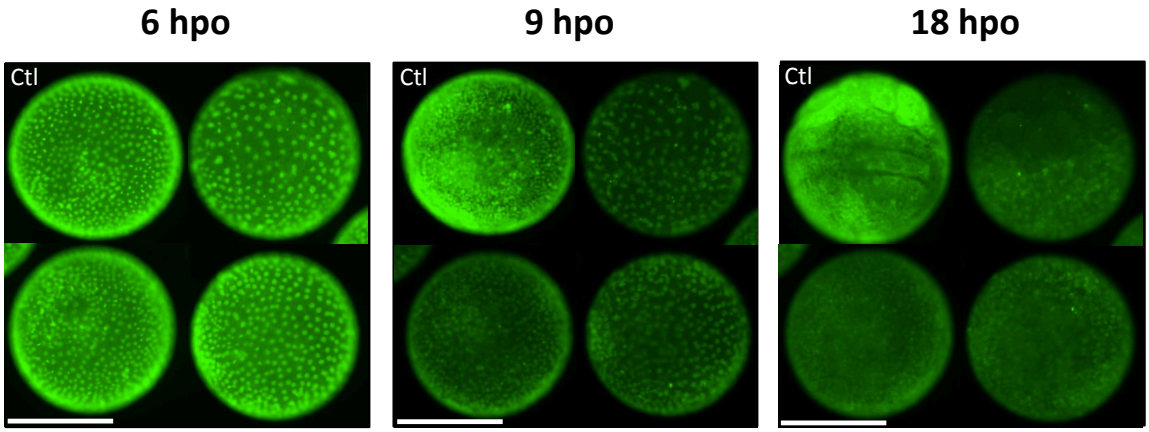

Figure 35: Development of *Ftz-F1* RNAi embryos. The snapshots at 6, 9 and 18-hpo of three *Ftz-F1* siRNA-injected male embryos with a non-injected control (Ctl) were taken from time-lapse imaging from 3 to 30-hpo. The control egg was normally developed until hatching. Scale bars: 200 µm.

Table 17: Summary of the siRNA microinjection experiment for phenotype observation. Excluding the Control_416 siRNA-injected embryos, all *Ftz-F1* siRNA-injected embryos developed abnormally, including failure to shed the outer egg membrane and slow development compared to that observed with normal eggs.

siRNA	Sex of egg	Number of injected eggs	Survived for 24 h	Developed eye pigment by 48 h
Control_416	Female	9	7	7
Control_416	Male	12	10 (*6)	4
Ftz-F1_699	Female	11	7	4
Ftz-F1_918	Female	10	8	8
Ftz-F1_918	Male	19	12 (*6)	6

* The embryos were subjected to total RNA isolation for qRT-PCR analysis.

To confirm that the *Ftz-F1* expression has been successfully knocked down during RNAi, total RNA from 24 h siRNA injected-male embryos was isolated, and then the *Ftz-F1* expression level was measured. The graph in Figure 36 is the qRT-PCR analysis result that shows 90 ± 5% of expression was suppressed when compared to the control, indicating that RNAi effectively occurred in the siRNA-injected embryos.

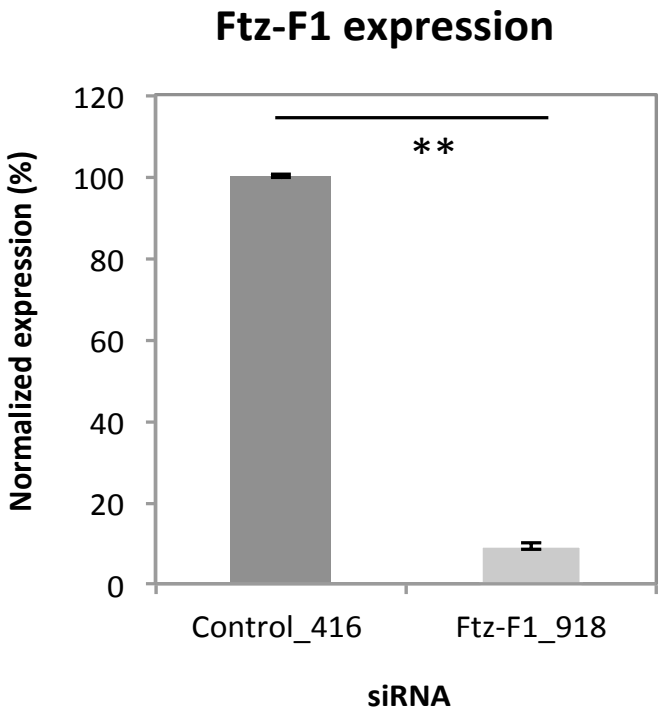

Figure 36: Normalized expression of *Ftz-F1* gene in RNAi male embryos. The normalized expression of *Ftz-f1* in Control_416 siRNA injected embryos was set as 100%. (Student's t-test; **, P<0.01).

4.3.5 Ftz-F1 binding site candidates on the *Dsx* promoter

To examine the possibility the Ftz-F1 transcription factor to activate *Dsx* genes expression in male, I performed computational analyses to identify possible Ftz-F1 binding site using the consensus binding sequence reported previously [89].

Based on computational identification result, seven hypothetical binding sites with high score value were found on the promoter/enhancer region of *Dsx* gene from *D. magna* (Table 18 (top)). To confirm whether those binding sites are conserved or are in *Daphnia* species, I performed the same computation analysis with the *Dsx* genes sequence from *D. pulex* and eight sequences were acquired (Table 18 (bottom)). I mapped the location of the hypothetical Ftz-F1 binding sites on the *Dsx* genes both from *D. magna* and *D. pulex* as illustrated in Figure 37.

Table 18: The identification of Ftz-F1 binding sites on *Dsx* genes promoter in *D. magna* (top) and in *D. pulex* (bottom). D represents direct strand while R represents reverse strand of the DNA. The same sequences between the two species are emboldened and the sequence pairs are indicated with the letter a, b and c.

Map	Strand	Start	End	Sequence	Score	ln(P)
Ftz-F1.m1[a]	R	-29483	-29473	tagt**CCAAGGTTGC**Cacgt	9.69	-11.83
Ftz-F1.m2[b]	D	-26569	-26559	gcaa**CCAAGGCCATC**gatt	9.49	-11.63
Ftz-F1.m3[c]	R	-23668	-23658	ttta**CGAAGGCCAAC**gaat	8.30	-10.34
Ftz-F1.m4	R	-13535	-13525	aatgGCAAGGACACCaaac	11.04	-13.47
Ftz-F1.m5	D	-9340	-9330	tttgTCAAGGTCGTCtccc	8.43	-10.46
Ftz-F1.m6	D	-4421	-4411	acctCCAAGTCCACCatct	7.78	-9.87
Ftz-F1.m7	D	-2328	-2318	gcatCGAAGGACGAAagac	7.89	-9.9

Map	Strand	Start	End	Sequence	Score	ln(P)
Ftz-F1.p1[a]	R	-32740	-32730	tagt**CCAAGGTTGCC**attg	9.69	-11.83
Ftz-F1.p2[b]	D	-30058	-30048	gcaa**CCAAGGCCATC**gatt	9.49	-11.63
Ftz-F1.p3	D	-28353	-28343	gttaCCACGGACACCacca	9.25	-11.33
Ftz-F1.p4	D	-27012	-27002	ctgaCGAAGGTCCCCcctt	7.98	-10.07
Ftz-F1.p5[c]	R	-26801	-26791	tttg**CGAAGGCCAAC**cgtc	8.30	-10.34
Ftz-F1.p6	D	-24263	-24253	gaagCCAAGGATGCTttga	8.95	-10.98
Ftz-F1.p7	D	-19508	-19498	accaCCACGGCCACCctcc	8.17	-10.28
Ftz-F1.p8	R	-2412	-2402	gttgCCAAGGACTCTagga	8.42	-10.44

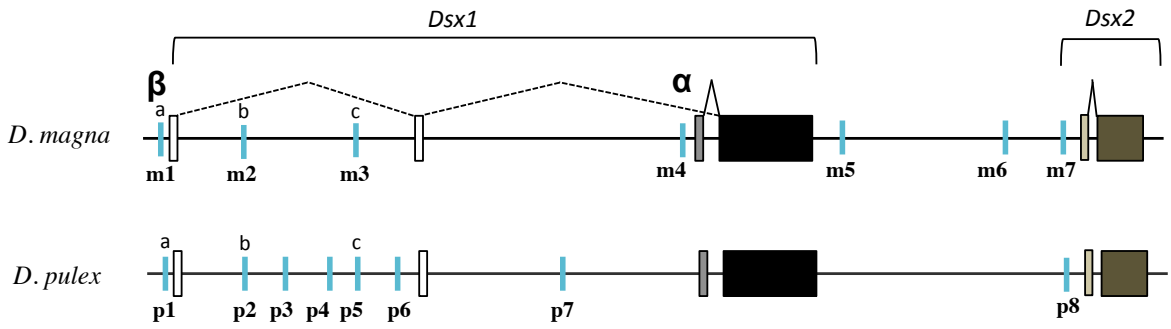

Figure 37: The schematic diagram of *Dsx* genes of *D. magna* and *D. pulex* with annotation of the hypothetical Ftz-F1 binding site locations. The blue lines indicate the location of binding sites obtained from Table 16.

By comparing both annotations, I found three conserved binding sites sequence that are labeled with a, b and c for each pair. Those binding sites contain the same "AAGG" core sequence for Ftz-F1 proteins [89] and are located near the exons of *Dsx1 β*-isoform. This result provides us with candidates for Ftz-F1 binding site on the promoter/enhancer of *Dsx1* gene.

4.4 Discussion

In this study, I have cloned and characterized the *Ftz-F1* orthologs in the *D. magna.* Similar to that observed in *Drosophila, D. magna Ftz-F1* produces two splicing variants, *αFtz-F1* and *βFtz-F1,* which encode 699 and 777 amino acids, respectively. Both isoforms share a DNA-binding domain, a ligand-binding domain, and an AF-2 activation domain and differ only at the A/B domain. The genomic organization and phylogenetic position of *Ftz-F1* suggested that *Ftz-F1* has diverged from an ancestral gene common to branchiopod crustacean and insect *Ftz-F1* genes. Glenner *et al.* (2006) hypothesized that insects originated from branchiopod crustacean and this study also supports the hypothesis in which the phylogenetic

relationship of Ftz-F1 from *Daphnia* that was more closely related to insect orthologs compared to the malacostracan crustaceans.

Based on qRT-PCR analysis, I discovered that both *αFtz-F1* and *βFtz-F1* transcripts exhibited dimorphism in their expression during embryogenesis, indicating that it has sex-specific functions. The *Ftz-F1* RNAi during *D. magna* embryogenesis led to slow and abnormal development after gastrulation stage, hatching failure, and stopped developing at 30 to 48-hpo, suggesting that *Ftz-F1* is essential for its embryonic development. Although this embryonic lethality prevented us from analyzing *Ftz-F1* sex-specific functions, its expression pattern suggested potential roles in *Daphnia* ESD as the following discussion.

First, in one-cell embryos at 0-hpo, male embryos exhibit two-fold higher expression in both isoforms compared to that observed in females (Table 16). Since adults exposed to the JH agonist Fenoxycarb at the critical stage of sex determination would ovulate eggs to developed as males [44], these expression patterns suggest activation of *Ftz-F1* expression occurred during oogenesis in response to JH stimuli, and the synthesized transcripts were deposited into eggs as maternal RNAs, which may imply that *Ftz-F1* may be a direct target of JH. Previous studies in *Drosophila* have shown that Ftz-F1 functions as a mediator that facilitates JH activation gene expression [87,94]. Since *D. magna* Ftz-F1 is evolutionarily close related to Ftz-F1 of the insects, it is rational to speculate the involvement of Ftz-F1 in JH signaling pathway in ESD to activate the downstream gene *Dsx1* in male sex-determining pathway.

Second, during the gastrulation stage, *βFtz-F1* was transiently activated and highly expressed in males. Importantly, this isoform was more abundant compared to the *αFtz-F1* transcript, suggesting that *βFtz-F1* may have a dominant role in sex

determination. Additionally, I found three candidates of Ftz-F1 binding sites in *Dsx1* *β*-promoter and this result may lead to the assumption that maternal transcripts and/or zygotic transcription of *Ftz-F1* may function in activating *Dsx1* during male sex determination and differentiation.

Third, in the later stages of embryogenesis, the expression of *αFtz-F1* transcript was observed to be dominant, which may suggest that this transcript is responsible for male trait development. In previous studies, *Me. Ensis* Ftz-F1 was also detected in testis [95], and Ftz-F1α of *X. laevis* was discovered in developing gonad and testis [96]. Moreover, the homolog of Ftz-F1 in mammalian Sf-1 is a critical regulator for normal development of hypothalamic-pituitary-gonadal axis during reproduction and sexual differentiation [97]. These findings indicated that the role of *Ftz-F1* orthologs in sexual development is evolutionary conserved among species.

Chapter 5 General discussion and conclusion

5.1 General discussion

Sex is widespread for reproduction in animal kingdom. In the sex determination process, through interactions of several genes in a hierarchical manner, an initial cue leads to sex-specific expression of the major effector of sexual differentiation, *Doublesex* (*Dsx*). Although how genetic factors on sex chromosomes control *Dsx* expression have been extensively studied in model organisms, there is limited knowledge about dependence of *Dsx1* on environmental signals. In this study, *D. magna* was chosen as model to study environmental sex determination that is implemented by male-specific expression of *Dsx* ortholog, *Dsx1*. Unlike most of insect *Dsx* that exhibit sex-splicing variants, *D. magna* shows sexually dimorphism of *Dsx1* expression at the transcriptional level. Because of the difference in these transduction mechanisms, it has been suggested that factors regulating expression of *Doublesex* are independently co-opted during evolution between crustacean and insects [17].

In *Daphnia,* unfavorable environmental conditions are conveyed through the endocrine system by releasing juvenile hormone as signals to sexually dimorphic cells. To understand the molecular nature on how this sex determination pathway controls the transcription of sexual major effector gene *Dsx1*, it is essential to know the temporal expression during early stages of the cells. Transcriptional regulation of *Dsx1* comprises at least three phases during embryogenesis: non-sex-specific initiation, male-specific up-regulation, and its maintenance. The first initiation occurs at gastrulation stage, the activation of α-promoter (Chapter 2). Interestingly, enhancer element harboring a consensus Vri binding site overlapped with Dsx binding site was found on the α-promoter. The transcription factor Vri exhibits male-specific

expression in early gastrulation before the *Dsx1* up-regulation phase begins, suggesting *Vri* role as an activator of *Dsx1*. Targeted mutagenesis to disrupt the enhancer sequence on genome in males also led to the reduction of *Dsx1* expression. When modulating Vri activity by RNAi-based suppression and mRNA overexpression, corresponding effects on *Dsx1* expression levels were observed, and these findings indicate that Vri directly regulates the transcription of *Dsx1* gene (Chapter 3).

In genetic sex-determining pathways, new genes have recently been identified in various organisms, which reveals the importance of gene co-option. Mechanisms for co-option of new sex-determining genes are largely divided into three categories: 1) allelic diversification, 2) duplication of genes related to sexual development and 3) recruitment of a novel gene with no homology to any known sexual development. First, by allelic diversification, transcription factor SOX3 was recruited as a master regulator for sex determination in mice [98] and Indian ricefish [99]. By the same mechanism, the DM-domain gene Dmrt1 and the gonadal soma-derived growth factor (Gsdf) were also co-opted at the top of sex-determining pathways in birds [100] and Luzon ricefish [101] respectively. Second, in frog [102] and Medaka [103], the *Dmrt1* gene was duplicated and one of the duplicates gained function as a master sex-determining gene. In insects, transformer orthologs, which are conserved components of the sex-determining cascades, were duplicated in honeybee [104,105], resulting in upstream regulators named the *Csd.* These findings suggested that orthologous genes are repeatedly co-opted for genetic sex-determining pathways in independent animal lineages. However, as the third category, novel factors such as a piRNA and the interferon regulatory factor irf9 have been reported as sex determiners in the silkworm and the rainbow trout. In this study, I identified *Vri* as an activator of *dsx1*

in *D. magna*. Interestingly, *Vri* gene was previously identified as one of the genes regulated by Dsx protein in male *Drosophila* [59]. Therefore, I speculated that *Vri* might be repeatedly employed in the sex-determining regulatory networks in organisms.

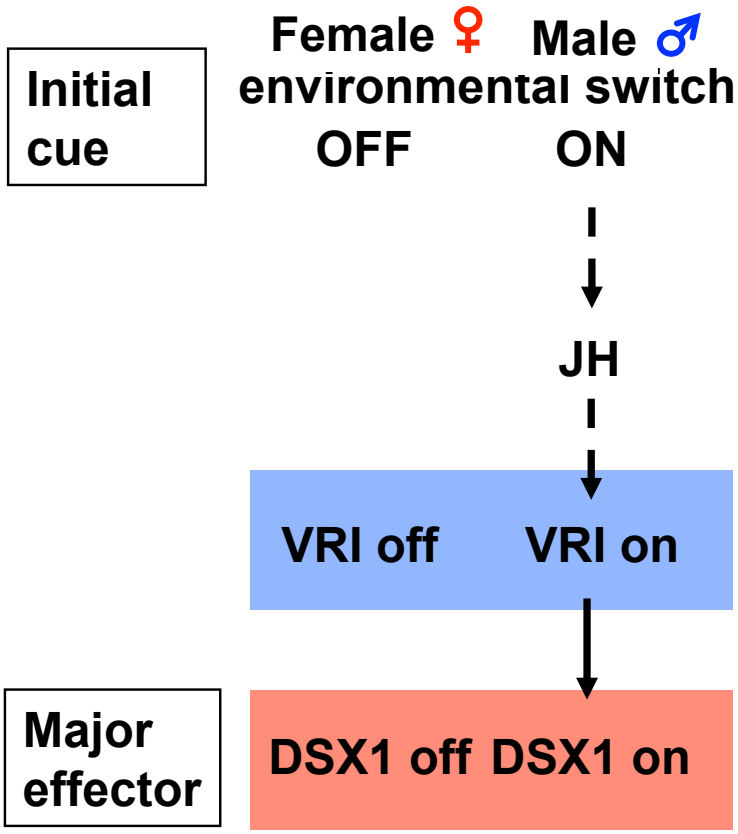

Figure 38: Simplified view of the environmental sex determining pathway in *D. magna*. Solid arrow indicaed direct interaction whereas dash arrows indicated possible interactios.

Based on the timing of JH action, Vri, and Dsx1, I would like to propose a hierarchy of signal transduction in *D. magna* sex determination as presented in Figure 38. In this hierarchy, JH first stimulates expression of *Vri,* which in turn activates *Dsx1* expression, thereby closing the gap between the JH signal and the pathway effector Dsx1. To examine the possibility that the JH-receptor MET directly regulates *Vri* activation, I have searched for sequences similar to the MET-binding site for the

Vri promoter/enhancer. One candidate sequence that is conserved in two *Daphnia* species was found, suggesting that this motif functions as an element to regulate the JH-dependent gene expression. However, because there is still time lag between JH signal and *Vri* activation (around 10 hpo), there might be other molecules that respond to JH signal and then direct the male-specific *Vri* transcription. Thus, discovering these early response genes of JH signal may improve the understanding of hormonal signaling and environmental sex determination pathway.

In the *D. magna* ESD molecular cascade, *Dsx1* is transcribed both in males and females at 3- to 6-hpo during the initiation phase of *Dsx1* transcription. The hypothesis is that in males, Vri might form a heterodimer with Dsx1, bind to the enhancer and up-regulate *Dsx1* expression 6 to 9-hpo. *Drosophila* Dsx is known to form a heterodimer with bZIP-domain transcription factor and bind to the fat body enhancer (FBE) of the yolk protein gene [72]. Transactivation of *Dsx1* by a truncated Vri lacking the bZIP domain in this study also suggests that heterodimeric combination of Dsx and bZIP transcription factor has function as a transcriptional regulator before divergence of insects and crustacean. Even though this study has provided genetic evidence of *Dsx1* activation by Vri function, the *Vri* functional analyses led to embryonic lethality due its pleiotropic nature averting the deduction that Vri is the sole component acting as a *Dsx1* activator necessary for male trait development. To understand more about how Vri functions in environmental sex determination, localization of Vri, specifically in early embryo, was clarified and knock down/overexpression in cell that endogenously express Vri was performed. This study would avoid alternation of non-sex specific function of Vri in later embryo.

Besides *Vri* gene, I also characterized the *Ftz-F1* gene in *D. magna* (Chapter 4), demonstrating that it is very closely related to insect *Ftz-F1* orthologs. I found that both two isoforms of *Ftz-F1* have sexually dimorphic expression and gene silencing led to embryonic lethality. These findings led to the speculation that Ftz-F1 may have its role in sex determination also conserved in *D. magna.* To confirm this hypothesis, studying the function of specific isoforms in sex determination and differentiation mechanisms of *D. magna* is necessarry. For that, more sophisticated methods for analyzing gene functions, such as tissue-specific and inducible knock down techniques would be required in future.

The insight into regulation of sex determination in *Daphnia* through this study could provide knowledge for the use of biotechnology to induce sex change in crustacean. For crustacean monosex culture, silencing a regulater of the male sexual differentiation, IAG gene, has been demonstrated to generate sex-reversal of male in *M. rosenbergii* (giant prawn), eventually facilitating the production all-male population in two generation [6]. However, because the IAG is located downstream of sexual development and it exhibit ongoing expression, continuous silencing of the IAG gene is necessary for this technology. Identification of other genes that position upstream of the sex-determination cascade or function as a master sex-determinant could solve this problem. In the decapods crustaceans, the initiation of sexual development occurs with a sex-specific genetic cascade that is mediated through a various chromosomal mechanism of sex determination [106]. However, there is no knowledge about regulators that trigger the genetic cascade of sex determination. Since genetic regulation of sex determination is still poor amongst the decapods crustaceans, their sex determination mechanisms could be learnt for its closest model species in the branchiopod crustacean *Daphnia*. Gene conservation in the sex-

determining pathway can be observed in the same clade as showin in the insect clade and therefore, the sex-determining genes identified in this study can be tested on their ability for decapod crustacean sex determination, ultimately contributing to development of monosex culture.

5.2 Conclusion

In this study, I discovered 1) the co-option of transcription factor Vrille as the activator of major effector *Dsx1* in *Daphnia* sex-determining pathway and 2) the conservation sequence and sexually dimorphic expression of Ftz-F1. These findings add new knowledge both on the molecular mechanisms that underlie environmental sex determination and on evolution of sex-determining mechanisms. In addition, this study provides molecular insights into sex determination of commercially important crustaceans, which in turn could contribute to the development of monosex culture in aquaculture fields.

References

1. Bull J. Sex determining mechanisms: an evolutionary perspective. Experientia. 1985; 1285–1296.
2. Eggers S, Sinclair A. Mammalian sex determination — insights from humans and mice. Chromosom Res. 2012; 20: 215–238.
3. Ocal G. Current Concepts in Disorders of Sexual Development. J Clin Pediatr Endocrinol. 2011; 3: 105–114.
4. Koukidou M, Alphey L. Practical Applications of Insects' Sexual. Sex Dev. 2014; 8: 127–136.
5. Sagi A, Eliahu DA. The androgenic gland and monosex culture of freshwater prawn Macrobrachium rosenbergii (De Man): a biotechnological perspective. Aquac Res. 2005; 36: 231–237.
6. Ventura T, Sagi A. The insulin-like androgenic gland hormone in crustaceans: From a single gene silencing to a wide array of sexual manipulation-based biotechnologies. Biotechnol Adv. 2012; 30: 1542–1550.
7. Barton NH, Charlesworth B. Why sex and recombination? Science. 1998; 281: 1986–1990.
8. Wilhelm D, Palmer S, Koopman P. Sex Determination and Gonadal Development in Mammals. Physiol Rev. 2007; 87: 1–28.
9. Levy A, Crown A, Reid R. Endocrine intervention for transsexuals. Clin Endocrinol (Oxf). 2003; 59: 409–418.
10. Cline TW, Meyer BJ. VIVE LA DIFFERENCE : Males vs Females in Flies vs Worms. Annu Rev Genet. 1996; 30: 637–702.
11. Williams TM, Carroll SB. Genetic and molecular insights into the development and evolution of sexual dimorphism. Nat Rev Genet. 2009; 10: 797–804.

12. Marin I, Baker B. The Evolutionary Dynamics of Sex Determination. Science. 1998; 281: 1990–1994.

13. Zarkower D. Establishing sexual dimorphism: conservation amidst diversity? Nat Rev Genet. 2001; 2: 175–185.

14. Pomiankowski A, Nothiger R, Wilkins A. The evolution of the Drosophila sex-determination pathway. Genetics. 2004; 166: 1761–1773.

15. Pane A, Salvemini M, Delli Bovi P, Polito C, Saccone G. The transformer gene in Ceratitis capitata provides a genetic basis for selecting and remembering the sexual fate. Development. 2002; 129: 3715–3725.

16. Gempe T, Hasselmann M, Schiott M, Hause G, Otte M. Sex determination in honeybee: Two separate mechanisms induce and maintain the female pathway. PLoS Biol. 2009 7: e1000222.

17. Kato Y, Kobayashi K, Watanabe H, Iguchi T. Environmental Sex Determination in the Branchiopod Crustacean Daphnia magna: Deep Conservation of a Doublesex Gene in the Sex-Determining Pathway. PLoS Genet. 2011; 7: e1001345.

18. Korpelainen H. Sex ratios and condition required for environmental sex determination animals. Biol Rev. Blackwell Publishing Ltd; 1990; 65: 147–184.

19. Organ C, Janes D. Evolution of sex chromosomes in Sauropsida. Integ Comp Biol. 2008; 48: 512–519.

20. Bulmer M, Bull JJ. Models of polygenic sex determination and sex-ratio control. Evolution (N Y). 1982; 36: 13–26.

21. Epper F, Bryant P. Sex-specific control of growth and differentiation in the Drosophila genital disk, studied using a temperature-sensitive transformer-2

mutation. Dev Biol. 1983; 100: 294–307.

22. Hodgkin J. Exploring the envelope: Systematic alteration in the sex-determination systemof the nematode Caeraorhabditis elegens. Genetics. 2002; 162: 767–780.

23. Shoemaker CM, Crews D. Analyzing the coordinated gene network underlying temperature-dependent sex determination in reptiles. Semin Cell Dev Biol. 2009; 20: 293–303.

24. Toyota K, Kato Y, Sato M, Sugiura N, Miyagawa S, Miyakawa H, et al. Molecular cloning of doublesex genes of four cladocera (water flea) species. 2013; 14: 239.

25. Sagi A, Cohen D. Growth, maturation and progeny of sex-reversed Macrobrachium rosenbergii males. World Aquac. 1990; 21: 87–90.

26. Ginsburger-Vogel T, Charniaux-Cotton H. Sex determination. In: Abele LG, editor. The biology of Crustacean. Orlando, FL, USA: Academic Press; 1982. pp. 257–281.

27. Ventura T, Manor R, Aflalo ED, Weil S, Khalaila I, Rosen O, et al. Expression of an androgenic gland-specific insulin-like peptide during the course of prawn sexual and morphotypic differentiation. Endocrinology. 2011; 2011: 476283.

28. Hebert PDN. The population biology of Daphnia (Crustacea, Daphnidae). Biol Rev. Blackwell Publishing Ltd; 1978; 53: 387–426.

29. Kleiven OT, Larsson. P, Hobk A. Sexual reproduction in Daphnia magna requires three stimuli. Oikos. 1992; 65: 197–206.

30. Sagawa K, Yamagata H, Shiga Y. Exploring embryonic germ line development in the water flea, Daphnia magna, by zinc-finger-containing VASA as a marker. Gene Expr Patterns. 2005; 5: 669–678.

31. Olmstead AW, LeBlanc GA. Effects of endocrine-active chemicals on the development of sex characteristics of Daphnia magna. Environ toxical Chem. 2000; 19: 2107–2113.

32. Mitchell SE. Intersex and male development in Daphnia magna. Hydrobiologia. 2001; 145–156.

33. Orsini L, Decaestecker E, Meester L De, Pfrender M, Colbourne J. Genomics in the ecological arena. Biol lett. 2011; 7: 2–3.

34. Colbourne JK, Pfrender ME, Gilbert D, Thomas WK, Tucker A, Oakley TH, et al. The ecoresponsive genome of Daphnia pulex. Science. 2011; 331: 555–561.

35. Watanabe H, Tatarazako N, Oda S, Nishide H, Uchiyama I, Morita M, et al. Analysis of expressed sequence tags of the water flea Daphnia magna. Genome. 2005; 48: 606–609.

36. Kato Y, Shiga Y, Kobayashi K, Tokishita SI, Yamagata H, Iguchi T, et al. Development of an RNA interference method in the cladoceran crustacean Daphnia magna. Dev Genes Evol. 2011; 220: 337–345.

37. Törner K, Nakanishi T, Matsuura T, Kato Y, Watanabe H. Optimization of mRNA design for protein expression in the crustacean Daphnia magna. 2014; 707–715.

38. Naitou A, Kato Y, Nakanishi T, Matsuura T, Watanabe H. Heterodimeric TALENs induce targeted heritable mutations in the crustacean Daphnia magna. Biol Open. 2015; 4: 364–9.

39. Nakanishi T, Kato Y, Matsuura T, Watanabe H. TALEN-mediated homologous recombination in Daphnia magna. Sci Rep. Nature Publishing Group; 2015; 5: 18312.

40. Nakanishi T, Kato Y, Matsuura T, Watanabe H. TALEN-mediated knock-in

via non-homologous end joining in the crustacean Daphnia magna. Sci Rep.; 2016; 6: 36252.

41. Nakanishi T, Kato Y, Matsuura T, Watanabe H. CRISPR / Cas-Mediated Targeted Mutagenesis in Daphnia magna. PLoS One. 2014; 9: e98363.

42. Hobaek A, Larsson P. Sex determination of Daphnia magna. Ecology. 1990; 71: 2255–2268.

43. Banta A, Brown L. Control sex in cladocera. III. Localization of the critical period for control of sex. Proc Natl Acad Sci. 1929; 15: 71–81.

44. Kato Y, Kobayashi K, Oda S, Tatarazako N, Watanabe H, Iguchi T. Sequence divergence and expression of a transformer gene in the branchiopod crustacean, Daphnia magna. Genomics. 2010; 95: 160–165.

45. Oda S, Tatarazako N, Watanabe H, Morita M, Iguchi T. Production of male neonates in Daphnia magna (Cladocera, Crustacea) exposed to juvenile hormones and their analogs. Chemosphere. 2005; 61: 1168–1174.

46. Tatarazako N, Oda S, Watanabe H, Morita M, Iguchi T. Juvenile hormone agonists affect the occurrence of male Daphnia. Chemosphere. 2003; 53: 827–833.

47. Burtis K, Baker B. Drosophila doublesex gene controls somatic sexual differentiation by producing alternatively spliced mRNAs encoding related sex-specific polypeptides. Cell. 1989; 56: 997–1010.

48. Ayoubi TAY, Van De Ven WJM. Regulation of gene expression by alternative promoters. FASEB J. 1996; 10: 453–460.

49. Kluttgen B, Dulmer U, Engels M, Ratte H. ADaM, an artificial freshwater for the culture of zooplankton. Water Res. 1994 ;28: 743–746.

50. Kato Y, Matsuura T, Watanabe H. Genomic integration and germline

transmission of plasmid injected into crustacean Daphnia magna eggs. PLoS One. 2012; 7: e45318.

51. Miyakawa H, Toyota K, Hirakawa I, Ogino Y, Miyagawa S, Oda S, et al. A mutation in the receptor Methoprene-tolerant alters juvenile hormone response in insects and crustaceans. Nat Commun. Nature Publishing Group; 2013; 4: 1856.

52. Nong Q, Mohamad Ishak NS, Matsuura T, Kato Y, Watanabe H. Mapping the expression of the sex determining factor Doublesex1 in Daphnia magna using a knock-in reporter. Sci Rep. 2017; 7: 13521.

53. True JR, Carroll SB. Gene Co-option in physiological and morphological evolution. Annu Rev Cell Dev Biol. 2002; 18: 53–80.

54. Rund SSC, Yoo B, Alam C, Green T, Stephens MT, Zeng E, et al. Genome-wide profiling of 24 hr diel rhythmicity in the water flea , Daphnia pulex: network analysis reveals rhythmic gene expression and enhances functional gene annotation. BMC Genomics. 2016; 17: 1–20.

55. George H, Terracol R. The vrille gene of drosophila is a maternal enhancer of decapentaplegic and encodes a new member of the bZIP family of transcription factors. Genetics. 1997; 146: 1345–1363.

56. Beckstead RB, Lam G, Thummel CS. The genomic response to 20-hydroxyecdysone at the onset of Drosophila metamorphosis. Genome Biol. 2005; 6: R99.

57. Cowell IG, Skinner A, Hurst HC. Transcriptional repression by a novel member of the bZIP family of transcription factors. Mol Cell Biol. 1992; 12: 3070–3077.

58. Zhang W, Zhang J, Kornuc M, Kwan K, Frank R, Nimer SD. Molecular

cloning and characterization of NF-IL3A, a transcriptional activator of the human interleukin-3 promoter. Mol Cell Biol. 1995; 15: 6055–6063.

59. Lebo MS, Sanders LE, Sun F, Arbeitman MN. Somatic , germline and sex hierarchy regulated gene expression during Drosophila metamorphosis. BMC Genomics. 2009; 10: 80–103.

60. Herpin A, Schartl M. Plasticity of gene-regulatory networks controlling sex determination: of masters, slaves, usual suspects, newcomers, and usurpators. EMBO Rep. 2015; 16: 1–15.

61. Tsunoda T, Takagi T. Estimating transcription factor bindability on DNA. Bioinformatics. 1999; 15: 622–630.

62. Turatsinze J, Thomas-chollier M, Defrance M, Helden J Van. Using RSAT to scan genome sequences for transcription factor binding sites and cis-regulatory modules. Nat Protoc. 2008; 3: 1578–1588.

63. Thompson JD, Higgins DG, Gibson TJ. CLUSTAL W: improving the sensitivity of progressive multiple sequence alignment through sequence weighting, position-specific gap penalties and weight matrix choice. Nucleic Acids Res. 1994; 22: 4673–4680.

64. Tamura K, Stecher G, Peterson D, Filipski A, Kumar S. MEGA6: Molecular Evolutionary Genetics Analysis Version 6.0. Mol Biol Evol. 2013; 30: 2725–2729.

65. Sumiya E, Ogino Y, Toyota K, Miyakawa H. Neverland regulates embryonic moltings through the regulation of ecdysteroid synthesis in the water flea Daphnia magna , and may thus act as a target for chemical disruption of molting. Appl Toxicol. 2016; 1476–1485.

66. Vandesompele J, Preter K De, Poppe B, Roy N Van, Paepe A De. Accurate

normalization of real-time quantitative RT -PCR data by geometric averaging of multiple internal control genes. Genome Biol. 2002; 3: 1–12.

67. Asada M, Kato Y, Matsuura T, Watanabe H. Early Embryonic Expression of a Putative Ecdysteroid-Phosphate Phosphatase in the Water Flea, Daphnia magna (Cladocera: Daphniidae). J Insect Sci. 2014; 14: 1–6.

68. Sasakura Y, Awazu S, Chiba S, Kano S, Satoh N. Application of Minos, one of the Tc1/mariner superfamily transposable elements, to ascidian embryos as a tool for insertional mutagenesis. Gene. 2003; 308: 11–20.

69. Sander JD, Maeder ML, Reyon D, Voytas DF, Joung JK, Dobbs D. ZiFiT (Zinc Finger Targeter): an updated zinc finger engineering tool. Nucleic Acids Res. 2010; 38: 462-468.

70. Gagnon JA, Valen E, Thyme SB, Huang P, Ahkmetova L, Pauli A, et al. Efficient mutagenesis by Cas9 protein-mediated oligonucleotide insertion and large-scale assessment of single-guide RNAs. PLoS One. 2014; 9: 5–12.

71. Honda Y, Tsuchiya K, Sumiyoshi E, Haruta N, Sugimoto A. Tubulin isotype substitution revealed that isotype composition modulates microtubule dynamics in C . elegans embryos. J Cell Science. 2017; 1652–1661.

72. An W, Wensink PC. Integrating sex- and tisue-specific regulation within a single Drosophila enhancer. Genes Dev. 1995; 256–266.

73. Glenner H, Thomsen PF, Hebsgaard MB, Sorensen M V., Willerslev E. EVOLUTION: The Origin of Insects. Science. 2006; 314: 1883–1884.

74. Szuplewski S, Kottler B, Terracol R. The Drosophila bZIP transcription factor Vrille is involved in hair and cell growth. Development. 2003; 130: 3651–3662.

75. Szuplewski S, Fraisse-Véron I, George H, Terracol R. Vrille is required to

ensure tracheal integrity in Drosophila embryo. Dev Growth Differ. 2010; 52: 409–418.

76. Glossop NRJ, Houl JH, Zheng H, Ng FS, Dudek SM, Hardin PE. vrille feeds back to control circadian transcription of Clock in the Drosophila circadian oscillator. Neuron. 2003; 37: 249–261.

77. Motomura Y, Kitamura H, Hijikata A, Matsunaga Y, Matsumoto K, Inoue H, et al. The transcription factor E4BP4 regulates the production of IL-10 and IL-13 CD4+ T cells. Nat Immunol. 2011; 12: 450–459.

78. Zhong C, Zhu J. Transcriptional regulators dictate innate lymphoid cell fates. Protein Cell. Higher Education Press; 2017; 8: 242–254.

79. Nandakumar V, Chou Y, Zang L, Huang XF, Chen S-Y. Epigenetic control of natural killer cell maturation by histone H2A deubiquitinase, MYSM1. Proc Natl Acad Sci. 2013; 110: 3927–3936.

80. Ueda H, Sonoda S, Brown JL, Scott MP, Wu C. A sequence-specific DNA-binding protein that activates fushi tarazu segmentation gene expression. Genes Dev. 1990; 4: 624–35.

81. Lala DS, Rice D a, Parker KL. Steroidogenic factor I, a key regulator of steroidogenic enzyme expression, is the mouse homolog of fushi tarazu-factor I. Mol Endocrinol. 1992; 6: 1249–1258.

82. Honda S-I, Morohashi K-I, Nomura M, Takeya H, Kitajima M, Omura T. Ad4BP Regulating Steroidogenic P-450 Gene Is a Member of Steroid Hormone Receptor Superfamily. J Biol Chem. 1993; 268: 7494–7502.

83. Gissendanner CR, Sluder AE. nhr-25, the Caenorhabditis elegans ortholog of ftz-f1, is required for epidermal and somatic gonad development. Dev Biol. 2000; 221: 259–272.

84. Ikeda Y, Lala DS, Luo X, Kim E, Moisan MP, Parker KL. Characterization of the mouse FTZ-F1 gene, which encodes a key regulator of steroid hydroxylase gene expression. Mol Endocrinol. 1993; 7: 852–860.

85. Luo X, Ikeda Y, Parker K. A cell-specific nuclear receptor is essential for adrenal and gonadal developement and sexual differentiation. Cell. 1994; 77: 481–490.

86. Hofsten J Von, Olsson P. Zebrafish sex determination and differentiation: Involvement of FTZ-F1 genes. Reprod Biol Endocrinol. 2005; 3: 1–11.

87. Dubrovsky EB, Dubrovskaya V a., Bernardo T, Otte V, DiFilippo R, Bryan H. The Drosophila FTZ-F1 nuclear receptor mediates juvenile hormone activation of E75A gene expression through an intracellular pathway. J Biol Chem. 2011; 286: 33689–33700.

88. Mittmann B, Ungerer P, Klann M, Stollewerk A, Wolff C. Development and staging of the water flea Daphnia magna (Straus, 1820; Cladocera, Daphniidae) based on morphological landmarks. Evodevo. 2014; 5: 12.

89. Bowler T, Kosman D, Licht J, Pick L. Computational identification of Ftz/Ftz-F1 downstream target genes. Dev Biol. 2006; 299: 78–90.

90. Lavorgna G, Ueda H, Clos J, Wu C. FTZ-F1, a steroid hormone receptor-like protein implicated in the activation of the fushi tarazu. Science. 1991; 252: 848–851.

91. Yamada M, Murata T, Hirose S, Lavorgna G, Suzuki E, Ueda H. Temporally restricted expression of transcription factor beta FTZ-F1: significance for embryogenesis, molting and metamorphosis in Drosophila melanogaster. Development. 2000; 127: 5083–5092.

92. Yussa M, Löhr U, Su K, Pick L. The nuclear receptor Ftz-F1 and

homeodomain protein Ftz interact through evolutionarily conserved protein domains. Mech Dev. 2001; 107: 39–53.

93. Wurtz JM, Bourguet W, Renaud JP, Vivat V, Chambon P, Moras D, et al. A canonical structure for the ligand-binding domain of nuclear receptor. Nat Struct Biol. 1996; 3: 87–94.

94. Bernardo T, Dubrovsky EB. The drosophila juvenile hormone receptor candidates methoprene-tolerant (MET) and germ cell-expressed (GCE) utilize a conserved LI XX L motif to bind the FTZ-F1 nuclear. 2012; 287: 7821–7833.

95. Chan SM, Chan KM. Characterization of the shrimp eyestalk cDNA encoding a novel fushi tarazu-factor 1 (FTZ-F1). FEBS Lett. 1999; 454: 109–114.

96. Takase M, Nakajima T, Nakamura M. FTZ-F1alpha is expressed in the developing gonad of frogs. Biochim Biophys Acta. 2000; 1494: 195–200.

97. Ikeda Y, Shen WH, Ingraham H a, Parker KL. Developmental expression of mouse steroidogenic factor-1, an essential regulator of the steroid hydroxylases. Mol Endocrinol. 1994; 8: 654–662.

98. Koopman P, Gubbay J, Vivian N, Goodfellow P, Lovell-Badge R. Male development of chromosomally female mice transgenic for Sry. Nature. 1991; 351: 117–21.

99. Takehana Y, Matsuda M, Myosho T, Suster ML, Kawakami K, Shin-I T, et al. Co-option of Sox3 as the male-determining factor on the Y chromosome in the fish Oryzias dancena. Nat Commun. 2014; 5: 4157.

100. Smith C a, Roeszler KN, Ohnesorg T, Cummins DM, Farlie PG, Doran TJ, et al. The avian Z-linked gene DMRT1 is required for male sex determination in the chicken. Nature. 2009; 461: 267–271.

101. Myosho T, Otake H, Masuyama H, Matsuda M, Kuroki Y, Fujiyama A, et al.

Tracing the emergence of a novel sex-determining gene in medaka, Oryzias luzonensis. Genetics. 2012; 191: 163–170.

102. Yoshimoto S, Okada E, Umemoto H, Tamura K, Uno Y, Nishida-Umehara C, et al. A W-linked DM-domain gene, DM-W, participates in primary ovary development in *Xenopus laevis*. Proc Natl Acad Sci USA. 2008; 105: 2469–2474.

103. Matsuda M, Nagahama Y, Shinomiya A, Sato T, Matsuda C, Kobayashi T, et al. DMY is a Y-specific DM-domain gene required for male development in the medaka fish. Nature. 2002; 417: 559–563.

104. Beye M, Hasselmann M, Fondrk MK, Page RE, Omholt SW. The gene csd is the primary signal for sexual development in the honeybee and encodes an SR-type protein. Cell. 2003; 114: 419–429.

105. Gempe T, Beye M. Function and evolution of sex determination mechanisms, gene and pathways in insects. BioEssays. 2010; 33: 52–60.

106. Crustacea D, Chandler JC, Aizen J, Chandler JC, Aizen J, Fitzgibbon QP, et al. Applying the power of transcriptomics: Understanding male sexual development in decapod crustacea. Integr Comp Biol. 2016; 1–13.

List of publications

1. **Mohamad Ishak, NS.**, Kato, Y., Matsuura, T., Watanabe, H. (2016) Sequence conservation and sexually dimorphic expression of the *Ftz-F1* gene in crustacean *Daphnia magna*. *PLoS ONE* 11(5):e0154636.

   (Chapter 4)

2. **Mohamad Ishak, NS.**, Nong, QD., Kato, Y., Matsuura, T., Watanabe, H. (2017) Co-option of the bZIP transcription factor Vrille as the activator of *Doublesex1* in environmental sex determination of the crustacean *Daphnia magna*. *PLoS Genet* 13(11):e1006953.

   (Chapter 3)

Acknowledgments

I would like to express my sincere gratitude to Professor Dr. Hajime Watanabe of Department of Biotechnology, Graduate School of Engineer, Osaka University, for his kindness in giving me the great opportunity to do research in Bioenvironmental Science Laboratory and his guidance. Furthermore, I would like to thank Associate Professor Dr. Tomoaki Matsuura for his helpful comments and thinking, and special gratitude to Assistant Professor Dr. Yasuhiko Kato for his personal guidance and teaching in the laboratory.

I am also very grateful to Professor Dr. Toshiya Muranaka and Professor Dr. Kazuhito Fujiyama from the Department of Biotechnology, Graduate School of Engineering, Osaka University, for their valuable comments and suggestions for this writing and the thesis presentation.

I would like to acknowledge the Department of Biotechnology, Osaka University and Monbugakusho Scholarship (MEXT) for the financial support.

Finally, I am also thankful to my family in Malaysia and family from Watanabe Laboratory for their encouragement and understanding during the ups and downs throughout this journey of research and growth.

Nur Syafiqah Mohamad Ishak.